Aus dem Max-Delbrück-Centrum für Molekulare Medizin

DISSERTATION

Electrical excitability and mechanosensitive currents in sensory neurons: developmental onset, calcium channels and NGF-mediated modulation of mechanotransduction.

zur Erlangung des akademischen Grades
Doctor of Philosophy in Medical Neurosciences
(PhD in Medical Neurosciences)

vorgelegt der Medizinischen Fakultät
Charité – Universitätsmedizin Berlin

von

Rui Wang

aus Beijing, China

Gutachter/in: 1. Prof.Dr. Gary Lewin

2. Prof. Dr. Rohini Kuner

3. Prof. Dr. med. Ulrich Dirnagl

Datum der Promotion: 05.10.2009

Acknowledgement

First of all, I would deeply thank my supervisor Prof. Gary Lewin for giving me the chance to do my PhD study in his well-equipped and internationally atmospheric laboratory. His passion and knowledge toward science has inspired me and motivated me to achieve the aim of my project. His sincere advice and encouragement guided me throughout all my work. I also thank him for understanding and being patient during the less productive periods. I am grateful for financial and academic support from the research training school ” The impact of inflammation on nervous system function” and International Graduate Program of Medical Neurosciences at Charité-Universitätsmedizin Berlin and helpful administrative assistance by Stefanie Korthal and Lutz Steiner.

I would like to thank Dr. Stefan Lechner and Dr. Jing Hu for teaching me laboratory techniques and helping me with experimental design and data analysis. Their useful suggestions and generous share of studying experiences made my work much straightforward and easier. I am also sincerely grateful to Prof. Stuart Bevan and Clive Gentry in King’s college London for teaching and helping me with the retrograde labeling experiment.

It has been a great pleasure to work with my fellow PhD students. Communicating skills and ideas between colleagues made my study more rich and colourful. Their encouragement and support have helped me pass through the tough times during my study. I am grateful for their advice and friendship. I also want to send my thanks to our technicians: Heike, Anke, Anja and irreplaceable secretary Manuela for enormous help in organising animals and lab issues.

My thanks also go to my family, especially my parents. I deeply appreciate their finical support, making my study in Germany possible and dedicatedly. Their endless love

and encouragement give me infinite braveness to overcome any difficulties at any stages of my life. And I am also sure their spiritual support will always accompany me for my further career, which I will never be able to return.

Finally, I would like to thank Dr. Ewan Smith for proof reading of my thesis and Soeren Markworth for translating the Summary of the thesis.

Studying in Germany is one of the most important decisions that I have ever made in my life. When I first time came to Germany, I was bewildered by my future and new life. During this six-year study period, I was gradually growing up not only in my knowledge but also in my personality. There are laughs and tears, successes and fails and applause and criticism. At the time of finishing my doctoral study, I would love to say all the friends I met in Germany will be my friends for ever and all the experience I had here will be invaluable treasure for all my life.

Table of Contents

List of Figures

List of Tables

List of Abbreviations

AM	A-mechanonociceptors
AP	Action potential
ASIC	Acid sensing ion channels
C-MiHi	C-Mechanoinsensitive, heat insensitive fibers
CV	Conduction velocity
DEG/ENaC	Degenerins/epithelial sodium channels
FDA	Fluorescent labeled dextran amine
GS	Gastrocnemius muscle
HTRMs	High threshold mechanoreceptors
HVA	High voltage-activated channel
IA	Intermediately adapting current
LTMRs	Low threshold mechanoreceptors
LVA	Low voltage-activated channels
MEC	Mechanosensory abnormal
MIA	Mechanically insensitive nociceptors
NGF	Nerve growth factor
RA	Rapidly adapting current
RAM	Rapidly adapting mechanoreceptors
RF	Receptive field
RP	Receptor potential
RUNX	runt-related transcription factor
SA	Slowly adapting current
SAM	Slowly adapting mechanoreceptors
TrK	Tyrosine kinase receptor
TRP	transient receptor potential

1. Introduction

The senses of cutaneous and deep touch, muscle tension, and joint position, as well as those of hearing and equilibrium, all rely on the activity of mechanoreceptors, which are specialized cells tailored to transduce mechanical input into electrical signals.

1.1 Cutaneous mechanoreceptors in mice

All somatosensory information from the limbs and trunk is conveyed by dorsal root ganglion (DRG) neurons. Among all organs, the skin is the most densely innervated. The cell bodies of these sensory neurons lie in the DRG and the axons bifurcate sending one branch to the periphery and the other one to the central nervous system. The terminal of the peripheral branch of the axon is the only portion of the DRG cell that is sensitive to mechanical stimuli. Different cutaneous sensory endings, characterized by their morphology (Iggo and Andres, 1982), are responsible for transducing touch, thermal, and potentially painful stimuli. Electrophysiologically, the sensory nerve fibers can be primarily classified by their conduction velocities and firing patterns. In the mouse, the cutaneous sensory fibers with the conduction velocity above 10m/s are designated as Aβ–fibers, which are large-diameter myelinated fibers, can be either slowly adapting (SAM) or rapidly adapting (RAM) (Koltzenburg et al., 1997)**.** RAM fibers fire only at the onset and offset of a skin displacement and are therefore associated with transmitting vibratory stimuli, or transient motion of hairs in the hairy skin. SAM fibers signal throughout skin displacement and preferentially encode texture and pressure (Toma and Nakajima, 1995). Thinly myelinated Aδ-fibers have conduction velocities between 1-10m/s. They can be further subdivided into rapidly adapting D-hair fibers which are very sensitive to small forces and may be associated with stimulation of the down hairs (Brown and Iggo, 1967; Koltzenburg et al., 1997) and slowly adapting A-fiber mechanonociceptor (AM) fibers which are much less sensitive and require large forces to evoke a

response. Both of these slowly conducting fibers have a thinner myelin sheath than the faster conducting Aβ-fibers. The slowest conducting fibers are C-fibers, which conduct slower than 1m/s and have unmyelinated axons. They primarily conduct signals produced by painful and/or thermal stimuli (Fig. 1).

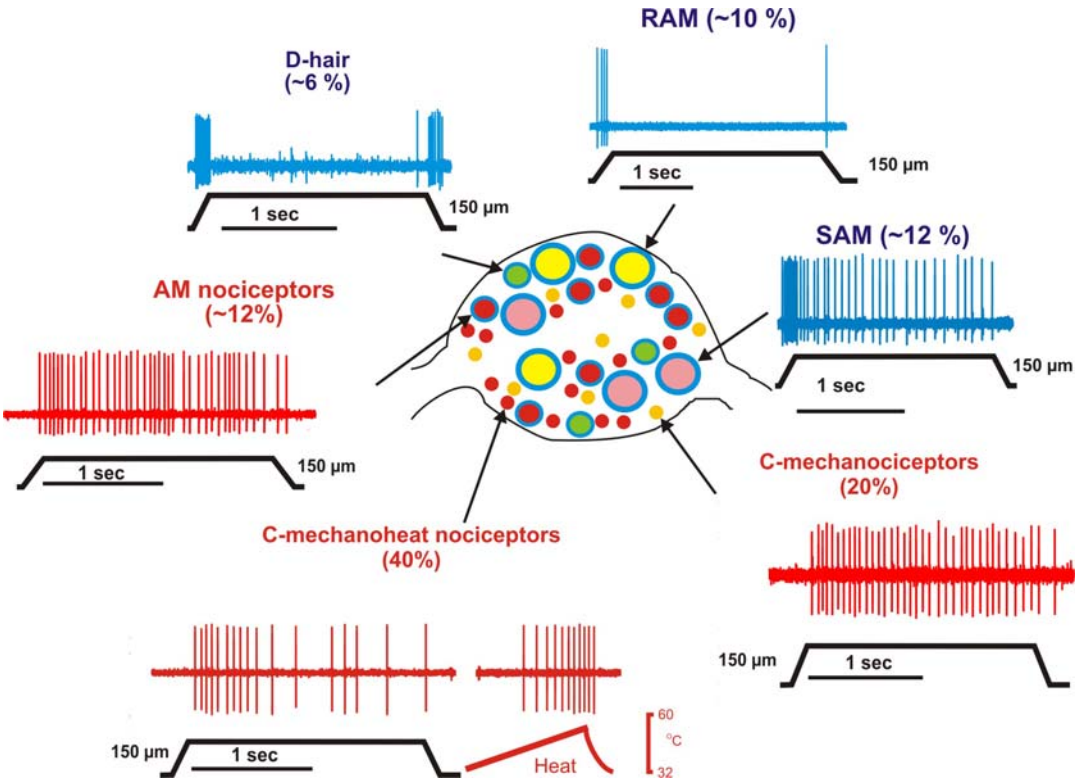

Fig. 1: Varieties of cutaneous mechanoreceptors and their firing patterns.
Typical response properties of mouse mechanoreceptors from the saphenous nerve to a standardized 2s ramp and hold indentation stimulus of 150µm are shown. In the center of this graph is the schematic diagram of the DRG cross section ensheathing the soma of different primary afferent fibers. Arrows indicate the counterpart soma size and myelination state of each kind of mechanoreceptor. The receptors indicated in blue are mechanoreceptors, which respond to vibration, touch and down hair stimuli. RAM and D-hair receptors only respond to the ramp phase of the stimuli, while SAM receptors do not only respond to the ramp phase but also continuously fire during the static phase. Those depicted in red are nociceptors, which detect noxious mechanical, thermal and chemical stimuli. They exclusively and continuously respond to the static stimuli. The approximate percentage of each receptor of the total cutaneous sensory neuron population is indicated in brackets (Lewin and Moshourab, 2004).

1.2 Candidate molecules involved in mechanotransduction in invertebrates and mammals

There are various proposed mechanisms underlying mechanotransduction in different systems. One favored viewpoint for mechanotransduction is the direct-gating model, which proposes that channels are tethered to the cytoskeleton and/or extracellular matrix, and that tension between these linkages controls channel gating.

The tether model emerged from biophysical studies of auditory and vestibular hair cells (LeMasurier and Gillespie, 2005); However, genetic screens for mechanosensory mutants in the fruit fly *Drosophila melonagaster* and the nematode worm *Caenorhabditis elegans* have identified a few of molecular candidates that fit this model. The general tether model applicable to many mechanosensory transduction systems has been established from these studies (Chalfie, 1997; Hudspeth, 1992; Tavernarakis and Driscoll, 1997) (Fig. 2A). A transduction channel integral to the cell membrane can detect the deflection of an extracellular link relative to an intracellular structure. Such a deflection could take the form of deformation of the skin, oscillation of a hair cell's stereocilia bundle, or the vibration of a fly's bristle. Deflection changes tension in all elements of the system, and the transduction channel responds by changing its open probability. Up to now, some of the blanks in this all-purpose general model have been filled by the studies of mutants in mice and the two most utilized invertebrate models – *C.elegans* and *D.melanogaster*. These studies have yielded possible candidate transduction channels and accessory molecules. Intensive studies have been conducted in hair cell mechanotransduction. Hair cells are located in the organ of corti in the cochlea. They are the auditory receptor cells, which convert mechanical energy into an inward electrical current causing depolarization. Each hair cell has many hairy-looking stereocilia extending from its top. The stereocilia contain aligned actin filaments and are deflected by the vibration caused by a sound wave. The deflection of stereocilia pulls on fine links that

join adjacent stereocilia at their tips. The tip link acts as a gating spring to open one or more transduction channels. Some recent work showed that Myosin 1c might be a component of the adaptation motor protein (Holt et al., 2002; Stauffer et al., 2005). Cadherin 23 and Procadherin15 are thought to constitute the hair bundle tip links, which are extracellular filaments that transmit force to the transduction channel's gate (Ahmed et al., 2006; Siemens et al., 2004), while TRPA1 was briefly viewed as a candidate for the mechanotransduction channel (Corey et al., 2004). However, the role of TRPA1 as mechanotransduction channel was quickly disproved by the normal hearing and vestibular function in *Trpa1*$^{-/-}$ mice (Kwan et al., 2006) (Fig. 2B). Furthermore, genetic screens from flies have revealed that an extracellular-matrix protein NompA (no mechanoreceptor potential) and three ion channels TRPN1 (NompC), Nan (Nachung) and IAV (Iactive) (belong to TRPV family) are necessary for bristle mechanotransduction (Chung et al., 2001; Gong et al., 2004; Kim et al., 2003; Walker et al., 2000) (Fig. 2C). However, later studies indicated that Nan played a role in electrical signal propagation rather than transduction (Gopfert et al., 2006; Kamikouchi et al., 2009).

In addition, the *mec* mutants in *C. elegans* have revealed that several of the *mec* genes encode components of the cytoskeleton, the extracellular matrix, or the links to them in the transduction complex (Du et al., 1996; Fukushige et al., 1999; Goodman et al., 2002; Gu et al., 1996; Huang et al., 1995; Savage et al., 1989) (Fig. 2D). Two of the *mec* genes encode similar but nonredundant proteins, called degenerins (DEGs), which are related to vertebrate epithelial sodium channels (ENaC) responsible for Na^+ absorption. A channel formed by the MEC-4 and MEC-10 and probably also by MEC-6 forms a cationic pore through the plasma membrane and produces depolarization of the membrane potential when it is opened. The channel may be associated on its intracellular surface with MEC-2, which may also be attached to the microtubules (MEC-7 and MEC-12). On its extracellular surface, the channel may be associated with the MEC-1, MEC-5 and MEC-9 proteins. Therefore, studies in worms, flies and vertebrates have shown that there are two general families of ion channels,

namely the DEG/EnaC and TRP families and some other sets of genes encoding the channel related proteins appear to be needed for the function of different mechanosensory receptors.

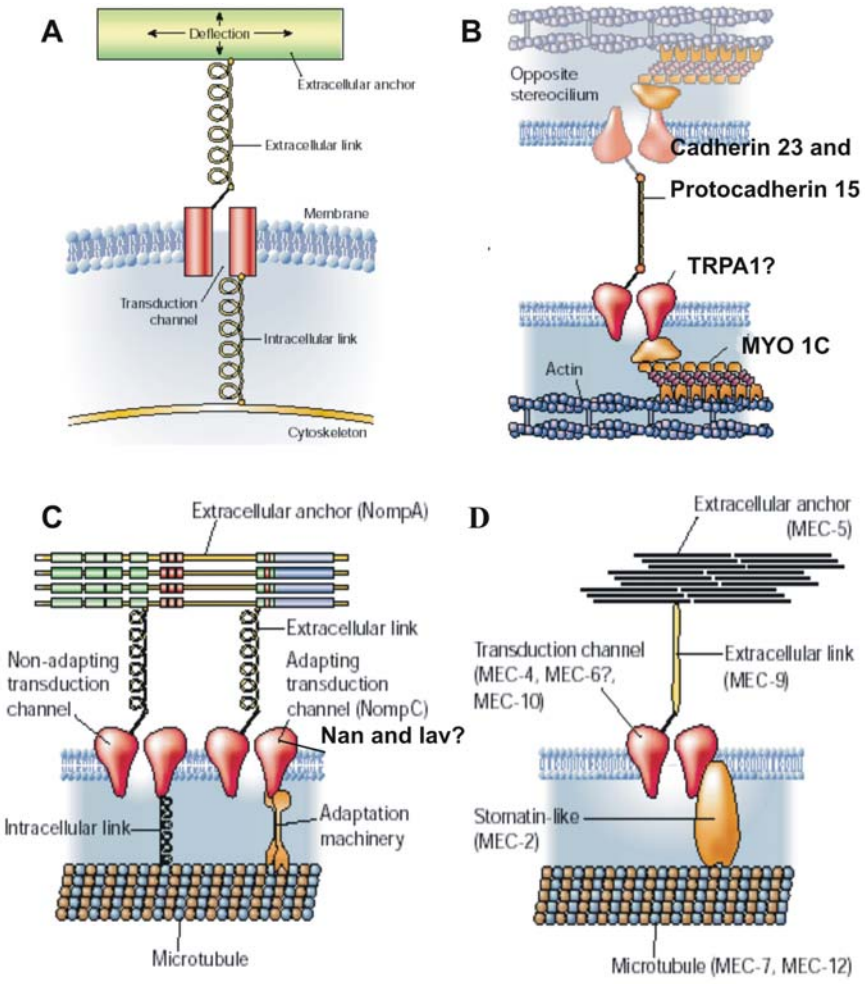

Fig. 2: Molecular components in different mechanotransduction models.
A: General model of mechanotransduction complex. A transduction channel is anchored by intracellular and extracellular anchors to the cytoskeleton and to an extracellular structure to which forces are applied. The transduction channel can be regulated in response to the relative deflection between intracellular and extracellular structure. Corresponding proteins to these structures were gradually identified in vertebrate hair cell, *D.melanogaster* and *C.elegans*. **B:** Proposed protein components in the hair cell transduction apparatus. **C:** The location of NompC and NompA in proposed molecular model of transduction for ciliated insect mechanoreceptors in *D.melanogaster*. **D:** MEC proteins are discovered and localized to the corresponding structures in the *C. elegans* touch-receptor transduction model (Gillespie and Walker, 2001).

Based on *C.elegans* research (Ernstrom and Chalfie, 2002)**,** acid-sensing ion channels (ASIC2 and ASIC3) have been identified in DEGs/ENaC channel family as potential components of the mechanotransducer in mature skin mechanoreceptors in mammals (Price et al., 2000; Price et al., 2001) (Fig. 3). The host lab have shown that ASIC2 and ASIC3 can form complexes with proteins of the stomatin family that have also been implicated in sensory mechanotransduction (Mannsfeldt et al., 1999; Wetzel et al., 2007). Using the skin-nerve preparation, certain classes of sensory axons in null mutants were shown to have aberrant response properites. ASIC2 mutants showed reduced sensitivity of low threshold RAM and SAM mechanoreceptors in the hairy skin in mice (Price et al., 2000). Whereas, ASIC3 mutants displayed an increased sensitivity of RAM fibers but a decreased sensitivity of Aδ- and C-fibre nociceptors (Lewin and Moshourab, 2004; Price et al., 2001). On the other hand no significant changes in the mechanically gated current were observed in isolated sensory neurons in ASIC2 and ASIC3 knockout mice (Drew et al., 2004; Lechner et al., 2009). In view of these contradictory findings, it is clear there is still a big gap in our knowledge about mechanotransduction in the mammalian sensory system.

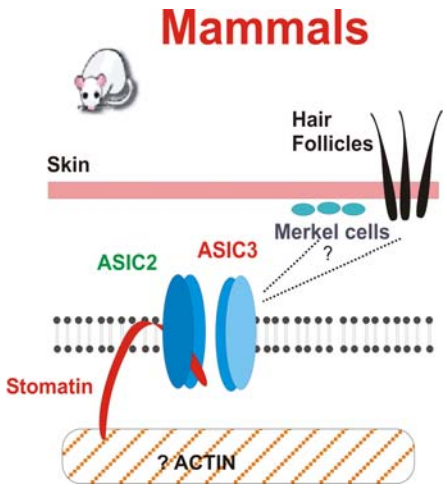

Fig. 3: Molecular model of mechanotransduction in mammals.
Homologous to C. *elegans* MEC-4, ASIC2 has been localized to the fine terminals of the mechanoreceptive organs such as Meissner corpuscles, merkel disks and the lanciform endings surrounding the follicles of simple hairs (Garcia-Anoveros et al.,

2001; Price et al., 2000). And it is expressed in many large diameter neurones. ASIC3 is co-expressed with ASIC2 in large diameter sensory neurones, but also found in medium and small size neurones in the DRG (Price et al., 2001). The mammalian protein stomatin is related to MEC-2 in *C. elegans*, which is also detected in the mammalian skin and proposed to play a role in mechanotransduction (Fricke et al., 2000; Mannsfeldt et al., 1999; Martinez-Salgado et al., 2007).

1.3 Mechano-electrical transduction

The transduction of mechanical stimuli is thought to take place via the direct gating of specialized ion channels in the membrane that are not voltage dependent. When a mechanical stimulus is applied to receptor's surface, a non-regenerative, non-propagated receptor potential (RP) is produced. When the RP reaches a threshold value, a regenerative, voltage-dependent action potential (AP) is initiated. The AP is propagated along the afferent axon to central locations. Since the earliest successful physiological studies on Pacinian corpuscles (Adrian and Umrath, 1929), a variety of techniques have been used to measure RPs and APs in different sensory organs from different species by extracellular, current-clamp or voltage-clamp recordings with the application of procaine, TTX and/ or sodium-free solutions (Hunt et al., 1978; Juusola and French, 1998; Loewenstein and Cohen, 1959a; Loewenstein and Cohen, 1959b; Rydqvist and Purali, 1993). It is proposed from these experiments that the RP is a result of ions flowing down their electrochemical gradient into the cell, the action somehow initiated by membrane stretch opening up some unidentified ion pathways. RPs are also graded in amplitude, increasing in size for increases in the strength of the stimulus, and there is a constant latency between a stimulus and the RP produced. It was also found in Pacinian corpuscles that the RP actually leaves a refractory state so that subsequent stimuli falling within the time course of the RP will elicit a smaller RP or no RP (Loewenstein and Altamiranoorrego, 1958). The size of the effect is inversely proportional to the preceding RP amplitude. However, APs can be generated with electrical stimulation and response all-or-none in amplitude and have response latencies, which are typically dependent upon stimulus intensity (Fig.

4). In general, both RPs and APs can be rapidly or slowly adapting. Adaptation describes the phenomenon whereby the response is initially large at stimulus onset but falls off in amplitude (RP) or in firing frequency (AP) despite a constant stimulus. Recordings of the RP made from cat Pacinian corpuscles showed that this receptor type had a rapidly adapting receptor current and AP discharge (Loewenstein and Skalak, 1966). Intracellular recordings made from crayfish muscle receptor organs and spider slit sensilla showed existence of both sustained and burst firing neuron types in these two species (Eyzaguirre and Kuffler, 1955; Juusola and French, 1998). Further voltage-clamp recordings revealed that rapid and slow adaptation kinetics of RP in the two types of neurons are relatively unimportant in determining AP adaptation (Juusola and French, 1998; Rydqvist and Purali, 1993). In addition, electrical stimulation produced the same differences in firing patterns between the neurons as mechanical stimulation, suggesting that voltage-gated channels define AP adaptation. Since a wide range of electrophysiological processes could occur during the mechanotransduction process, how much of the adaptation and intrinsic properties of the receptor current and membrane electrical properties of different sensory neuronal cells contribute the overall firing pattern of the AP and further affect the receptor and tissue sensitivity remains enigmatic.

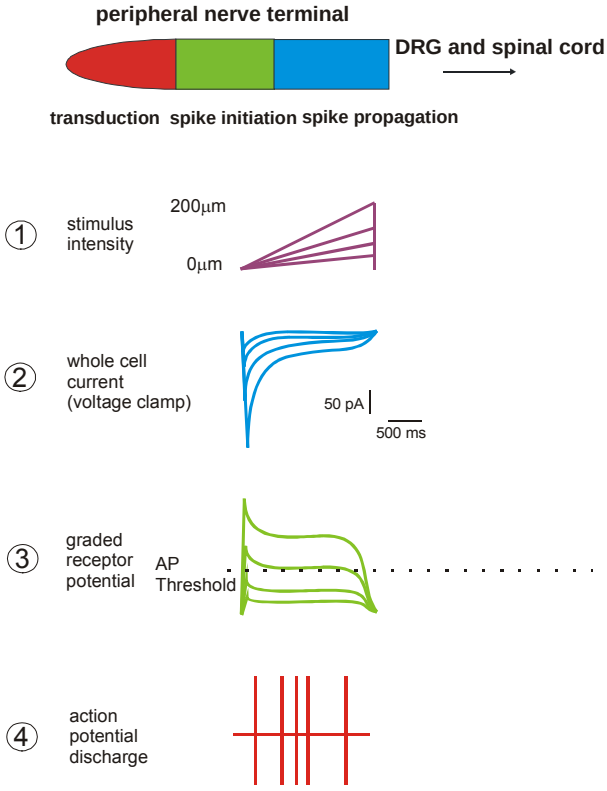

Fig. 4: A schematic diagram of the mechanotransduction process.
1.When increasing indentation stimuli are applied to a nerve ending, the inward currents can be measured at the receptor ending of the sensory cell body under voltage clamp. **2.** This current is thought to be generated by the opening of mechanically gated ion channels. **3.** As a consequence of increasing stimuli, a series of membrane depolarizations could be recorded under current clamp. **4.** Finally, when depolarization reaches the threshold for AP generation, APs are evoked and can be recorded with extracellular recording (Hu et al., 2006).

1.4 In vitro RP recording from cultured mouse sensory neurons

In the past, we have characterized the mechanosensitivity of single sensory neurons using an *in vitro* skin nerve preparation where AP discharge to defined receptive field stimulation has been measured (Koltzenburg et al., 1997; Milenkovic et al., 2008). However, this technique does not allow one to directly measure the activity of ion channels that are opened by the mechanical stimulus, as these are located on

endings that are too small for intracellular recordings. One would like to directly measure the ionic currents that underlie mechanosensory transduction in mechanoreceptors. Using acutely isolated sensory neurons grown in culture with whole cell patch-clamp technique McCarter and Levine demonstrated that some sensory neurons exhibit mechanosensitive inward currents upon mechanical stimulation of the cell soma. In subsequent more detailed studies Drew and colleagues also showed similar mechanically gated conductances again by stimulating the cell body of both rat and mouse DRG neurons in culture (Drew et al., 2004; Drew et al., 2002; McCarter et al., 1999). In general two major kinetic types of current have been observed in response to step displacements of the somal membrane, a rapidly inactivating and a slowly inactivating inward current. Our lab has also developed a technique that allows us to directly measure mechanically gated conductances evoked from the neurites of mouse sensory neurons in culture. In this way, we could observe three types of mechanically activated currents in adult mouse DRG neurons. These currents can be distinguished by their inactivation kinetics and are classified into rapidly adapting (RA: τ_{iac}<5ms), intermediately adapting (IA:5ms< τ_{iac}<50ms) and slowly adapting currents (SA: τ_{iac}>50ms) (Hu and Lewin, 2006).

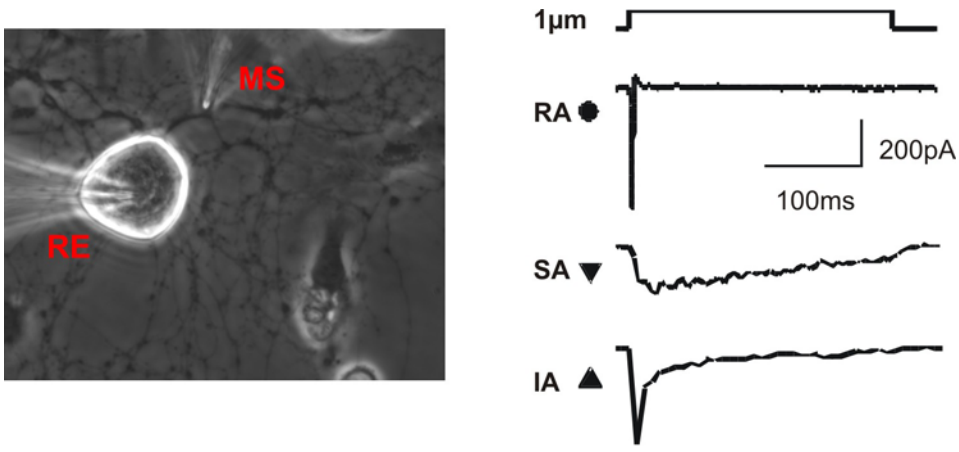

Fig. 5: Mechanically activated currents in adult cultivated mouse sensory neurons.
Left is shown an example of a recorded cell. RE stands for the recording electrode that is being used to record whole cell currents from the cell soma. The mechanical

stimulus (MS) is a single-step displacement of ~750 µm delivered to the neurite of the recorded cell. On the right are examples of the three types of mechanically activated currents observed with the standard mechanical stimulus. According to their inactivation time constant, they are classified into rapidly adapting (RA), slowly adapting (SA) and intermediately adapting current (IA). Note that in all cases voltage sodium channels were blocked with 1µM TTX (Hu and Lewin, 2006).

1.5 Developmental acquisition of mechanosensitivity in DRG neurons

Gene mapping studies in both mice and humans with inherited syndromic and non-syndromic deafness have identified a myriad of genes expressed in the hair cell that are essential for normal hearing. In contrast, genetic mapping of monogenic inherited sensory disorders in mice or humans has not led to the identification of candidate genes essential for the transduction of somatic mechanical stimuli by sensory neurons. This may be because the diversity of sensory mechanoreceptors in the DRG might make obvious sensory phenotypes that are a consequence of single gene defects less easy to recognize or that the overlapping sensitivities of mechanoreceptors to different modalities of mechanical stimuli leads to a functional compensation of the loss of any individual mechanoreceptor.

However, developmental studies in hair cells have shed light on searching for molecues involved in somatosensory mechanotransdution The ability of sensory neurons and hair cells to transduce mechanical stimuli is thought to start very early during embryonic development. The relative ease of making direct recordings of the transduction event in hair cells with whole cell patch-clamp techniques has enabled physiologists to pinpoint the time of onset of hair cell mechanotransduction with a high degree of accuracy (Corey et al., 2004; Geleoc and Holt, 2003; Si et al., 2003). Thus, transduction in mouse utricle hair cells starts between embryonic day 16 and 17 (E16-17) and correlates with the acquisition of hair bundle tip links, adaptation motor proteins like Myosin 1c (Holt et al., 2002), and the appearance of the previously

believed transduction channel TRPA1 (Corey et al., 2004; Geleoc and Holt, 2003). Because of the abundance of molecular candidates identified as being essential for hair cell mechanotransduction, the coordinated onset of mechanically activated currents during the development of these cells has become a useful experimental tool to identify the most important molecular players.

The identification of the exact time point when different classes of DRG neurons acquire their mechanosensitivity during development has not been adequately addressed. Several studies have shown that the mechanosensory behavior of sensory neurons matures over time during the post-natal period (Ferrington et al., 1984; Fitzgerald, 1987a; Koltzenburg and Lewin, 1997). The retrograde labeling studies showed that the earliest examined stage when the lateral femoral cutaneous nerve of chick reaches the skin was E5 (Honig, 1982). And the supramaximal stimulation of lumbosacral spinal nerves of chick embryo could be recorded at E10.

The innervation of the embryonic rat hindlimb starts at around E14 to the proximal part and reaches the distal part by E16.5 (Mirnics and Koerber, 1995), while single nerve recordings showed the cutaneous mechansensitivity is clearly observed from E17 on, just after innervation is completed (Fitzgerald, 1987b). Extracellular recordings from these two species have suggested that mechanosensitivity is present as soon as or after innervation of peripheral tissues (Fitzgerald, 1987b; Honig, 1982; Scott, 1982). The timing of peripheral target innervation in mouse has been shown to start at E11 and is completed by E13.5 in the forelimb followed with a slight delay by the hindlimb (Berg and Farel, 2000). Due to the lack of high resolution electrophysiological techniques, which enable the direct measurement of mechanically gated currents in developing sensory neurons, the time when the mechanosensitivity starts in mouse has not been addressed up to now.

In the present study, we used the *in vitro* mechanical stimulation method in cultured mouse DRG neurons to study the developmental acquisition of mechanotransduction in mouse DRG neurons and hypothesized that candidate channel genes must be

expressed in the receptor cell by the time during developmental age that the mechanically sensitive current is detected. These candidate channel proteins should be located at the site of mechanical transduction within the cell. Based upon the electrophysiological findings, we could execute a series of molecular studies (e.g. real-time PCR and *in situ* hybridisation) to search for the putative proteins belonging to the members of the TRP and DEG/EnaC families, since they have been shown to be important components of mechanotransduction complexes in invertebrate sensory neurons as well as in vertebrate hair cell transduction.

1.6 Function of $Ca_v3.2$ in sensory neuron mechanosensitivity

The variety of different mechanoreceptor neurons makes it increasingly important to have specific molecular markers that reliably distinguish between receptor types (Fig.1). This is particularly important when one isolates sensory neurons from their in vivo environment. One type of very sensitive cutaneous receptor is the D-hair receptor. It is named so because this type of receptor can be selectively activated by moving small sinus or down hairs within the skin (Brown and Iggo, 1967). It has also been observed in primates, rodents, and humans (Adriaensen et al., 1983; Burgess and Perl, 1967; Koltzenburg et al., 1997; Leem et al., 1993; Lewin and McMahon, 1991; Perl, 1968). When recording from peripheral nerve, D-hair receptors can be easily recognized by their relatively large receptive fields and extremely low mechanical thresholds. It has been acknowledged as by far the most sensitive mechanoreceptor in the skin and has von Frey thresholds that are 10 times lower than for other low-threshold receptors (Koltzenburg et al., 1997; Lewin and McMahon, 1991; Lewin et al., 1992). The hallmark of its special physiological properties makes it of particular interest. Its supersensitivity could arise due to a specific mechanosensitive ion channel, voltage-gated ion channel or peculiar structural ending, which has not yet been unravelled, but seems like to be associated with hairs (Stucky et al., 1998). Recently, our group used a DNA array and cDNA library based screening approach to

identify a calcium channel gene that is specifically expressed in D-hair receptor neurons at high levels (Shin et al., 2003). Using neurotrophin knockout mice that lack D-hair receptor neurons we found that a subpopulation of medium-sized neurons expressing the low-voltage activated T-type calcium channel Cav3.2 gene were missing.

Voltage-gated Ca^{2+} channels play a key role in controlling Ca^{2+} entry during cell depolarization. They can be broadly divided into high voltage-activated (HVA) and low voltage-activated (LVA) channels. The HVA family (L, N, P/Q and R-Types) requires a strong depolarization for activation. These channels are primarily involved in muscle contraction, hormone secretion and fast synaptic transmission. In contrast, the LVA (T-type) channels are activated by weak depolarization (at -50 to -40 mV in 5 mM Ca^{2+}) and are transient. These channels ($Ca_v3.1$, $Ca_v3.2$ and $Ca_v3.3$) have been functionally described in DRG neurons (Carbone and Lux, 1984a) and are associated with AP generation and repetitive electrical activity. Reverse transcription (RT)- PCR and *in situ* hybridisation analyses have shown that a subset of small- and medium-diameter primary afferent neurons express $Ca_v3.2$ almost exclusively, wherein D-hair cells show the highest density of $Ca_v3.2$ (Shin et al., 2003; Talley et al., 1999). T-type currents are congregated in small and medium diameter rat sensory neurons, but are not present in large diameter neurons (Scroggs and Fox, 1992). Small diameter cell bodies had small T-type Ca^{2+}. Medium diameter cells had considerably larger currents providing the dominant means of Ca^{2+} entry, whereas large cells did not express any T-type current.

Functional experiments using a drug (Mibefradil) that blocks T-type channels revealed that the mechanosensitivity of D-hair receptors was selectively reduced (Shin et al., 2003). Some other studies showed that redox agent (e.g. L-cysteine) sensitized a unique subpopulation of periperal nociceptors (capsaicin+ and isolectin B_4+) via the T-type Ca^{2+} channel and promote cutaneous thermal and mechanical hyperalgesia following injection into the peripheral receptive fields (Nelson et al., 2005; Todorovic et

al., 2001). Consistently, high doses of Mibefradil reversed behavioral responses to acute mechanical and thermal stimuli and to hyperalgesia in animal models of pain. Similarly, antisense targeting of the $Ca_v3.2$ channel, reduced T-type currents in rat sensory neurons and resulted in antinociceptive and antihyperalgesic effects (Bourinet et al., 2005). Furthermore, behavioural studies from knockout mice showed that the $Ca_v3.2^{-/-}$ mice showed decreased pain responses to tonic noxious stimuli under normal condition, but no differences in spontaneous pain or mechanical and thermal hyperalgesia induced by nerve ligation were observed when compared with wild type (Choi et al., 2007). Since the contradictory findings about the involvement of $Ca_v3.2$ channel in nociception processing and mechanoreceptor sensitivity, in the present study, we will make use of $Ca_v3.2^{-/-}$ mice to test the functional properties of D-hair mechanoreceptors and nociceptors with the *in vitro* skin nerve preparation. In particular such experiments will allow us to determine whether the behavioral phenotypes observed are due to changes in the transduction properties of primary afferents.

1.7 Sensitization mechanism of deep tissue receptors after inflammation

The major sensation from deep tissues such as joints and muscles is pain. Deep tissue pain is often dull and aching, and poorly localized, and is thus different from cutaneous pain. Some studies have suggested that deep tissue and visceral afferents might detect mechanical stimuli using fundamentally different mechanisms than cutaneous afferents.

Deep tissues including joints and muscles are predominantly innervated by nociceptors, which are normally activated by non-physiological painful stimuli. Unmyelinated C-fibers account for about 40% of joint afferent (Schaible and Grubb, 1993) and 33% of the muscle afferent (Mense, 1993), respectively. Aδ-fibres account

for less than 10% in each tissue. Both Aδ- and C-fibers terminate as free nerve endings in the fibrous capsule, adipose tissue, ligaments menisci and the periosteum in joints, while in the wall of arterioles in the muscle belly and in the surrounding connective tissue (Schaible and Grubb, 1993; Stacey, 1969).

1.7.1 Mechanoinsensitive neurons

Meyer and Campbell identified a substantial group of C-fibers, which display little or no mechanosensitivity under physiological conditions (Meyer et al., 1991). This class of nociceptors that were termed mechanically insensitive nociceptors (MIA) had also been identified in experimental studies on visceral and deep tissue receptors and have sometimes been called “silent” or “sleeping” nociceptors (McMahon and Koltzenburg, 1990). Because these fibers by definition have high mechanical thresholds or are unresponsive to mechanical stimuli, finding the mechanical receptive field of these fibers is difficult. Using microneurography and electrocutaneous search techniques, about 12-25% of cutaneous C-fibers were estimated as C-mechanoinsensitive, heat insensitive (C-MiHi) in human and monkeys (Davis et al., 1993b; Meyer et al., 1991; Schmidt et al., 1995; Weidner et al., 1999). They also appear to be present in rodent skin, but most studies have found them to be present in much smaller numbers (~10%) than observed in higher mammals (Handwerker et al., 1991; Kress et al., 1992; Lewin and Mendell, 1994). In addition, about half of the Aδ-fibers are mechanical insensitive in monkey skin (Meyer et al., 1991). In the joint, it is difficult to make a valid estimate of the proportion of initially mechanoinsensitive joint afferents. A rough estimate would be that about 30% of the C-fibers and a small percentage of the Aδ-fibers (about 24%) are initially mechanoinsensitive (Fig. 6). Several distinct features allow the separation of C-MiHi from other C-fibers: 1.C-MiHis have higher electrical thresholds for activation than mechanosensitive C-fibers (Schmidt et al., 1997); 2.Although they have comparable conduction velocities to other nociceptors, human C-MiHis exhibit stronger activity-dependent slowing. This is a phenomenon whereby low frequency

suprathreshold electrical stimulation of C-fiber axon or terminal ending induces a slowing of the apparent conduction velocity.

As to why these mechanically insensitive afferents are silent, we have to take a closer look at how mechanotransduction happens. If we apply mechanical stimuli on the peripheral nerve terminal, mechanical RPs can be recorded. As the stimuli increase, the mechanical currents increase and reach the threshold for voltage-gated ion channels activation, therefore causing AP generation. So the silence of these neurons could either be at mechanotransduction level due to the lack of inactive state of the mechanotransduction ion channel or due to its specific membrane properties for harder AP generation (Fig. 4).

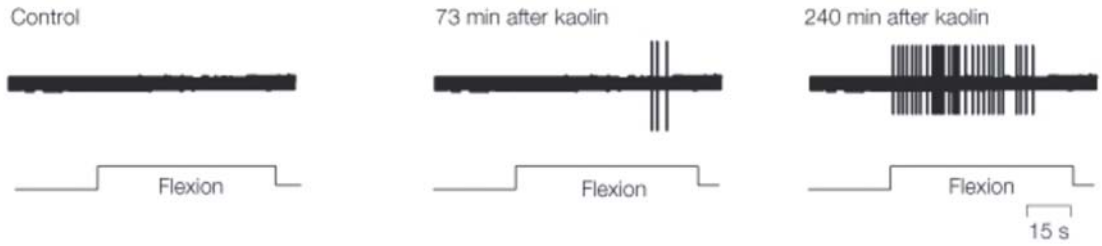

Fig. 6: Mechanosensitivity changes of a mechanoinsensitive C-fibrer in a cat's knee joint.
Extracellular recording showed that the joint silent neuron had no response to mechanical stimulation (probing, movements) before inflammation (control). However, after inflammation, induced by kaolin/carrageenan injection, AP were produced by mechanical stimulation (modified from Schaible & Schmidt 1988b).

1.7.2 Thermal and mechanical hyperalgesia

Upon sensitization with algogens some mechanoinsensitive neurons can become responsive within minutes to tonic pressure and heat stimuli (Kress et al., 1992; Meyer et al., 1991; Schmidt et al., 1995). For example, C-MiHi fibers recorded in humans and rats have been shown to acquire mechanosensitivity within minutes after stimulation with capsaicin or mustard oil (Kress et al., 1992; Schmidt et al., 1995). This

phenomenon is of considerable interest, as it strongly suggests that some sensory afferents possess a latent mechanotransducer that can be rapidly reactivated by algogenic compounds. This phenomenon may be of even more importance in the case of primary afferents that innervate deep tissue including muscle, joint and viscera (McMahon and Koltzenburg, 1990; Schaible and Grubb, 1993). The recruitment of these initially insensitive neurons is thought to be one factor contributing to the hyperalgesia during inflammation.

Hyperalgeisa is an increased response to a painfull stimulus, which may be caused by damage to nociceptors or peripheral nerves. It can be produced experimentally using a chemical or electrical stimulus in normal animals and human subjects (Koltzenburg, 2000; Koltzenburg et al., 1992; Lewin et al., 1994; Simone et al., 1989; Treede et al., 1992). Hyperalgesia to noxious heat stimuli only develops in the area of the initial insult: primary hyperalgesia (Treede et al., 1992). Neurophysiological recordings as well as molecular and cellular experiments indicate that heat hyperalgesia could be explained by a sensitization of the peripheral endings of nociceptors to thermal stimuli (Baumann et al., 1991; Julius and Basbaum, 2001; Simone et al., 1991; Treede et al., 1992). Following inflammatory insults in mice, heat hyperalgesia requires the presence of the heat and capsaicin sensitive cation channel TRPV1 (Caterina et al., 2000; Davis et al., 2000). In addition, hyperalgesia to mechanical stimuli has long been observed in the large area around the site of application of the initial noxious stimulus: sencondary hyperalgesia (Hardy et al., 1950). Up to now, only afferents supplying deep tissues have been shown to respond to inflammatory agents with increases in mechanosensitivity [muscle: (Berberich et al., 1988; Hoheisel et al., 2005); joint: (Grigg et al., 1986; Schaible and Schmidt, 1988a)]. The findings about cutaneous mechanical hyperalgesia are contradictory (Kocher et al., 1987; Reeh et al., 1986). However, due to the lack of a molecular identity for the mechanotransduction ion channel, one cannot deduce the increased sensitivity of nociceptors or newly appeared sensitivity of MIA nociceptors as being due to the activation or expression of mechanosensitive ion channels or membrane property changes caused by some

modification of voltage-gated ion channels during inflammation.

1.7.3 Nerve growth factor and its function in hyperalgesia

In response to tissue damage, many types of cell (e.g. endothelial cells, white blood cells and primary sensory afferent neurons) release inflammatory mediators, such as endothelin, prostaglandin E_2 (PGE_2), leukotrienes, cytokines, platelet activating factor, byradykinin, glutamate, nerve growth factor (NGF). Among these mediators, NGF is widely recognized as a key component in the generation of inflammatory hyperalgesia after injury, and NGF signaling is now seen as an attractive target for analgesic therapy. The neurotrophin family of proteins, comprising NGF, brain-derived neurotrophic factor (BDNF), neurotrophin-3 and neurotrophin-4. Their tyrosine kinase receptors TrKA, TrKB, TrKC bind NGF, BDNF and neurotrophin-3, respectively. In addition, a low- affinity transmembrane receptor $p75^{NTR}$ binds all neurotrophins. The TrK receptors are tyrosine kinase receptors, in dimers with or without $p75^{NTR}$. Activation of TrK by their ligands leads to dimerization of the receptor and phosphorylation of different tyrosine residues that in turn promote the activation of different signaling pathways, notably the ras-raf-MAPK, PI3K-akt-GSKIII, PLC_{γ}-DAG-PKC, and S6kinase. Activation of these pathways during early development blocks apoptosis and promotes cell survival and differentiation. Additionally, TrK activation in terminals leads to a retrograde signal (internalization of TrK-neurotrophin complex) and regulates neuronal responsiveness and synaptic function in adult, with important consequences for pain-signaling systems.

In the present study, we will focus on the effect of NGF on mechanical hyperalgesia. This is because some in vivo studies demonstrate that administration of NGF produces hypersensitivity and pain in humans (Petty et al., 1994; Svensson et al., 2003) in addition to reducing nociceptive mechanical thresholds in animal models of pain (Lewin et al., 1993). Previous studies have shown that long-term exposure to NGF increases the expression of a number of ion channels in TrKA-expressing

neurons, such as TRPV1, $P2X_3$ and ASIC3 (Bron et al., 2003; Ji et al., 2002; Mamet et al., 2002; Ramer et al., 2001; Winston et al., 2001; Zhuang et al., 2004). Stucky and Lewin found that cultivation of neurons in the presence of NGF markedly increased the proportion of neurons with a noxious heat-activated inward current, whereas the mean magnitude of the current evoked was not altered (Stucky and Lewin, 1999). The increased ASIC3 expression induced by NGF is paralleled by enhanced ASIC-mediated currents in the DRG (Mamet et al., 2002). In addition, the expression of some voltage-gated ion channels, including potassium (Park et al., 2003) and particularly sodium channels (Fjell et al., 1999; Leffler et al., 2002; Okuse et al., 1997), are increased in DRG neurons after NGF treatment. The above two groups of ion channels are either transducing ion channels primarily determining response specificity or voltage-gated ion channels determining the timing and extent of AP firing, thus molding the nociceptive sensory neuron response to noxious stimuli. Therefore, two major mechanisms for sensitizing these responses can be postulated: 1) enhanced efficacy of transducing ion channels in afferent nerve terminals yielding larger transduction currents and depolarizations, or 2) modified responsiveness of voltage-gated ion channels to graded depolarizations reducing firing thresholds and increasing responses to suprathreshold stimuli. These physiologic changes may occur at the transcriptional, translation, or post-translation (e.g. TRPV1) levels (Fig. 7).

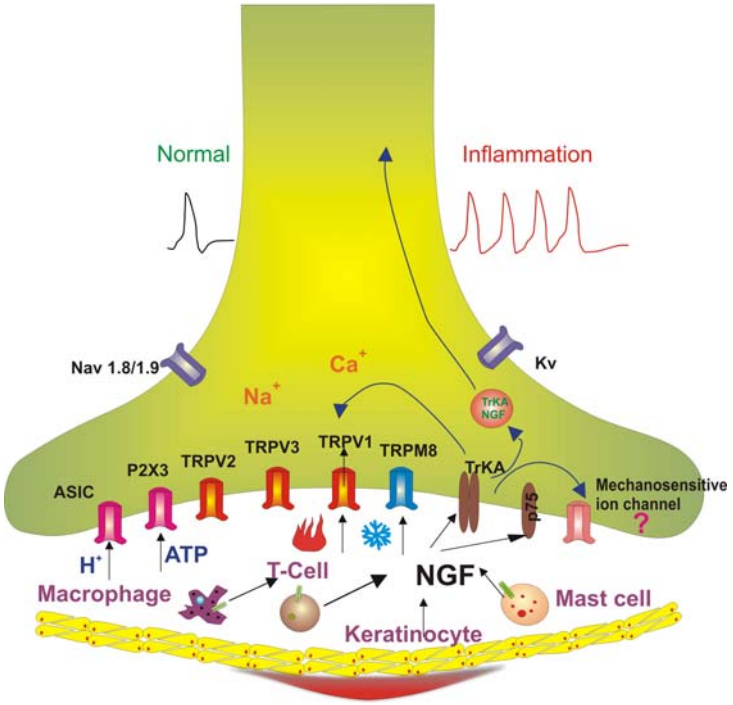

Fig. 7: Release of NGF sensitizes the peripheral terminals of sensory neurons. Upon localized tissue damage, a variety of immune cells and keratinocytes release NGF, which can then interact with its receptors, TrkA and p75, on the nerve endings. This interaction activates interacellular signaling cascades that can modulate the activity of different ion channels in the nerve ending directly, e.g., phosphorylation of ion channels or by transcription whereby the TrkA-NGF complex is retrogradely transported back to the cell body where it can modify the expression of multiple genes, e.g., ion channels. Under normal conditions, noxious stimuli might elicit a single AP, whereas after treatment with NGF or as a consequence of inflammation, the nerve gives rise to multiple APs. This is due to be the result of the reduced threshold of activation of transducer receptors and the increased excitability of the peripheral terminal membrane.

1.7.4 Mechanoinsensitive neurons in cultured mouse DRG neurons

Although we still don not know the molecular basis of mechanotransduction channels in the sensory neurons, mechanically activated currents can be physiologically recorded from cultivated DRG neurons (Drew et al., 2002; Hu and Lewin, 2006). A population of mechanical insensitive DRG neurons has been noted in cultures, about 10% from neurite stimulation and 40% from soma stimulation of the cultivated mice DRG neurons do not respond to mechanical stimulation (Hu and Lewin, 2006). This

group of neurons has the characteristics of typical nociceptors with small cell size and wide AP (Fig. 8). It has been reported from neonatal rat DRG neurons that a subset of capsaicin-sensitive, IB4+ neurons was refractory to mechanical stimulation (Drew et al., 2002). These data raise the possibility that different classes of nociceptors detect mechanical stimuli by using distinct mechanisms. In the present study, we would like to use cultured sensory neurons as a model of peripheral terminal and combine with retrograde labeling, so that cells innervating specific tissues can be examined in order to investigate: 1) whether sensory neurons innervating different tissues display different mechaosensitivity, which may indicate their mechanical detection mechanisms. 2) The effect of proinflammatory neurotrophin (NGF) on mechanosensitive ion channels.

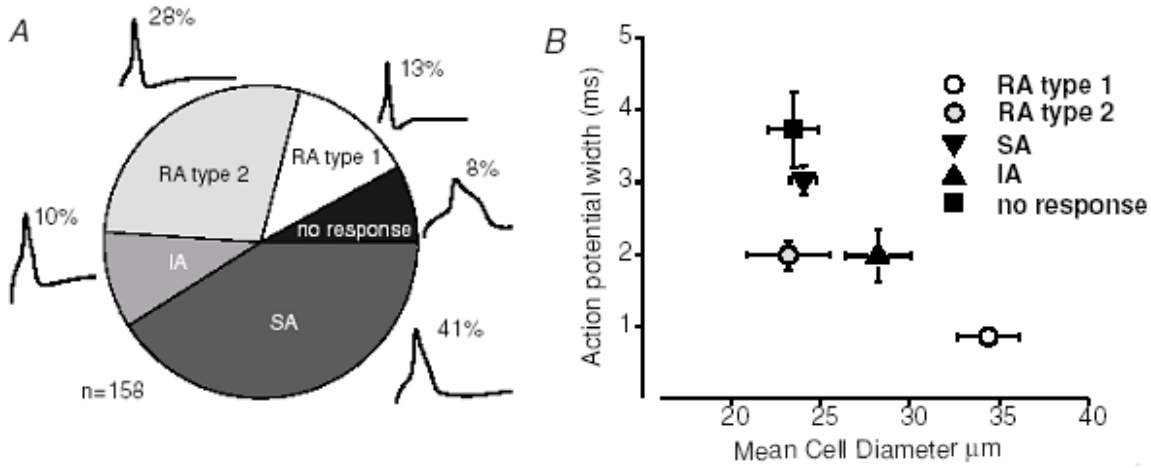

Fig. 8: Distribution of mechnosensitive and insensitive neurons in mechanoreceptors and nociceptors.
A: RA currents appear in both mechanoreceptors and nociceptors, whereas IA and SA currents are mainly distributed in the nociceptors. Notably mechnoinsensitive neurons are exclusively in the nociceptors. Example traces of the measured AP configuration for each cell type are shown together with the individual percentage of the total population adjacent to each pie chart slice. B: The AP width (half-peak duration) is plotted against the soma diameters of RA, SA, IA and mechanoinsensitive cell types. Compared with each type of mechanosensitive neurons, the mechanoinsensitive neurons possess relative small cell diameters and very broad AP widths, which represent the typical nociceptor characteristics (Hu and Lewin, 2006).

1.8 Aims

Early physiological studies from Pacinian corpuscles, crayfish muscle receptor organs and spider sensilla indicated that mechanotransduction is mediated by two processes: First is the generation of receptor current induced by the opening of mechanosensitive ion channels in response to mechanical stimuli. Second is the generation of APs controlled by voltage-gated ion channels opened by an increasing receptor current. We reason that both hitherto unknown proteins involved in mechanosensitive machinery and variety of voltage-gated ion channels play roles in the different sensitivity of heterogeneous mechanoreceptors.

Since the studies on the above sensory organs, no one has managed to record mechanosensitive currents from other mechanoreceptor types. Using whole cell patch-clamp technique, we can directly measure the ionic currents upon mechanical stimulation of the cell soma and neurite. The first aim of this study is to detect the acquisition sequence and maturation changes of RP and AP. Secondly, upon findings of specific expression of a low threshold voltage-gated T-type calcium channel $Ca_v3.2$ in a subtype of DRG neurons, we will use the *in vitro* skin nerve preparation to characterize its function in cutaneous afferents. I will further investigate its role in RP and AP generation using the whole cell patch-clamp technique. Finally, because deep tissue and cutaneous tissue exhibit different mechanosensitivity, we will use a retrograde labeling technique together with the whole cell patch-clamp technique to address which of the two process in mechanotransduction contribute to the tissue specific mechanosensitivity. Moreover, the same approach will be used to elucidate the mechanisms of NGF induced myalgia at the cellular level.

2. Materials and Methods

2.1 Materials

2.1.1 Technical equipment

ADInstruments PowerLab/4s

BDK Laminar flow hood

Leica CM 3000 Cryostat

Digitimer Ltd. NeuroLog Amplifier

EPC-9 amplifier, Heka

Forma Scientific -80°C Freezer

Forma Scientific Steri-Cult 200 Incubator

Gilson Minipuls 3 Peristaltic Pump

Hamamatsu Digital Camera C4742-95

Heraeus Biofuge 13

Heraeus Megafuge 1.0

Hereaus Biofuge 15R

Ikamag Reo Magnetic Stirrer

Julabo MP and Medingen Waterbaths

Kleindieck Nanomotor

Leica DM 500B with Metamorph software

Leica DM RBE Upright Fluorescence Light Microscope

Leica KL 750 Fiber Optic Light Source

Leica MS5 dissecting microscope

Mettler Toledo 320 pH Meter

Sartorius Weigh machine

Scientific Industries Vortex-Genie 2

SPOT-RT-SE18 CCD camera

Tektronix TDS 220 Two Channel Digital Real Time Oscilloscope

WAS02 automated perfusion system

2.1.2 Analytical software

AnalySIS 3.2 Software, Soft Imaging System

Chart v5.2 for Windows, ADI instruments

MetaVue v6.2, Universal Imaging Corp.

Openlab 3.0.4

Fitmaster software, HEKA

Spot advanced image analysis software, Diagnostic Instruments. Inc.

2.1.3 Chemicals and reagents

REAGENT/CHEMICAL	COMPANY
Bovine Serum Albumin (BSA)	Invitrogen Life Technologies
Gelatine	Sigma-Aldrich
Glycogen	Promega Corporation
Horse serum	PAA Laboratories GmbH
Paraformaldehyde	Sigma-Aldrich
Phenol/chloroform/isoamyl alcohol	Roth
poly-L-Lysin	Sigma
Laminin	Invitrogen
Tissue Tek	Sakura Finetek
Triton X-100	Sigma-Aldrich
Goat serum	PAA Laboratories GmbH
Tween-20	Pierce Chemical

2.1.4 Buffers and solutions

BUFFER/SOLUTION	COMPOSITION
10x TBS	0.5M Tris/HCl pH 7.9 1.5M NaCl
4% PFA	4% paraformaldehyde in 0.1M PBS pH 7.4
Patch-clamp buffer - intracellular solution	110 mM KCl 10 mM NaCl 1 mM $MgCl_2$ 1 mM EGTA 10 mM HEPES pH7.3, adjusted with KOH
Patch-clamp buffer - extracellular solution	140 mM NaCl 1 mM $MgCl_2$ 2 mM $CaCl_2$ 4 mM KCl 4 mM glucose 10 mM HEPES pH 7.4, adjusted with NaOH
PBS	PBS Dulbecco w/o Ca^{2+}, Mg^{2+}
Phosphate buffer	0.1M KH_2PO_4 0.1M Na_2HPO_4 x $2H_2O$
SIF (synthetic interstitial fluid)	2mM $CaCl_2$ 5.5mM glucose 10mM Hepes 3.5mM KCl 0.7mM $MgSO_4$ 123mM NaCl 1.5mM NaH_2PO_4 9.5mM Na-gluconate 7.4mM saccharose set to pH 8.4 with 10N NaOH; carbogene used for oxygenation during the experiment will bring it to pH 7.4

2.1.5 Culture media

DRG medium: 10% HS (PAA)

8mg/ml glucose (Gibco)

2mM glutamine (Sigma)

200u/ml penicillin/200µg/ml streptomycin (Sigma)

in D-MEM/F12 (Gibco)

2.1.6 Enzymes and molecular weight markers

ENZYME	COMPANY
Collagenase TypeIV	Sigma
Trypsin	Sigma

2.1.7 Consumables

PRODUCT	COMPANY
15ml and 50ml tubes	Falcon, Greiner
Cell culture dishes	Falcon
Coverslips	Roth
Dissection scissors (14mm and 8mm Blades)	F.S.T
Dissection Forceps (Dumont #5)	F.S.T
Eppendorf tubes	Eppendorf
Glass rod	In house made
Insect needles	F.S.T
Micro spin columns	Amersham
Needles	Sterican
Pipettes	Eppendorf or Biohit
Slides and coverslips	Roth or Menzel-Gläser
Sterile filters	Nalgene, Millipore
Syringes	Braun
Whatman filters	Schleicher & Schuell
Needle hypodermic regular clear 0.5 inch 30 gauge Microlance	Becton Dickinson

2.2 Animals

C57BL/6N mice were obtained from Charles River Breeding Laboratory, Inc., Wilmington, Massachusetts and kept in the animal house of the MDC until they were used for experiments.

For embryonic experiments, overnight mated C57BL/6N mice were used. The morning of the vaginal plug was considered as embryonic day 0.5 (E0.5). Accordingly, embryos obtained 14 days after positive plug check were staged as E14.5, 15 days later as 15.5, etc. Very young embryos (between E10.5and E13.5) were staged by a combination of somite number and maturity of limb development (Kaufman, 1994).

Cav3.2$^{-/-}$ mice are provided by C.C. Chen and K.P. Campbell from the University of Iowa Animal Care Unit and kept in the animal house of the MDC until they were used for experiments. Cav3.2$^{-/-}$ mice were generated by homologous gene targeting. The targeting vector was designed to delete the IS5 region of murine *Cacna1H* gene, which resulted in deletion of exon 6, corresponding to amino acid residues 216 to 267 (Chen et al., 2003).

.

2.3 Methods

2.3.1 Immunocytochemistry

Animals were anesthetized with 2% Rompun / 10% Ketavet and perfused first with 0.1 M PBS then with 4% PFA in 0.1M PBS, pH 7.4 and 4°C. Immediately after perfusion the DRGs were dissected and post-fixed in the perfusion fixative 4% PFA at 4°C for 1 hour. Tissue was immersed in 20% sucrose in 0.1M PBS for 1-3 days until the DRGs sank to the bottom of the sucrose solution. Fresh sucrose solution was replaced daily. DRGs were embedded in Tissue-Tek O.C.T. Compound (Sakura Finetek) and quickly chilled on dry ice. The frozen tissue can be stored at –80 °C for later cutting. DRG sections were cut on a freezing microtome at –20 °C into 14 µm sections.

DRG sections were pre-incubated in 1% serum albumin (BSA) and 0.05% Triton

X-100 in 1x TBS for 2hrs and incubated overnight at RT with primary antibody PGP9.5 (goat anti rabbit polyclonal, UltraClone Ltd, Wellow, UK) diluted 1: 500 in 1xTBS with 0.05% Triton X-100 and 5% normal goat serum. The next day, DRG sections were washed by rinsing slides in excess 1xTBS 3 times, every time 10 minutes and then incubated for 2 hours at room temperature with Cy-3-conjugated secondary antibodies (Jackson Immuno Research, West Grove, PA) diluted 1:250 in 1xTBS containing 0.05% Triton X-100 and 5% normal goat serum. DRG sections were washed 3 times in excess 1xTBS for 10 mins each time and then mounted in Aqua-Polymount. Cy3 light emission was captured with the XF22 filter (excitation 535nm, emission 605DF50, Omega Optical).

2.3.2 Cell culture

Timed pregnant mice were euthanized by placing the animal into a chamber filled with carbon dioxide. For each culture, DRGs from all spinal segments from at least two embryos were dissected, collected in Ca^{2+} and Mg^{2+}-free PBS and treated with trypsin (0.05%, Invitrogen, Karlsruhe, Germany,) for 12-20min at 37°C. DRGs taken from E16.5 and older embryos were additionally treated with collagenase IV (1mg/ml, Sigma-Aldrich) for 15min at 37°C, prior to trypsin-treatment. Digested DRGs were washed twice with growth medium [DMEM-F12 (Invitrogen) supplemented with L-glutamine (2mM, Sigma-Aldrich), Glucose (8mg/ml, Sigma-Aldrich), Penicilin(200U/ml)– Streptomycin(200µg/ml) (both Sigma) and 5% horse serum (PPA)], triturated using fire-polished Pasteur pipettes and plated in a droplet of growth medium on a glass coverslip precoated with 100µg/ml poly-L-lysine (20µg/cm², Sigma-Aldrich) and 20µg/ml laminin (4µg/cm², Invitrogen). To allow neurons to adhere, coverslips were kept for 3-4 hours at 37°C in a humidified 5% incubator before being used for patch-clamp experiments. For overnight cultures, fresh medium was added after 4 hours. When neurotrophic factors were used, they were added at the time of cell plating.

2.3.3 Retrograde labeling

Dextrans are hydrophilic polysaccharides synthesized by *Leuconostoc* bacteria that are characterized by their high molecular weight, good water solubility, low toxicity, and relative inertness. These properties make dextrans effective water-soluble carriers for dyes, indicators, and reactive groups in a wide variety of applications. Moreover, their biologically uncommon α-1,6-poly-glucose linkages are resistant to cleavage by most endogenous cellular glycosidases; therefore dextran conjugates make ideal long-term tracers for live cells. Here we used Alexa fluor 488 conjugated Dextran (D34682, Dextran- Alexa Fluor 488, 3000 MW, anionic, Molecular Probe, Eugene, OR) because of its small molecular weight, which gives good peripheral neuronal processe penetration and fast diffusion. Absorption and fluorescent emission wavelengths of the Alexa Fluor 488 conjugate were 495 and 519 nm, respectively. 4 3ul injections of 2.5% dye were made into each side of the gastrocnemius-soleus muscle. And 5 1ul intradermal injections of 2.5% dye were made at the glabrous hairy border and plantar sulface of the hind paw skin. 3 days after injection the animals were sacrificed and the DRG (L1-S3) dissected out from both sides for cell culture or histochemical analysis (Fig. 9).

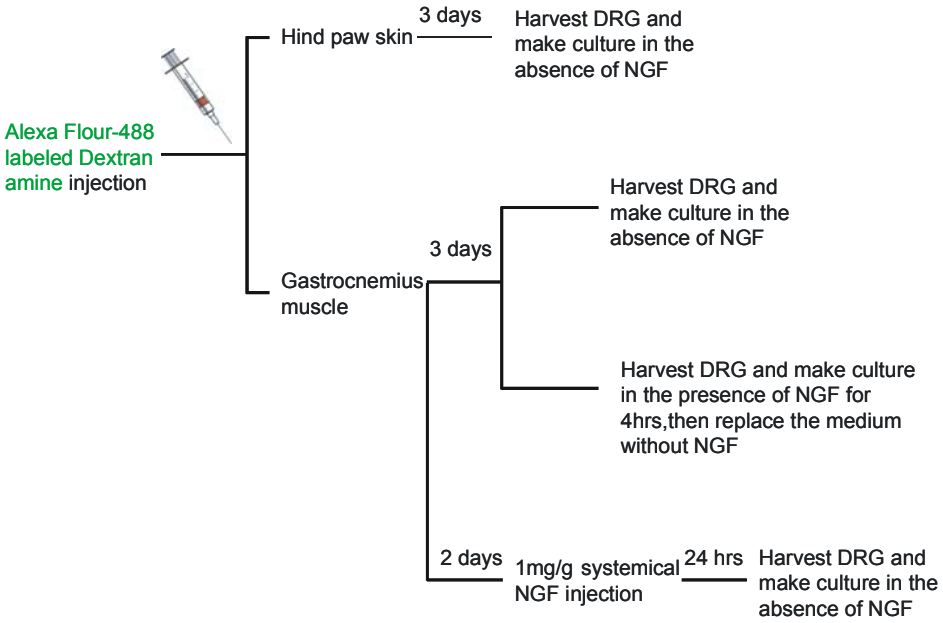

Fig. 9: Experimental flowchart of dye and NGF injection.

2.3.4 The *in vitro* skin nerve preparation

Animals were killed by exposure to a rising concentration of CO_2 gas, a method in accordance with German national guidelines. The hair over the hindlimb was shaved and the skin from the area innervated by the saphenous nerve was removed with the nerve intact. To facilitate oxygenation of the tissue, the skin was placed corium-side up in an organ bath, where it was fixed with insect needles, and superfused with 32°C warm oxygen-saturated synthetic interstitial fluid (SIF) at a flow rate of 10ml/min. The saphenous nerve was pulled through a gap to the recording chamber and laid on top of a small mirror that served as the dissection plate. The aqueous solution in the recording chamber was overlaid by mineral oil in such a way that the interface of the two phases was located just below the surface of the mirror. F.S.T. forceps Dumont #5 were used to desheath the nerve, carefully removing its surrounding epineurium, and to tease small filaments from the nerve so that the activity from single units could be recorded by placing the individual strands of the nerve onto the silver recording electrode installed in the wall of the chamber.

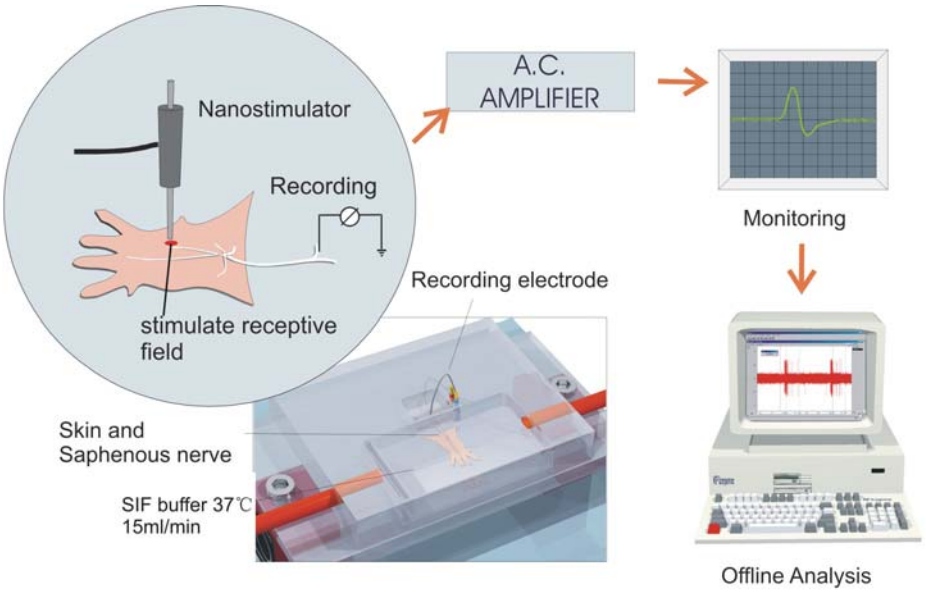

(Modified from Dr. Paul Heppenstall)

Fig. 10: Scheme of the *in vitro* skin-nerve preparation.

Electrophysiological recordings were performed using the NeuroLog™ system from Digitimer Ltd., which included a low-noise differential amplifier for recording from identified units. The recordings were visualized on a connected Tektronix TDS 220

two-channel digital real time oscilloscope, while simultaneously acquired on a PC by a PowerLab/4s converter from AD Instruments. The receptive fields (RF) of individual units were identified by manually probing the corium-side of the skin with a mechanical search stimulus, a blunt-end glass rod (Koltzenburg et al., 1997). Individual units were characterised by the constant shape of the APs they fired in response to stimulation, as the shape of an AP depends on the composition of voltage-gated ion channels expressed by each neuron.

All data were collected and saved to disk using Chart 5 software for the Powerlab system running on a PC (AD Instruments). For each single unit the data were analysed off-line using the Spike histogram extension of Chart software. This software allows calculation of histograms of spikes discriminated on the basis of a constant height and width. The receptive fields of identified fibers were found by probing the skin with a glass rod. In this way up to 90% of thin myelinated or unmyelinated nociceptors and virtually all of the low-threshold mechanoreceptors can be activated (Kress et al., 1992). Once the borders of the receptive field were determined, a teflon-coated silver electrode with a non-insulated tip (∅ <0.5mm) was set on the most sensitive spot of the receptive field, and electrical pulses of constant current in square-wave pulses were used to excite the unit. The stimulus intensity was set at approximately two-times the threshold with a pulse duration of 50-500µsec depending on the afferent under investigation. The latency between the stimulus artefact and the resulting AP was measured. To calculate the conduction velocity the distance between the stimulating and the recording electrode was divided by this latency. Units could thus be grouped into three classes: Aβ-fibers, which are thickly myelinated units, have a conduction velocity faster than 10m/sec, Aδ-fibers are thinly myelinated units with a conduction velocity of 1-10m/sec, and non-myelinated C-fibers conduct slower than 1m/sec (Koltzenburg et al., 1997).

The mechanical threshold was established using calibrated von Frey hairs applied perpendicular to the receptive field. The weakest von Frey filament in this study exerted a bending force of 0.4 mN. After electrical stimuli, by using a probe fixed to a linear stepping motor under computer control (Nanomotor Kleindiek Nanotechnic), a

standard ascending series of displacement stimuli were applied to the receptive field at 30s intervals and each displacement was maintained for 10s (Fig.11). Each stimulus-response function started at threshold as the probe was adjusted so that the first 5 µm displacement evoked spikes. The delay between the start of the mechanical probe movement and the first spike, corrected for the electrical conduction delay of the tested fiber, was designated as the mechanical latency. For further characterizing the rapidly adapting neurons RAM and D-hair, an increasing velocity program was applied at 48 and 96 micra step stages. By changing the time course used to reach certain displacement, the stimulating velocities were varied from 6 µm/s to 3000 µm/s at 48 µm and 96 µm steps.

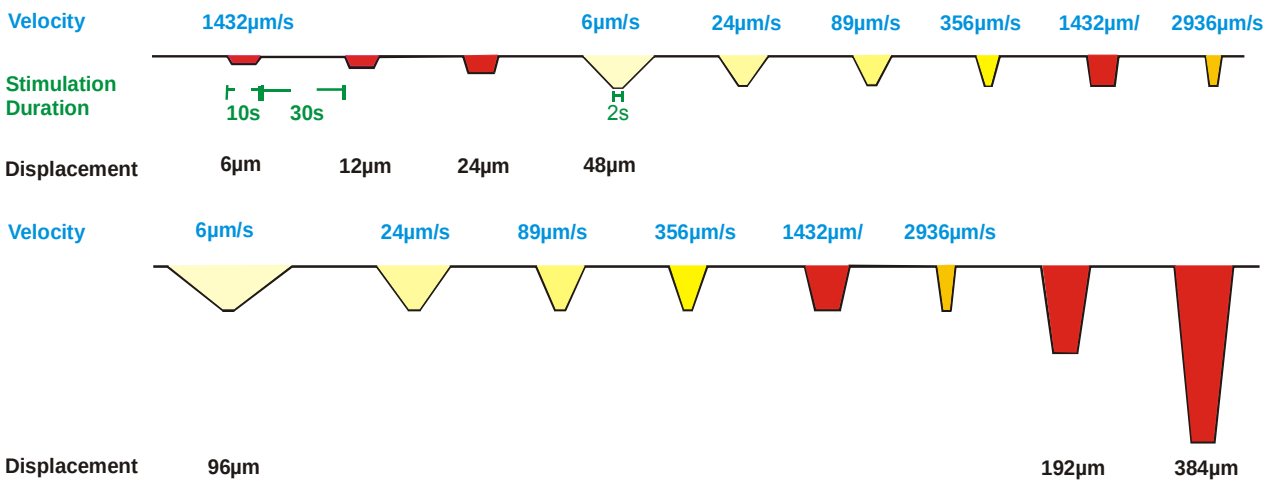

(Milenkovic et al., 2008)

Fig. 11: Velocity stimulus protocol
Rapidly adapting neurons, RAM and D-hair, are stimulated with increasing displacements (noted in black underneath the orange coded stimuli) as well as increasing velocities at 48 µm and 96 µm steps (noted in blue above the yellow coded stimuli). The stimuli at normal velocity are maintained for 10s at certain displacement with 30s interval. The stimulus is maintained for 2s in varing velocity stimuli after it reached the desired displacement.

2.3.5 Cell size measurement

To determine the soma diameters for cell size distribution histograms and of each single recorded neuron, photomicrographs were taken at 10-fold and 40-fold magnification during recording, respectively using an Axiovert 200 microscope (Zeiss),

equipped with a SPOT-RT-SE18 CCD camera (Visitron Systems, Puchheim, Germany). Soma diameters were then calculated from the mean of the longest and the shortest diameters of each cell measured with MetaFluor Imaging software (Molecular Devices), which was calibrated with a stage micrometer (Zeiss).

2.3.6 Patch-clamp experiments

Whole cell patch-clamp recordings were made at room temperature (20-24°C) from cultures prepared as described above. Patch pipettes were pulled (Flaming-Brown puller, Sutter Instruments, Novato, CA, USA) from borosilicate glass capillaries (Hilgenberg, Malsfeld, Germany), filled with a solution consisting of (mM) KCl (110), NaCl (10), MgCl2 (1), EGTA(1) and HEPES (10), adjusted to pH 7.3 with KOH and had tip resistances of 6-8MΩ. The bathing solution contained (mM) NaCl (140), KCl (4), CaCl2 (2), MgCl2 (1), glucose (4), HEPES (10), adjusted to pH 7.4 with NaOH. Drugs were applied with a gravity driven multibarrel perfusion system (WAS-02). All recordings were made using an EPC-9 amplifier (HEKA, Lambrecht, Germany) in combination with Patchmaster© and Fitmaster© software (HEKA). Pipette and membrane capacitance were compensated using the auto function of Patchmaster and series resistance was compensated by 70% to minimize voltage errors. APs were evoked by repetitive 80ms current injections increasing from 80pA to 1040pA with increments of 80pA. The second AP evoked with this pulse protocol was used for analysis. Mechanically activated currents were recorded as previously described (Hu and Lewin, 2006; Wetzel et al., 2007). Briefly, neurons were clamped to -60mV, stimulated mechanically with a fire-polished glass pipette (tip diameter 2-3µm) that was driven by a piezo based micromanipulator called nanomotor© (MM3A, Kleindiek Nanotechnik, Reutlingen, Germany) and the evoked whole cell currents were recorded with a sampling frequency of 200 kHz. The stimulation probe was positioned at an angle of 45° to the surface of the dish and moved with a velocity of 4.3µm/ms. In contrast to our previous work (Hu and Lewin, 2006; Wetzel et al., 2007), here only the cell soma was stimulated. Stimulation of neurites was not possible, as we have mostly used embryonic acutely dissociated DRG neurons, which at the time of recording

have few neurites and in addition these neurites are very thin compared to those found in adult neurons. Currents were fitted with single exponential functions and classified as RA-, IA- and SA type currents according to their inactivation time constant (Hu and Lewin, 2006). Electrophysiological experiments on acutely dissociated DRG neurons were carried out between 3 and 8 hours after plating.

2.3.6 Data and statistical analyses

All APs were counted in a time period of 10s after the onset of a mechanical stimulus because this time window contained all spikes during the rise time, the plateau and the discharge during the release of the stimulus. Further quantitative analysis of the recorded APs was carried out by repeated measures ANOVA tests with Graphpad Prism 4 software by Graphpad software Inc. All values are presented as means ± S.E.M. A level of 5% was taken as evidence of statistical significance.

3.Results

3.1 Developmental acquisition of electrical excitability and mechanosensitivity in mouse DRG neurons

3.1.1 Maturation of electrical properties in diverse DRG neurons

Mechanosensitive ion channels are located on the nerve terminals. If we apply a mechanical stimulus on the peripheral nerve terminal, the opening of the mechanosensitive ion channels will induce a mechanical evoked RP. As stimulus strength increases, the RP also increases until it reaches the activation threshold for voltage-gated ion channels and elicits AP generation in DRG neurons (Fig. 4). The train of APs is conveyed to the spinal cord and then to our brain, allowing us to form sensory experiences. Primary sensory neurons of the DRG have diverse but characteristic physiological properties. These properties have been shown to be associated closely with the types of peripheral receptor innervated in the periphery. For example, mechanoreceptors have narrow somal spikes without inflections (Koerber et al., 1988; Rose et al., 1986), whereas afferent fibers innervating nociceptors in the periphery always have broad somal spikes with inflections on the falling phase of the spikes. The presence or absence of such a hump is of some significance, because it is a reliable indicator of physiological function for myelinated afferents. Low-threshold mechanoreceptors (LTMRs) with relatively large soma sizes and thickly myelinated axons that respond to hair movement, gentle pressure, or vibration do not have a hump, whereas, afferents responding to high-intensity, potentially noxious stimulation of the skin [high-threshold mechanoreceptors (HTMRs)] are always found to have an inflected spike (Koerber et al., 1988; Ritter and Mendell, 1992; Rose et al., 1986)

Previous studies indicated that mechanical responses cannot be elicited before embryonic day 17 in rat, whereas electrical responses can already be evoked at E16

(Fitzgerald, 1987b). To determine whether electrical responses or mechanical responses appear first in the mouse and when the diversification of electrical properties occurs, we dissected DRGs from E11.5 embryos shortly before the target innervation, since the nerve fibers extend from the DRG into the pre-forelimb mesenchyme at E11.5 and reach the distal margin of the forelimb by E13.5 in mouse (Berg and Farel, 2000). We made whole cell patch-clamp recordings from cultivated sensory neurons thereafter until birth between 3-8 hours after plating in the absence of all neurotrophins to ensure that the electrophysiological properties measured best reflect those found *in vivo*. We routinely measured the voltage-gated currents in the recorded cells using a standard voltage step protocols and evoked APs in current-clamp recordings.

From E11.5 on, along with the whole developmental stages until birth, 3 types of APs were observed. At the earliest stage E11.5, the majority of neurons (83%, 5/6 tested neurons) exhibited an immature AP, which lacked a rapid upstroke and failed to repolarize normally (Fig. 12A, black trace). Correspondingly, this immature AP can be reconfirmed by the lack of apparent burst of inward sodium current in response to stepped voltage depolarization (Fig. 12C, black trace) and explained by insufficient density of voltage-gated sodium channels (Na_v). Only 17% of neurons (1/6 tested neurons) at this stage fired normal APs in response to current injection (Fig. 12A, blue trace). This was characteristic of a mechanoreceptor, relatively narrow and humpless. At the time of E13.5 a new population of neurons appeared and accounted for 69% (18/26) of tested cells. They exhibited an obvious nociceptive hump on the falling phase of the AP spike and a relatively broad half-peak duration (Fig. 12A, red trace). The determination of the presence of an inflection was made by calculating and plotting the first derivative (dV/dt) of the trace (Fig. 12B). The latter two populations with mature APs possessed abrupt Na_v current shoot at the average voltage step of –32.39±1.04 mV (Fig. 12C, blue and red traces). Mean voltage-gated Na^+ current amplitudes measured at holding potentials of –20mV at stages E11.5 and E13.5 in immature neurons (0.611±0.11 nA) were significantly smaller than in neurons with

mature APs (1.66±0.13 nA; *P*<0.0001, t-test, n=9,23; Fig. 12D).

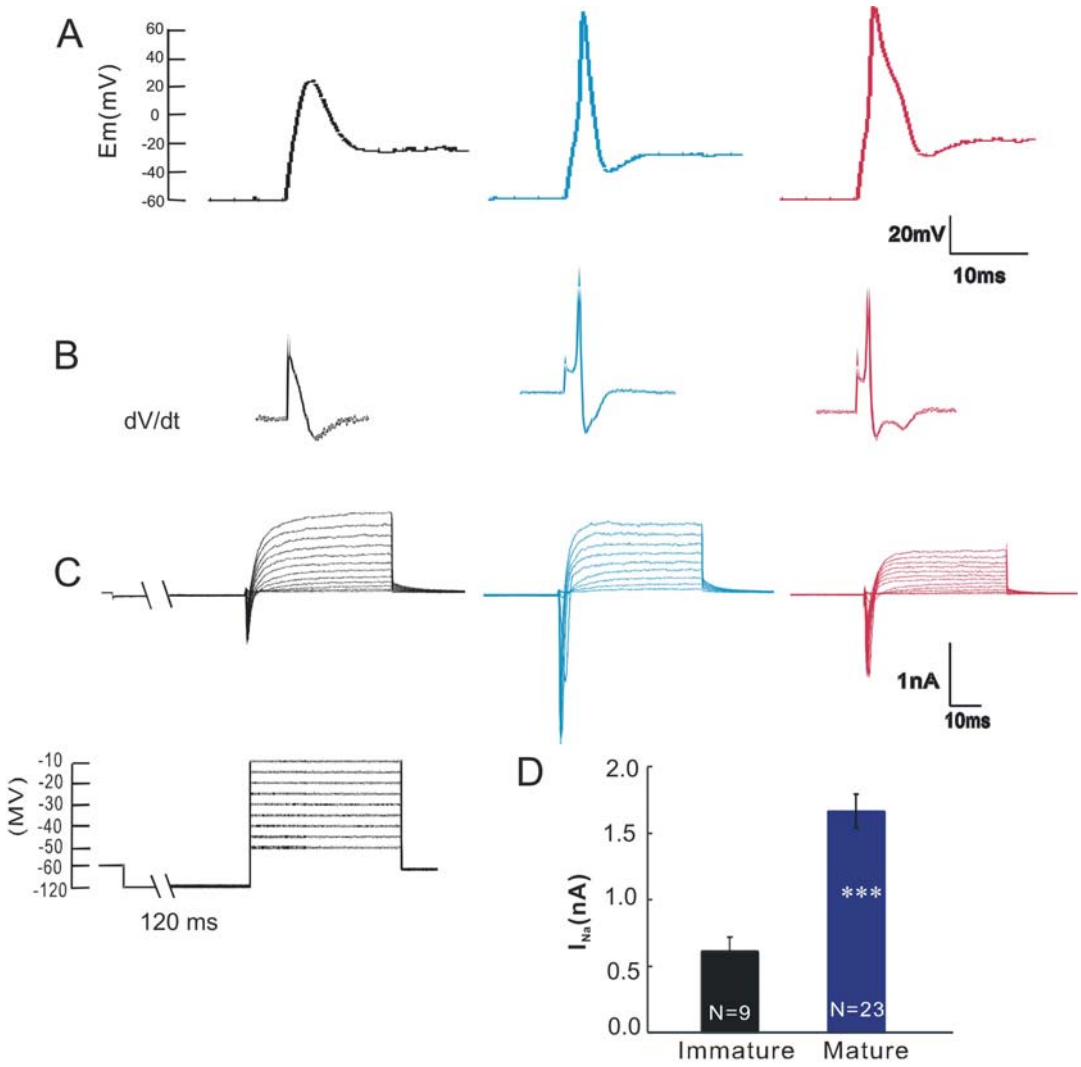

Fig. 12: Emergence and maturation of APs.
A: Example traces of immature (black trace) and mature APs (blue: mechanoreceptor and red: nociceptor) evoked in response to current injection. **B:** The presence of a hump on the falling phase was determined by plotting the first derivative, which for humped spikes exhibits two relative minima (dV/dt). **C:** Corresponding Na_v currents evoked in neurons with the immature and mature APs with the indicated voltage-step protocol. Smaller Na_v current was observed in neurons with immature APs. **D:** Bar graph summarized the peak inward Na_v current measured at –20 mV. (∗, *P*<0.05; ∗∗, *P* <0.01; ∗∗∗, *P* <0.001, unpaired t-test; Bars represent means±SEM; numbers of recorded neurons were indicated at the bottom of each bar)

From E11.5 the proportion of neurons with immature APs decreased from 83% to 15%

by E13.5 (*P*=0,0008, χ^2) and vanished by E14.5 (Fig. 13). Within the same time frame (E11.5-14.5), a new population of neurons that exhibited APs with a hump on the falling phase of the spikes appeared and increased to 69% of the total population at E13.5 (*P*=0,002, χ^2) and kept increasing to 89% at E14.5, then fluctuated between 70% to 90% with each day after E14.5. The proportion of this type of neurons did not have a dramatic change between consecutive stages until birth (*P*>0.05, χ^2). Neurons with narrow APs without hump already existed at E11.5 (17% of total) and the proportion fluctuated around 17% without major changes at later stages.

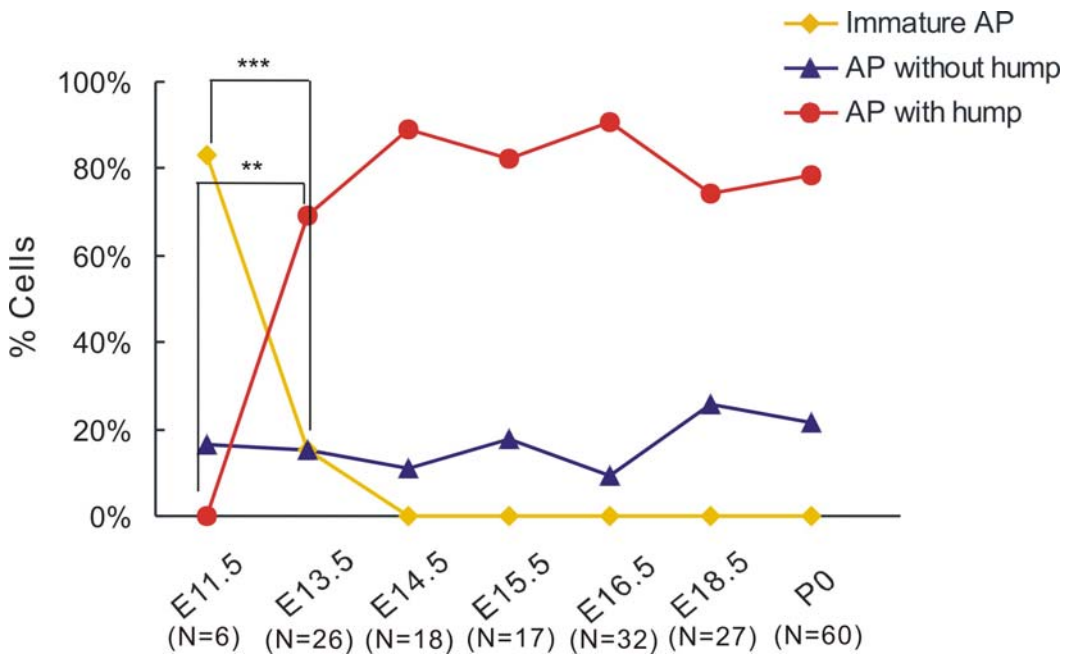

Fig. 13: Developmental wave of mechanoreceptors and nociceptors.
The proportions of neurons with immature APs (yellow squares), mechanoreceptive (blue triangles) and putative nociceptive APs (red circles) are plotted as a function of development. Mechanoreceptive neurons with narrow APs (no hump) have existed from E11.5 on and their proportions remain stable at around 17% during developmental stages. The appearance of neurons with nociceptive APs starts later at E13.5 and is accompanied by the disappearance of neurons with immature APs. Their proportions fluctuate between 70% and 90% after E14.5. (∗, *P*<0.05; ∗∗, *P* <0.01; ∗∗∗, *P* <0.001; χ^2; Numbers of recorded neurons are indicated beside each stage)

From E11.5, the stage, when the first mechanoreceptors gained electrical properties, until birth, the mean AP amplitudes of neurons lacking humps fluctuated between

E13.5 and E15.5, but stablized at around 70 mV from E16.5 onward (Fig. 14A). No dramatic changes in AP amplitudes were observed until birth. In contrast, nociceptors characterized by humped APs showed increasing AP amplitudes during development after their birth at E13.5 and they were significantly bigger at E15.5 (77.55±3.16 mV) than at E13.5 (62.11±3.33mV; $P<0.05$, one-way ANOVA, Post Bonferroni test) and remained stable afterwards at about 80 mV until birth. From stage E13.5 when both mechanoreceptive and nociceptive APs had differentiated, their half-peak durations were gradually fine tuned. At the beginning, half-peak durations were not significantly different in both types until E15.5 (Fig. 14B). At E16.5 the half-peak durations of APs with or without humps appeared to be different from each other, although this difference did not reach statistical significance at this stage. Until E18 and P0 half-peak durations of both types are clearly segregated and the narrow ones (about 1ms) were always in APs without a hump, whereas the broad ones had humped APs. If we compare the changes of half-peak durations within APs with or without humps respectively, we could observe a dramatic drop in AP width at E16.5 (1.18±0.08 ms) compared to E13.5 (3.30±0.85 ms; $P<0.05$, one-way ANOVA, Post Bonferroni test) in narrow spiked APs lacking a hump. The widths of APs lacking humps stayed around 1ms until birth. The humped AP width fluctuated between E13.5 and E15.5, but stabilized around 2.5 ms from E15.5 on. Humped AP widths at birth P0 (2.93±0.13 ms) were much wider than those measured at E14.5 (1.77±0.12 ms; $P<0.001$, one-way ANOVA, Post Bonferroni test).

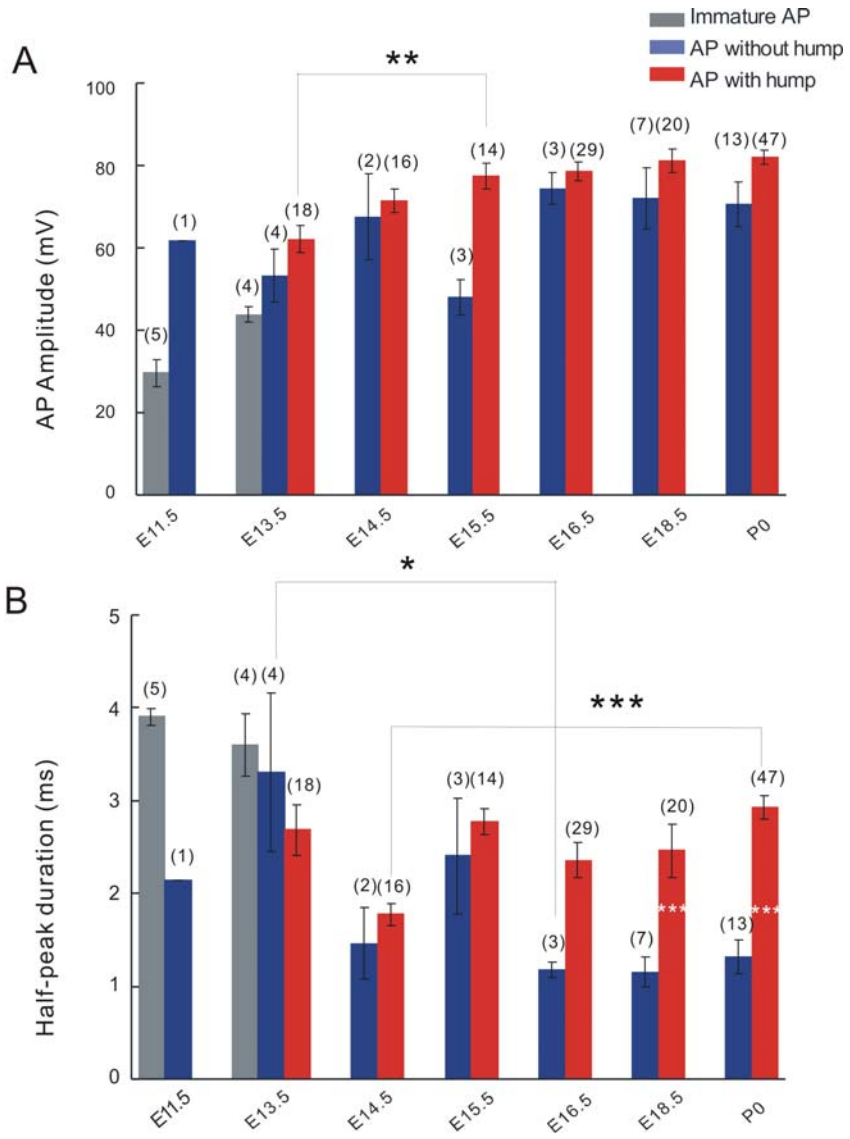

Fig. 14: Developmental changes of amplitude and half-peak duration of APs.
A: Summary of the developmental changes in the mean AP amplitudes in APs with or without humps. APs lacking humps did not show dramatic changes in amplitudes until birth, whereas humped APs showed increasing AP amplitudes from E13.5 to E15.5 and stayed stable until birth. **B:** Summary of the developmental changes in the mean AP half-peak durations in APs with or without humps. In general, APs without humps showed decreasing half-peak durations during development. After the fluctuation between E13.5 and E15.5, the significant reduction in AP width was noticed between E13.5 and E16.5. In contrast, humped APs showed increasing half-peak durations during development. AP width at P0 was much bigger than that at E14.5. The significant differences in AP amplitudes and half-peak durations during developmental stages were indicated with black asterisks (∗, P<0.05; ∗∗, P <0.01; ∗∗∗, P <0.001; one-way ANOVA, Post Bonferroni test; Bars represent means±SEM; numbers of recorded neurons are indicated above each bar). A final segregation in width of APs with or without humps at E18.5 and P0. The significant differences in widths of APs with or without humps occurred at E18.5 and P0 are indicated with white asterisks (∗,

P<0.05; **, *P* <0.01; ***, *P* <0.001; Paired T-test)

The late increase in AP-width in nociceptors also coincided with changes in electrical excitability. A standard 80 s duration current injection never evoked more than one AP in nociceptors taken from embryos younger than E16.5. In contrast, at E18.5 neurons repetitive firing emerged (19% of total) and after P0 increasing numbers of neurons (35% at P0 and 40% at P7) showed repetitive firing to current injections (Fig. 15 A, B). Repetitively firing neurons also had relatively wider APs (2.73±0.17ms) than those firing a single AP (2.34±0.14ms), but the difference was not significant. (Fig. 15C; *P* >0.05, unpaired T-test).

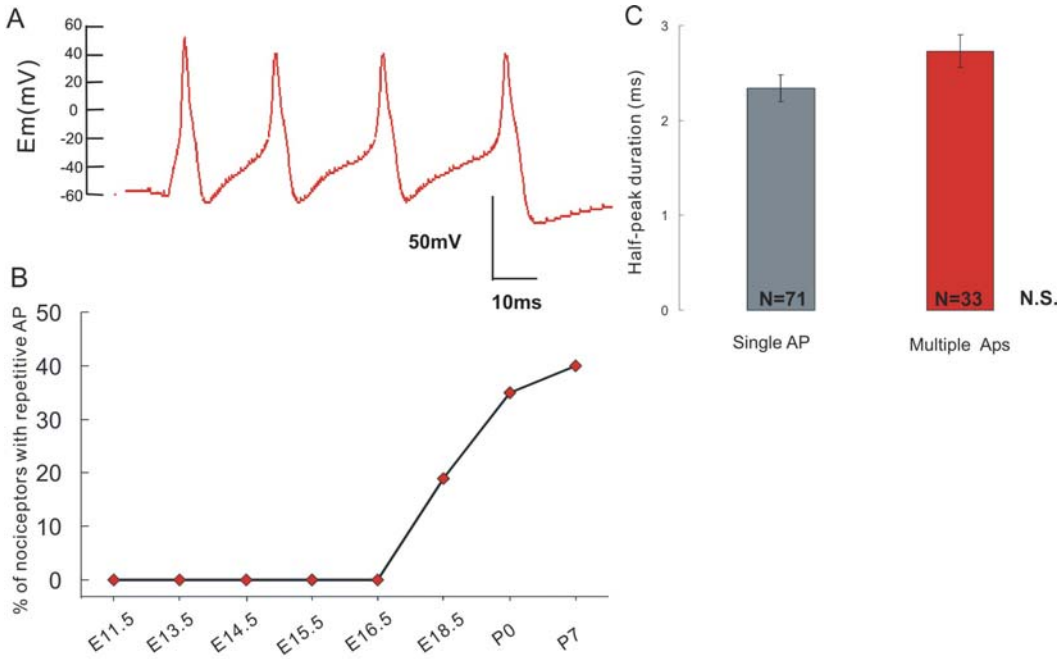

Fig. 15: Emergence of repetitive firing in nociceptors.
A: Example trace of AP trains evoked with a 160pA/80ms current injection at E18.5. **B:** The proportion of nociceptors with repetitive firing is plotted as a function of development. Neurons, which could fire repetitively, first appeared at E 18.5 with19%. The proportion of repetitively firing neurons increased to 35% at P0 and reached 40% one week later. **C:** Neurons with AP trains showed relatively wider width than those with single APs in half-peak duration. Half-peak durations are summarized from E18.5 to P14. (Bars represent means±SEM; numbers of recorded neurons are indicated at the bottom of each bar)

3.1.2 Acquisition and maturation of mechanosensitivity in sensory neurons

Since the first mechanically activated current in cultured rat DRG was reported by McCarter and colleagues (McCarter et al., 1999), we and others have shown the presence of three types of mechanically activated currents in both adult rat and mouse DRG neurons by either stimulating their somata or neurites. These currents can readily be distinguished by their inactivation kinetics (Fig. 16A) and are classified into rapidly adapting (RA type), intermediately adapting (IA type) and slowly adapting (SA type) currents (Drew et al., 2002; Hu and Lewin, 2006). RAs were more frequently found in larger sensory neurons with narrow APs characteristic of mechanoreceptors, whereas SAs and IAs were found more predominantly in nociceptors. We recorded mechanosensitive currents by stimulating the soma with very small ($\geqslant$ 550nm) and rapidly applied (~4μm/ms) displacement stimuli. At E11.5, none of the neurons (0/6) tested responded with inward current to mechanical stimulation (Fig. 16B). Just two days later, at E13.5 two types of mechanically activated current appeared at the same time, namely RA and IA (Fig. 16B). The proportion of responding neurons at E13.5 was 67% (14/21) , which was much higher than that at E11.5 (P<0.01, χ^2). The proportion of responding neurons stayed above 50% during the later tested embryonic stages without dramatic changes at the consecutive stages (P>0.05, χ^2) and reached 85% (50/59) at birth. Neurons with RA and IA type currents appeared at E13.5 with the proportion of 52% (11/21) and 14% (3/21), respectively, whereas neurons with SA type current only appeared from E16.5 on with very low proportion of 7% (2/30). After their appearance, neurons with RA type current fluctuated between 41% and 65% without significant changes in proportion for consecutive developmental stages (Fig. 16B). Neurons with IA type current showed a constant low incidence from E13.5 until birth, which was less than 15% at all stages. In spite of an increasing proportion from E16.5 (7%) to P0 (15%), SA type neurons always exhibited in a very low percentage.

At early stages only the large neurons possessed mechanosensitive currents. We used 14 μm as a criterion to distinguish the large and small neurons and checked their mechanical response properties, respectively. A much higher proportion (76%) of the large neurons (>14μm) responded to mechanical stimuli at E13.5 than the small neurons (<14μm)(25%, P<0.05, χ^2; Fig. 16C), but the proportion of responding neurons in the large and small diameter range did not show differences during developmental stages at E15.5, E16.5, E18.5 and P0. The proportion of mechanosensitive neurons in large neurons resembled those of all tested neurons at all developmental stages. But the proportion of small neurons with mechanosensitivity gradually increased from 25% (1/4) at E13.5 to 100% (3/3) at P0. Due to the sampling bias, only E13.5, E15.5, E16.5, E18.5and P0 had small neurons.

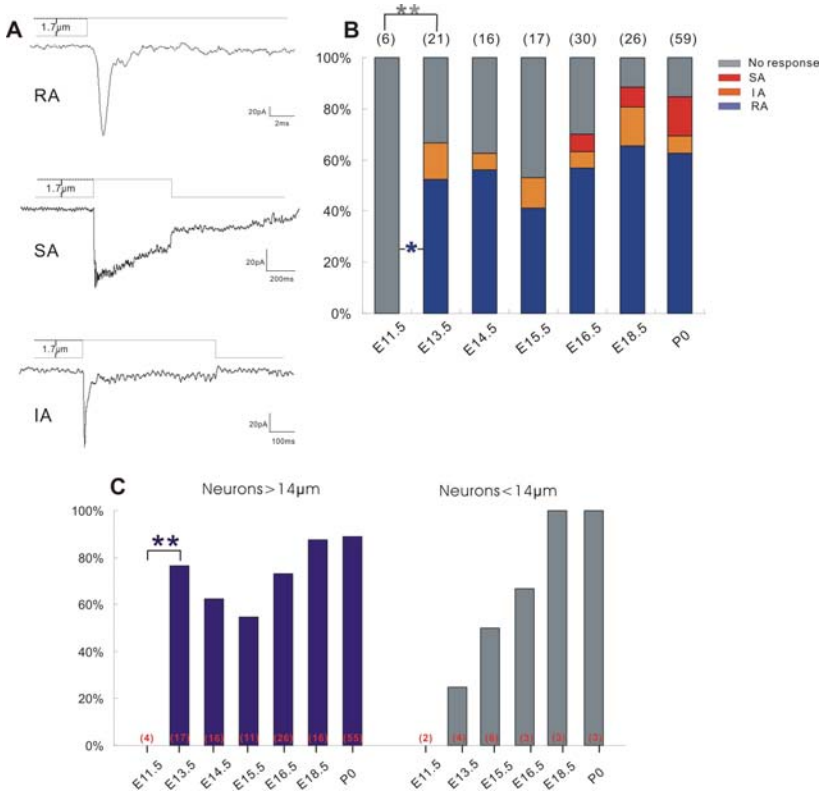

Fig. 16: Sequential acquisition of mechanosensitivity in sensory neurons.
A: Example traces of 3 types of mechanosensitive currents recorded from embryonic sensory neurons by stimulating cell soma. Mechanical thresholds are indicated above each current trace. The observed mechanosensitive currents are classified according to their inactivation time constant as RA (<5ms), IA (5-50ms) and SA (>50ms) (fit with single exponential function). **B:** Stacked histogram shows proportions of sensory

neurons with different mechanosensitive currents at different developmental stages. Significant change in responding neurons is noticed between E11.5 and E13.5 (gray asterisk). And a significant change in the incidence of RA type currents is observed between E11.5 and E13.5 (blue asterisk). **C:** the proportion of responding neurons are plotted for large neurons (>14μm, dark blue) and small neurons (<14μm, gray), respectively. The proportion of responding neurons drastically increased at E13.5 in large neurons (dark blue asterisk) (∗, P<0.05; ∗∗, P <0.01; ∗∗∗, P <0.001; χ^2; Numbers of recorded neurons are indicated above or at bottom of the bar).

We examined the distribution of the current types in more detail. Large neurons had two types of mechanosensitive current at E13.5 with proportions of 59% (RA) and 18% (IA) respectively. The proportion of neurons with RA type current stayed above 45% without dramatic changes during whole embryonic stages and increased to 67% at birth (Fig.17A). Neurons with IA type current were rare among all tested stages and their proportions did not change dramatically at each measured stage until birth (P>0.05, χ^2). The proportion of large neurons with SA currents was always lower than 16% from E16.5 onwards and remained stable until birth. For small neurons (<14μm), only the RA type current appeared at E13.5 with a very low percentage of 25% (1/4), but showed a gradually increasing proportion until birth (100%, 3/3). The neurons with IA type current only appeared at E15.5 with a proportion of 17%. No SA type current was observed, but this probably due to the relatively small sample (n≤6 at all tested stages).

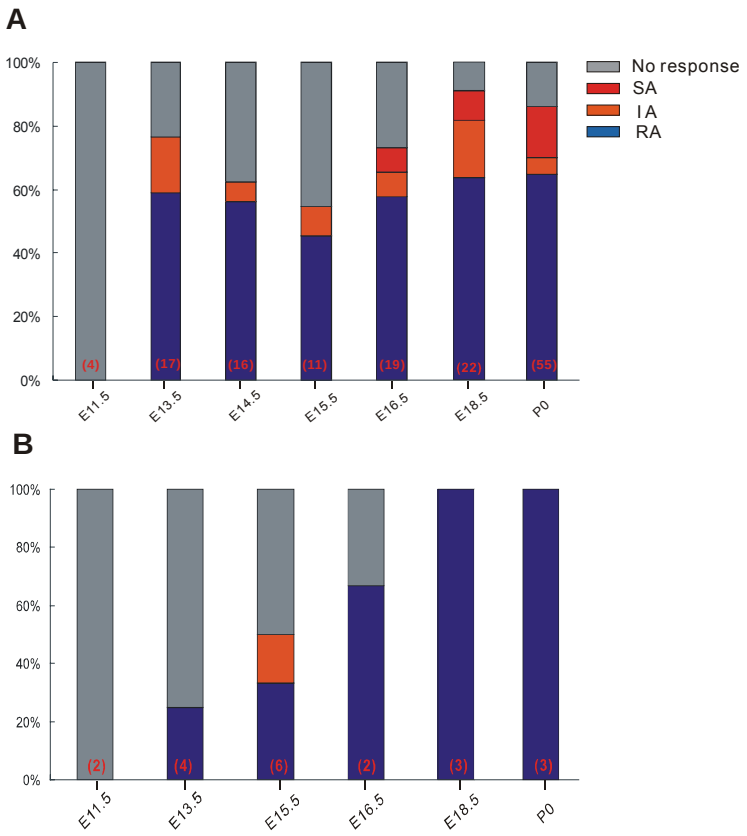

Fig. 17: Mechanosensitivity changes in large and small sensory neurons during development.
A: Stacked histogram shows proportions of large neurons (>14µm) with different mechanosensitive currents at different developmental stages. **B:** Stacked histogram shows proportions of small neurons (<14µm) with different mechanosensitive currents at different developmental stages. (Numbers of recorded neurons are indicated at bottom of the bar).

If we plotted the mechanical current types in large and small neurons (Fig. 18), we noticed that at E13.5 the mean diameter of RA possessing neurons (16.34±0.62 µm, N=11) was higher than that of the non-responsive neurons (14.74±0.59 µm, N=7), although this difference did not reach significance (*P*>0.05, unpaired t-test). Interestingly, in later tested embryonic stages the mean cell sizes of RA type neurons (**E14.5**: 18.89±0.40 µm, N=8; **E15.5**: 15.31±0.81µm, N=8; **E16.5**: 19.11±0.75µm, N=17; **E18.5**: 17.92.39±0.95µm, N=17) were in general bigger than that of non-responsive neurons (**E14.5**: 16.57±0.67µm, N=6; **E15.5:** 16.16±1.00µm, N=8; **E16.5**: 15.58±0.41µm, N=8; **E18.5:** 15.47±1.34µm, N=3) (E14.5: *P*<0.01, E16.5:

P<0.01; unpaired t-test), meaning that RA type neurons were restricted to larger neurons, whereas non-responsive neurons were restricted in the small nociceptive neurons during the embryonic stages. However, this size difference between RA type (P0: 19.35±0.76μm, N=37) and non-responsive neurons (P0: 19.17±0.78μm, N=9) was eliminated by P0, probably because some small neurons also developed RA type currents (P0: *P*>0.05, unpaired t-test). With regards to SA type neurons, the SA type current first appeared in relatively large neurons at E16.5 and E18.5 (E16.5: 17.87± 0.86μm, N=2; E18.5: 24.09 ± 2.05μm, N=2) compared to the non-responsive neurons (E16.5: 15.58± 0.41μm, N=8; E18.5: 15.47±1.34μm, N=3) (E16.5: *P*<0.05; E18.5: *P*<0.05, unpaired t-test). At birth, the mean cell size of SA type neurons (P0: 18.40±1.07μm, N=9) was no different to that of the non-responsive neurons (P0: 19.17±0.78μm, N=9), which may indicate the appearance of the SA type current in small neurons. IA type currents were present in all the developmental stages after E13.5 with very low percentage in neurons of no particular size.

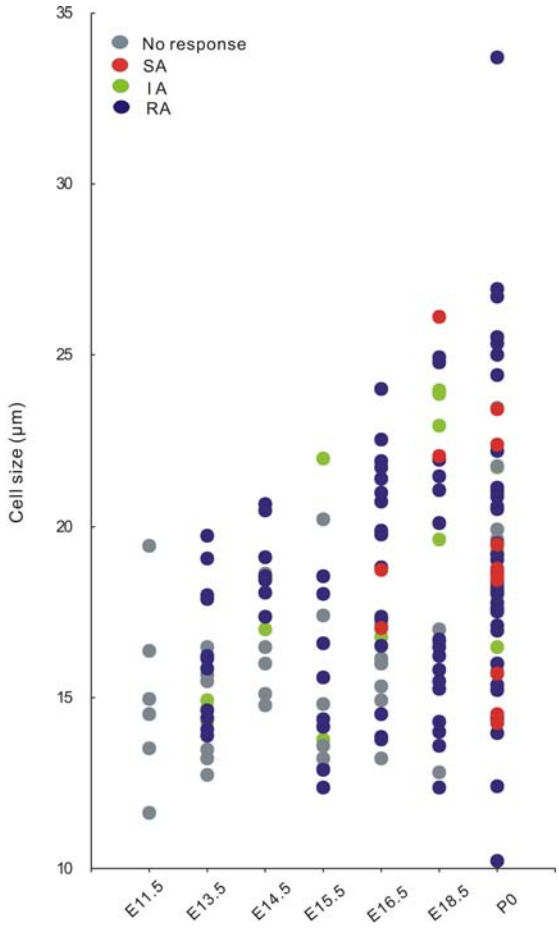

Fig. 18: Distribution of mechanosensitive currents in different cell sizes during development.
Different types of mechanosensitive current were plotted against cell size as a function of developmental stages. RA (blue dots) and IA type (green dots) currents first appeared at E13.5. And RA type currents were initially confined to relatively large neurons before E15.5. SA type currents (red dots) appeared from E16.5 onwards and were rare for all the tested stages. At birth, RA and SA type currents became widely distributed in both large and small neurons.

The kinetics of different mechanosensitive currents are summarized in table.1. In regard of the current amplitude, latency, activation time constant and inactivation time constant, RA type currents in embryonic stages showed much faster inactivation time constants than after birth (P<0.01, unpaired t-test) (Table.1). The amplitude of the SA current at P0 was significantly bigger than that during embryonic stages (P<0.05, unpaired t-test) (Table.1).

	E13.5-E15.5		E16.5-E18.5	P0		
	RA *(n=26)*	IA *(n=6)*	SA *(n=4)*	RA *(n=35)*	IA *(n=4)*	SA *(n=9)*
Current Amplitude (pA)	87.05±12.84	135.67±42.33	80.34±17.28	115.24±18.62	125.89±57.97	232.13±43.16 *
Latency (ms)	0.56±0.04	0.63±0.17	0.41±0.06	0.66±0.06	1.84±1.06	0.81±0.21
τ_{act} **(ms)**	0.58±0.08	0.63±0.06	0.87±0.08	0.62±0.08	1.13±0.42	0.64±0.14
τ_{inact} **(ms)**	0.66±0.07	12.22±3.05	896.61±801.2	1.26±0.19 **	8.20±0.87	215.39±72.32

Table. 1: Comparison of kinetics of mechanosensitive currents during embryonic stages and at birth
Kinetic changes were only observed in the inactivation time constant of RA currents and the current amplitude of SA currents. Other parameters of these two types of mechanosensitive currents were comparable before and after birth. The kinetics and amplitude of the IA current remained the same during embryonic stages and at birth. (Kinetic changes before and after birth were indicated on the corresponding item; *, $P<0.05$; **, $P<0.01$; ***, $P<0.001$, unpaired t-test)

3.1.3 Summary

The two crucial processes involved in mechano-electrical transduction, the electrical excitability and mechanosensitivity of embryonic mouse DRG neurons were examined from E11.5 to P0 with whole cell patch-clamp technique. The electrical excitability is acquired by DRG neurons as early as E11.5. The first APs to appear were characteristic of mechanoreceptors (narrow and no hump). The APs with characteristic of nociceptors (wide and hump) reached significant numbers only from E13.5 onwards. The electrical properties characterized by AP amplitude and half-peak duration were also fine tuned during development in both mechanoreceptors and nociceptors. The AP amplitudes of mechanoreceptors were relatively stable during all tested developmental stages, whereas that of nociceptors showed a dramatic increase between E13.5 and E15.5. The general tendency of half-peak duration was to get wider in nociceptors and to get narrower in mechanoreceptors during development. The phenomenon of repetitive AP firing in

small nociceptors was observed from E18.5 on and exhibited an increasing incidence in the first two postnatal weeks.

On the basis of these findings and classification of three types of mechanosensitve currents in adult mouse DRG neuron culture, the mechnanosensitive currents in embryonic DRG neurons first appeared at E13.5 with the RA type being major form and lower incidence of IA type mechanosensitive currents. SA type mechnaosensitive currents appeared with a very low incidence at E16.5 and exhibited an increasing proportion only at birth.

3.2 Role of $Ca_V3.2$ in sensory mechanotransduction

In the previous chapter, the mechanotransduction has been demonstrated to be two developmentally segregated transduction processes. Based on a *C.elegans* study (Ernstrom and Chalfie, 2002), homology screens in mammals have implied that ASCI2, ASCI3 and SLP3 might be components of the mechanotransducer in mammalian mature skin mechanoreceptors (Price et al., 2000; Price et al., 2001; Wetzel et al., 2007). In addition, our lab has shown that the T-type calcium channel $Ca_V3.2$ was exclusively expressed by a subtype of DRG neurons, D-hair receptors, by using subtracted cDNA library (Shin et al., 2003). However, other labs have shown expression of $Ca_V3.2$ in other types of DRG neurons and its functional involvement in nociception with pharmacological and behaviour experiments (Choi et al., 2007; Nelson et al., 2005; Todorovic et al., 2001). In this part of the study, the potential function of $Ca_V3.2$ in the two stages of mechanotransduction will be addressed in $Ca_V3.2$ null mutant mice by using *in vitro* skin nerve preparation and whole cell patch-clamp technique.

3.2.1 The general properties of different types of afferent fibers

To learn whether $Ca_V3.2$ has a role in somatic sensory mechanotransduction, we used $Ca_V3.2$ null mutant mice (Chen et al., 2003) and examined the mechanosensory properties of single sensory neurons of the saphenous nerve using an *in vitro* skin nerve preparation. Myelinated and unmyelinated single fibres were classified by their conduction velocity (CV), von Frey mechanical sensitivity, and mechanical stimulus response function. Thickly myelinated Aβ-fibres (CV>10m/s) can be subdivided into RAM and SAM low-threshold mechanoreceptors, which respond to light touch. Their von Frey thresholds are normally lower than 3.3 mN. Thinly myelinated Aδ-fibers have conduction velocities between 1-10m/s, but the two subtypes of Aδ-fibers display dramatically different mechanical sensitivity and response properties. One type, D-hair receptors are the most sensitive mechanoreceptor. Their von Frey thresholds

are always 0.4mN and probably lower. In addition D-hair receptors have large receptor fields and show rapidly adapting responses at the onset and offset of a constant displacement stimuli. In contrast, AMs respond to high intensity mechanical stimuli, do not respond to the movement phase of the stimuli, and adapt slowly to constantly applied stimuli. C-fibers (CV<1m/s) possess unmyelinated axons and respond to noxious mechanical stimuli. The proportion, conduction velocity and von Frey threshold of each type of afferent fiber recorded in the present study are summarized below (Table. 2). The ratios of RAM and SAM in Aβ-fibers in both genotypes were in line with that from previous studies, where it was found that RAM and SAM accounted for 45% and 55% of Aβ-fibers, respectively. But the ratio of AM to D-hair was lower in contrast to a previous study that AM was 65% and D-hair was 35% of total Aδ-fibers. This was because we over sampled D-hair receptors. We also had reason to believe that they might be affected (Koltzenburg et al., 1997).

	Wild type			Cav 3.2-/-		
Receptor Type	% Total	CV m/s	vFT (mN)	% Total	CV m/s	vFT (mN)
Aβ-Fibers						
RAM	44.4% (20/45)	13.7±0.8	0.4 (0.4-2)	48.7% (18/37)	14.7±0.8	0.4 (0.4-2)
SAM	55.6% 25/45)	12.6±0.4	1 (0.4-6.3)	51.4% (19/37)	13.8±0.7	1 (0.4-3.3)
Aδ-Fibers						
AM	53.3% (16/56)	5.7±0.6	3.3 (0.4-6.3)	37.5% (18/48)	4.4±0.6	3.25 (1-3.3)
D-hair	46.7% (40/56)	5.2±0.2	0.4	62.5% (30/48)	5.2±0.2	0.4
C-Fibers	44 (all unit)	0.5±0.02	3.3 (1-6.3)	21 (all unit)	0.5±0.02	3.3 (1-10)

Table. 2: The proportions and physiological properties of individual primary afferent mechanoreceptors recorded in wild-type and Cav 3.2 mutant mice.
The proportions, average conduction velocity and median von Frey thresholds for different physiological types of afferent fibers among the Aβ-, Aδ- and C-fiber groups recorded in the current experiment are listed above.

To investigate the relationship between the strength of the stimulus and the neural response, a standard ascending series of displacement stimuli (described in methods) was applied to each fiber. Increasing stimulation strength should produce increasing firing rates in wild-type mechanoreceptors. The total frequency of firing (spikes/s) was calculated over the entire 10 s of the stimulus. The mechanical latency was calculated by subtracting the electrical latency from the delay time between the start of the mechanical probe movement and the first spike (Fig. 24A). Since SAM receptors responded to both the movement and static phase of stimuli, we took a closer look into the two phases by analyzing separately the firing frequencies during the ramp phase (movement phase) and tonic firing frequency (static phase), respectively. In

addition, we compared the velocity sensitivity of RAMs and D-hairs in $Ca_V3.2$ mutants and wild types. The neurons were tested with two constant amplitude displacement stimuli (48µm and 96µm) with a series of varying ramp velocities of between 6 and 3000µm/sec (Fig. 11).

3.2.2 Comparison of mechanical sensitivity of nociceptors

In the present study we examined the mechanosensitivity of identified nociceptors under normal conditions. The AM fibers of $Ca_V3.2^{-/-}$ mice did not display any differences in either discharge frequency ($F_{(1,\ 196)}$=0.25, *P*>0.05; Fig. 19A) or mechanical latency ($F_{(1,\ 168)}$=0.54, *P*>0.05; Fig. 19B) compared to wild type mice. In C-fibers, the firing frequencies ($F_{(1,\ 252)}$=0.33, *P*>0.05; Fig. 19C) and mechanical latencies ($F_{(1,\ 252)}$=0.34, *P*>0.05; Fig. 19D) of $Ca_V3.2^{-/-}$ mice were also similar to wild types for each displacement stimulus.

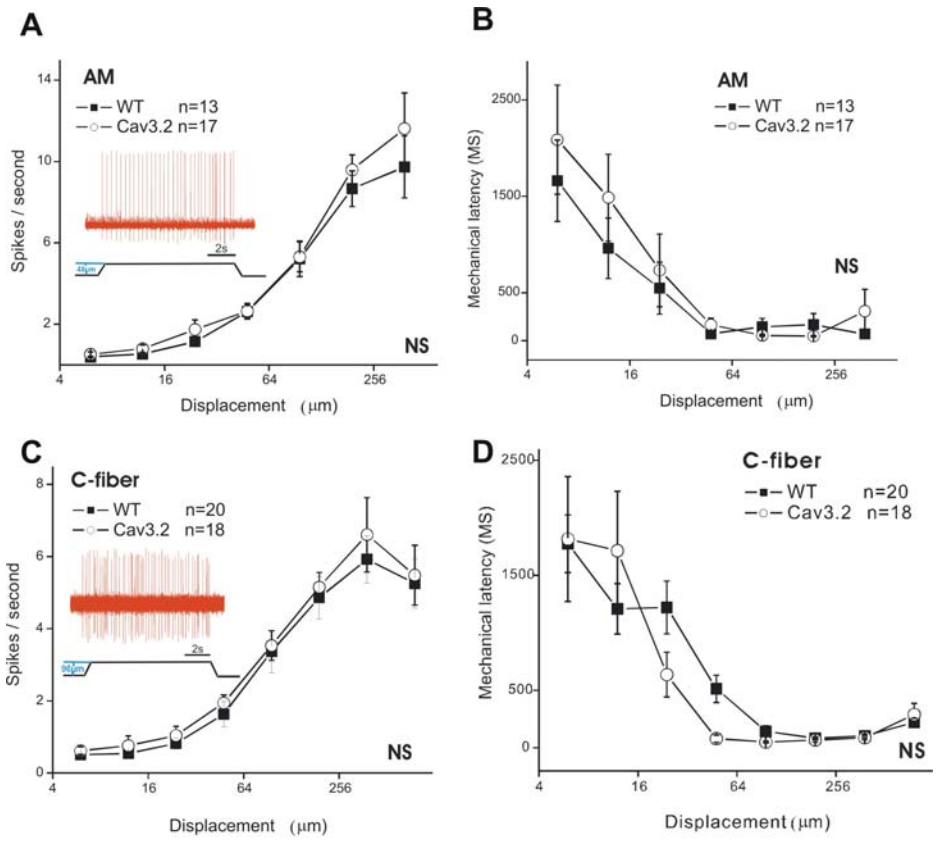

Fig. 19: Mechanical sensitivity of AM and C-fibres in wild-type and $Ca_v3.2^{-/-}$ mice measured by single-fiber recording with the skin nerve preparation.
The total stimulus-response function was measured as firing frequency against displacement amplitude for identified single fibers. The total firing frequency (spikes/s) was calculated over the entire 10 s of the stimulus. The same calculation was also applied to other mechanoreceptors. AMs **(A and B)** and C-fibers **(C and D)** did not display any changes in the firing frequency nor in transduction latency in control (black closed square) and $Ca_V3.2^{-/-}$ mice groups (open circle). The number of recorded fibers for each type of nociceptor was indicated on the graph and the statistical significance was assessed using a repeated ANOVA. Example traces of raw recordings for AM at 48μm and C-fibers at 96μm from wild type are shown as inset.

3.2.3 Comparison of mechanical sensitivity of low threshold mechanoreceptors

Among Aβ-fibers, SAMs are the receptors responding to both phasic and tonic phase of the stimulus, therefore besides total firing frequency, we also further compared the phasic and tonic firing frequencies separately. Neither the total, phasic nor tonic firing

frequencies were altered between the wild type and $Ca_V3.2^{-/-}$ mice (Total: $F_{(1, 186)}$=0.31, *P*>0.05, Fig. 20A; phasic: $F_{(1, 186)}$=1.19, *P*>0.05, Fig. 20C; tonic: $F_{(1, 162)}$=1.34, *P*>0.05, Fig. 20D). Although SAMs in $Ca_V3.2^{-/-}$ mice tended to have a shorter mechanical latency, it was not significantly different from the wild type ($F_{(1, 186)}$=3.90, *P*>0.05; Fig. 20B).

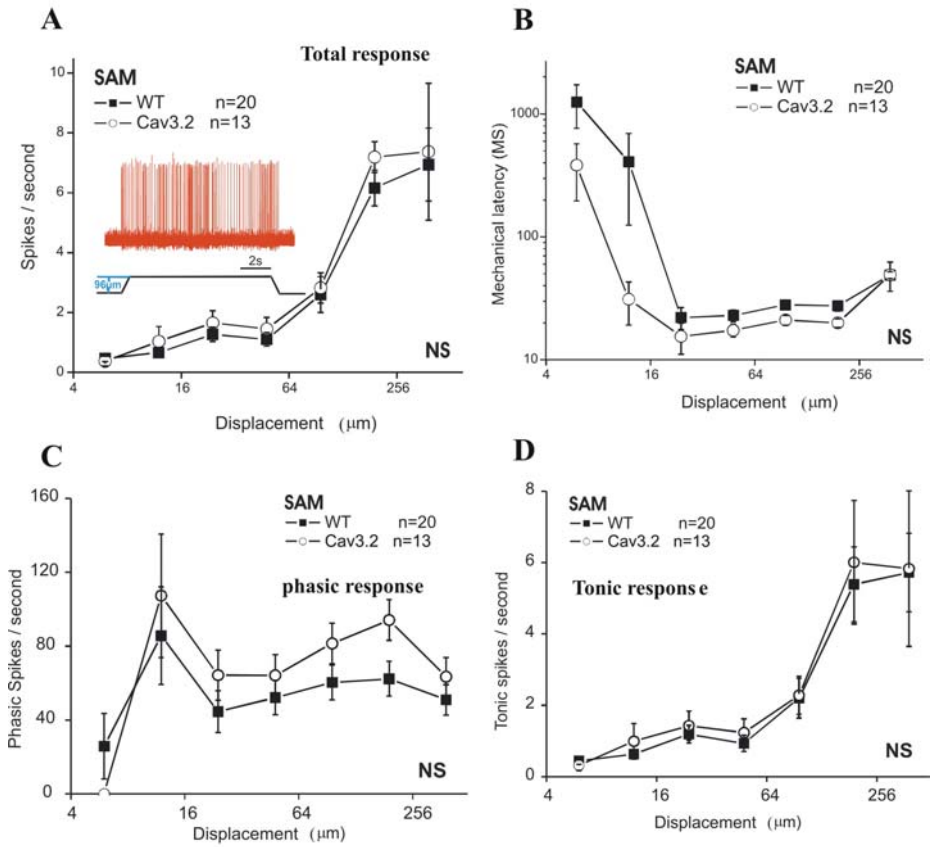

Fig. 20: Mechanical sensitivity and mechanotransduction latency of SAMs in wild type and $Ca_V3.2^{-/-}$ mice.
The total firing frequency of SAM fibers remained unaltered in the $Ca_V3.2^{-/-}$ compared to wild type **(A)**. Since they did not only respond to the movement of the probe, but also to the static phase of the stimulus, further analysis for phasic and tonic response was also applied, but no differences were found between two genotypes **(C and D)**. However, SAMs in $Ca_V3.2^{-/-}$ responded to mechanical stimuli with slightly shorter latencies but this was not significant **(B)**. Example trace of a SAM at 96µm from wild type is shown in the inset.

Another type of Aβ-fibers is the RAM, which only responds to the movement of the

probe. The total firing frequency analysis did not show any difference between wild type and $Ca_V3.2^{-/-}$ mice ($F_{(1, 156)}$=1.02, *P*>0.05; data not shown). If we analyzed the phasic firing frequency of RAM by dividing the total number of spikes on the phasic phase with the duration of the movement, we could observe a declining phasic firing frequency. This is because that RAMs stop firing within the first tens of milliseconds in spite of continuous stimulation. The comparison of phasic firing frequency also showed no significant difference between the two groups of animals ($F_{(1, 156)}$=4.20, *P*>0.05; Fig. 21A). However, the mechanical latency for $Ca_V3.2^{-/-}$ mice was consistently slower than the wild type ($F_{(1, 156)}$=5.16, *P*<0.05; Fig. 21B)

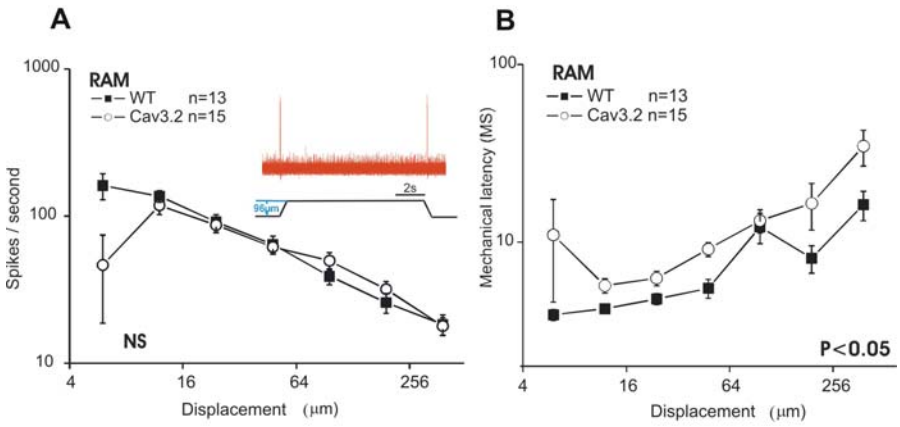

Fig. 21: Mechanical sensitivity of RAM in wild type and $Ca_V3.2^{-/-}$ mice.
The phasic firing frequencies of RAM **(A)** from wild type and $Ca_V3.2$ mutant were not significantly different for increasing stimuli. RAM in $Ca_V3.2$ mutant had significantly longer mechanical latencies for every step stimulus compared with wild type **(B)**. Example traces of raw recordings for RAM at 96µm from wild type are shown in the inset.

Another rapidly adapting receptor, D-hair, is the most sensitive receptor among all cutaneous receptors. Their von Frey thresholds are always 0.4mN or lower (Lewin and Moshourab, 2004). Since D-hair receptors respond only to the movement of the stimulus, we only analyzed the phasic firing frequency by dividing the total number of spikes on the phasic phase by the corresponding movement duration for each indentation. Then we found its phasic firing frequency stayed constant for increasing

displacement (Fig. 22A). D-hairs in $Ca_V3.2^{-/-}$ mice showed consistently lower firing frequency than in the wild types ($F_{(1, 420)}$=5.86, p<0.05; Fig. 22A). More noticeably, the mechanical latency in the $Ca_V3.2^{-/-}$ mice was significantly slower than in wild types $F_{(1, 420)}$=10.32, p<0.01; Fig. 22B).

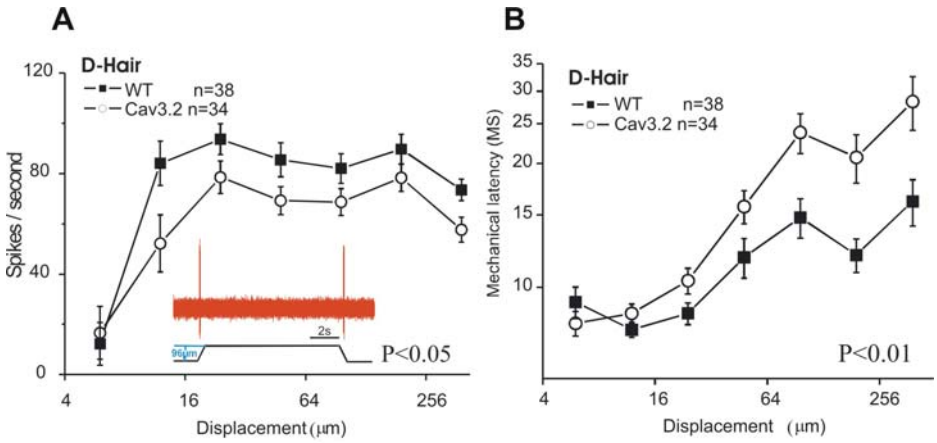

Fig. 22: Mechanical sensitivity of D-hair in wild-type and $Ca_V3.2$ mutant.
D-hair afferents in mutants showed a dramatically lower sensitivity **(A)**. And its mechanical latency was significantly postponed in mutant compared with the wild type **(B)**. Example traces of raw recordings for D-hair at 96µm from wild type were shown as inset.

3.2.4 The effect of $Ca_V3.2$ on velocity coding mechanoreceptors

We also tested the velocity response of low threshold RAM and D-hair receptors in both control and $Ca_V3.2^{-/-}$ mice. The velocity ranged from 6-3000µm/s and was applied at two constant indentations of 48 and 96 microns, respectively and the phasic response was analyzed. Since not every tested unit responded to each velocity, especially the lower velocity, only the responding units were analyzed. The percentages of the responding units at each tested velocity were plotted in the insets of Fig. 23 A, B. Increased firing frequencies with increased velocity indicated that these fibers do code the velocity.

There was no change detected in RAM velocity sensitivity in mutants ($F_{(1, 130)}$=0.19, *P*>0.05; Fig. 23A). However, the analysis of firing frequency during the ramp phase revealed that the movement response of D-hair receptors in $Ca_V3.2^{-/-}$ was remarkably lower than in wild type ($F_{(1, 280)}$=4, *P*<0.05; Fig. 23B). This result was also consistent with the previous finding that with the increasing indentations, the phasic firing rate of D-hairs was decreased in the $Ca_V3.2^{-/-}$. If we made more detailed analysis for the phasic firing frequency by dividing the stimulus durations at 356µm/s and 1432µm/s into five equal parts, we found that the difference of firing frequency between wild type and $Ca_V3.2^{-/-}$ was due to the lower firing frequency of $Ca_V3.2^{-/-}$ at the beginning of the ramp stimulus. At both velocities, D-hairs in wild type mice started to respond during the first 54ms at 356µm/s and 13.4ms at 1432µm/s and most of them reached plateau in firing frequency at 162ms (356µm/s) and 40ms (1432µm/s) and maintained this firing frequency until the end of the stimulus. However, D-hairs in $Ca_V3.2^{-/-}$ hardly responded at the beginning of the stimuli and started to respond gradually with increasing displacements. Most of D-hairs in $Ca_V3.2^{-/-}$ reached the same firing frequency as in wild type at the end of the stimulus, but the difference in firing frequencies between wild type and $Ca_V3.2^{-/-}$ was noted at a velocity of 356µm/s (Fig. 23C, D; at 356µm/s, $F_{(1, 280)}$=16.05, *P*<0.0001; at 1432µm/s, $F_{(1, 345)}$=0.39, *P*>0.05). The percentages of the responding RAMs per stimulus were in the same range (around 40% to 24µm/s and 100% to 3000µm/s) at each velocity stimulus in both animals. But the D-hairs of mutants (26% to 24µm/s and 97% to 3000µm/s) showed a lower responding percentage to each stimulus than of wild types (34% to 24µm/s and 100 % to 3000µm/s), however, the velocity thresholds for both genotypes were comparable (*P*>0.05, unpaired t-test).

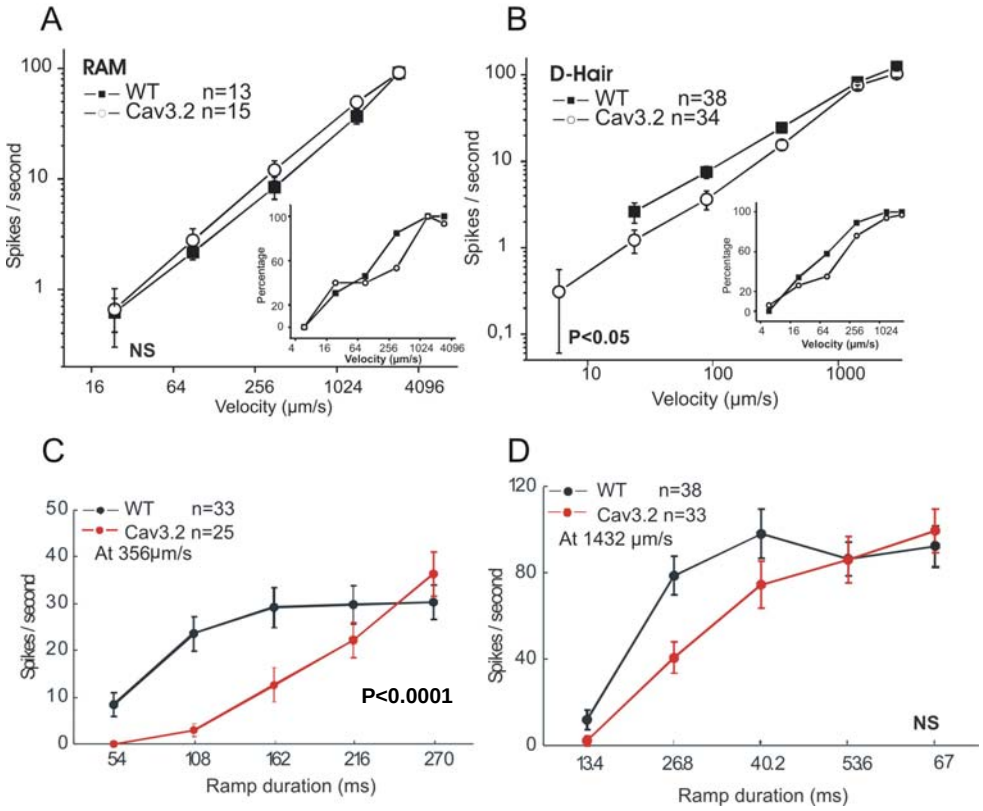

Fig. 23: Velocity sensitivity of RAM and D-hair mechanoreceptors in wild-type and $Ca_V3.2^{-/-}$ mice at 96 microns.

The indentation applied to evoke AP is constant, at different ramp velocities ranging from 6 to 3000µm/s, both RAM and D-hair receptors showed increasing firing frequencies with the rising velocities. This indicated that both receptors functioned as velocity receptors. As the velocity increased by 500 times, the coding frequency of RA in wild type was increased from 0.6 spike/s abruptly to 90 spikes/s by almost 150 times while that of D-hair was increased from 2.6 spikes/s to 124 spikes/s by about 50 fold. It was shown that RAMs and D-hairs had nearly the same sensitivity (around 100 spikes/s) to the highest velocity stimuli, but D-hairs were more exquisitely sensitive to slow movement (about 2.6 spike/s) compared with RAM (less than 1 spike/s). In **A**, the firing rate of RAM receptors at 96 microns in wild-type and $Ca_V3.2^{-/-}$ mice nearly overlapped at each velocity stimulus. But $Ca_V3.2^{-/-}$ D-hairs displayed a much lower firing rate at each velocity, especially at lower velocities **(B)**. Furthermore, fewer single D-hair receptors in mutants than in wild types responded to each velocity stimulus. In A and B, the percentage of responding RAM and D-hair fibers at that corresponding velocity step is in the inset. Detailed analysis in phasic firing frequency at velocities of 356µm/s **(C)** and1432µm/s **(D**).

The mechanical latency was calculated by subtracting the electrical latency from the delay time between the start of the mechanical probe movement and the first spike

(Fig. 24A). If the fibers respond at a certain threshold, the faster the stimulus velocity, the shorter time is required to reach this displacement. So along with the increasing velocities, D-hairs exhibited gradually shortened latencies. The mechanical latencies of D-hairs in $Ca_V3.2^{-/-}$ were also consistently longer than in wild type ($F_{(1,280)}$=55.15, *P*<0.0001; Fig. 24B).

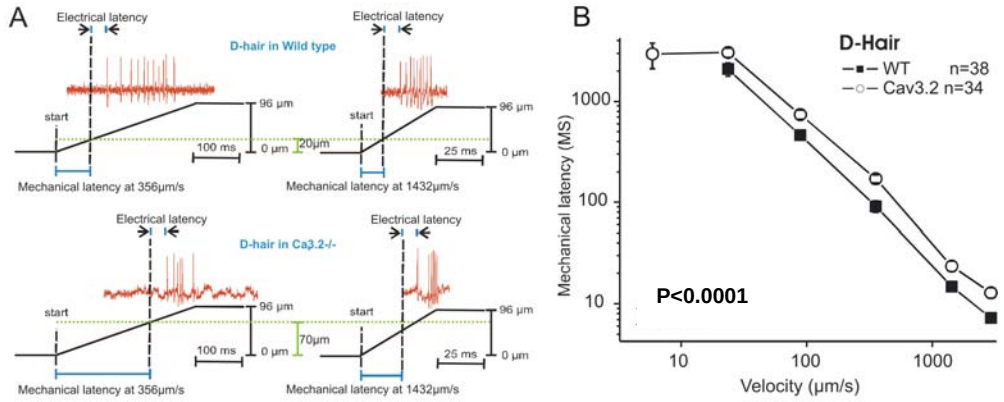

Fig. 24: The measurement of mechanical latencies at two consecutive velocities.
A: Calculation of mechanical latencies of D-hair receptors in both wild type and $Ca_V3.2$ mutant mice at velocities of 356µm/s and 1432µm/s. **B:** Statistical analysis of mechanical latencies in wild type and $Ca_V3.2$ mutant mice from 6 µm/s to 3000 µm/s at 96 µm.

3.2.5 Unchanged mechanosensitive current and somal AP threshold in $Ca_V3.2^{-/-}$ mice

Although considerable research has been made to try and elucidate the cellular and molecular mechanisms for mechanotransduction in the somatosensory system, the molecular basis of mechanotransduction is still poorly understood. The reason for different adaptation patterns of different cutaneous receptors remains mysterious. Mechanotransduction is a two step processes starting with the opening of mechanically activated ion channels and depolarization induced AP generation. Different sensitivity of mechanoreceptors could be caused either by changes in

specific mechanotransdution channels per se or by receptor specific voltage-gated ion channels, which underlie axonal excitability. The question of whether the lack of $Ca_V3.2$ affects the gating properties of the unknown mechanotransduction channel directly or the threshold of AP generation, cannot be answered by extracellular recording using the skin nerve preparation. This is because the *in vitro* skin nerve preparation does not allow one to directly measure the mechanosensitive ion channels, as they are located on endings that are too small for intracellular recording methods. The above observed changes of AP generation in RAM and D-hair receptors from skin nerve experiments can be further dissected by using the patch-clamp technique. This technique allows us to directly measure mechanically gated currents evoked from the neurite of mouse sensory neurons in culture (Fig. 25). We cultivated adult mouse sensory neurons and made whole cell patch-clamp recordings from the cell body. Under voltage clamp conditions and in the presence of TTX, mechanical stimulation of the neurite evoked very fast inward currents in most sensory neurons (Fig. 25A). These currents can be classified by their inactivation time constant into rapidly adapting (τ_{iac}<5ms) , intermediately adapting (5ms< τ_{iac}<50ms) and slowly adapting (τ_{iac}>50ms) (Fig. 25B).

Since I found lowered firing frequency to both displacement and velocity stimuli in D-hairs and also delayed mechanical latencies in both D-hairs and RAMs, in the patch-clamp experiment I intended to patch characteristic low threshold mechanoreceptors (Fig. 25A), which have middle to big sized neurons with narrow (half-peak duration<1ms) and humpless APs (Stucky and Lewin, 1999). After establishing whole cell configuration the amplifier was switched to current clamp mode and action current injection was used to evoke APs (pulses varied from 0.2 to 0.5 nA for 80 ms). After confirmation of mechanoreceptor specific AP the recording mode was switched back to voltage clamp to record mechanically activated currents at a holding potential of –60mV in the presence of 1μ M TTX. I found three types of mechanically gated current all existed in the selected neurons (Fig. 25B).

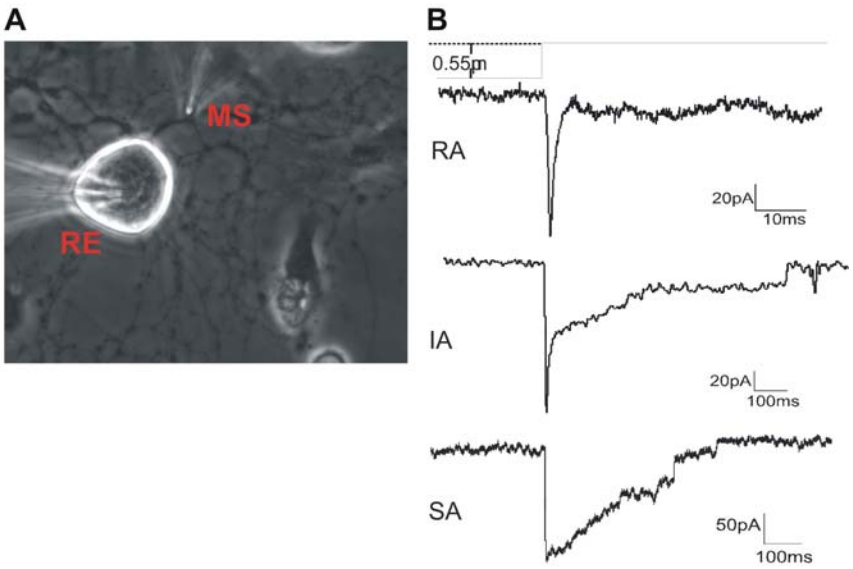

Fig. 25: Mechanically gated currents in DRG neurons cultured on PLL/Laminin substrate.
A: Bright field image of a single DRG neuron in the whole-cell recording configuration with the mechanical stimulator (MS) poised to stimulate one of the neurites. RE stands for recording electrode. **B:** Sample traces of the different types of mechanically gated currents obtained by neurite stimulation in the presence of TTX (1μM): RA: rapidly adapting; SA: slowly adapting; IA: intermediate adapting.

Because that the delayed mechanical latencies were observed in both RAMs and D-hairs in the $Ca_V3.2^{-/-}$, I analyzed the latency between onset of probe movement and current activation. In cells displaying RA, SA or IA responses all the currents activated within 300μs and there was no significant difference in latencies among three types of currents in wild types. The comparison of the mechanical latencies between wild types and $Ca_V3.2$ mutants in any types of current also did not show any dramatic differences (**RA** : WT: 0.28±0.07ms,n=10; $Ca_V3.2^{-/-}$: 0.27±0.02ms, n=12; *P*>0.05; **SA** : WT: 0.27±0.04ms, n=7; $Ca_V3.2^{-/-}$: 0.28±0.03ms, n=10; *P*>0.05; **IA** : WT: 0.25±0.03ms, n=3; $Ca_V3.2^{-/-}$: 0.24±0.03ms, n=6; *P*>0.05, Unpaired t-test: Fig. 26A). In addition to the mechanical latency, the mechanical current amplitude is another factor that could affect the timing of AP generation and firing frequency**.** It was found that in cells with RA currents the latency for AP initiation was very short, but in cells with IA

and SA currents there was often an appreciable delay of several milliseconds before AP initiation compared to the very short latency of mechanically gated current (Hu and Lewin, 2006). Therefore I also compared the mean peak amplitude from different types of mechanical currents. In general, RA type currents showed bigger amplitude than the IA and SA type currents in both wild type and $Ca_V3.2^{-/-}$. If we compared the mean peak amplitudes of different types of mechanical currents between wild type and mutant, we could not find any significant difference between two groups of animals (**RA** : WT: 253.79±48.92pA,n=10; $Ca_V3.2^{-/-}$:341.20±71.44pA, n=12; *P*>0.05; **SA** : WT:130.09±22.4pA, n=7; $Ca_V3.2^{-/-}$: 142.66±22.64pA, n=10; *P*>0.05; **IA** : WT: 117.68±30.12pA, n=3; $Ca_V3.2^{-/-}$: 161.15±50.68pA, n=6; *P*>0.05, Unpaired t-test: Fig. 26B). Now we can primarily conclude that the lack of $Ca_V3.2$ in the low threshold mechanoreceptors does not affect the gating properties of mechanically gated ion channels.

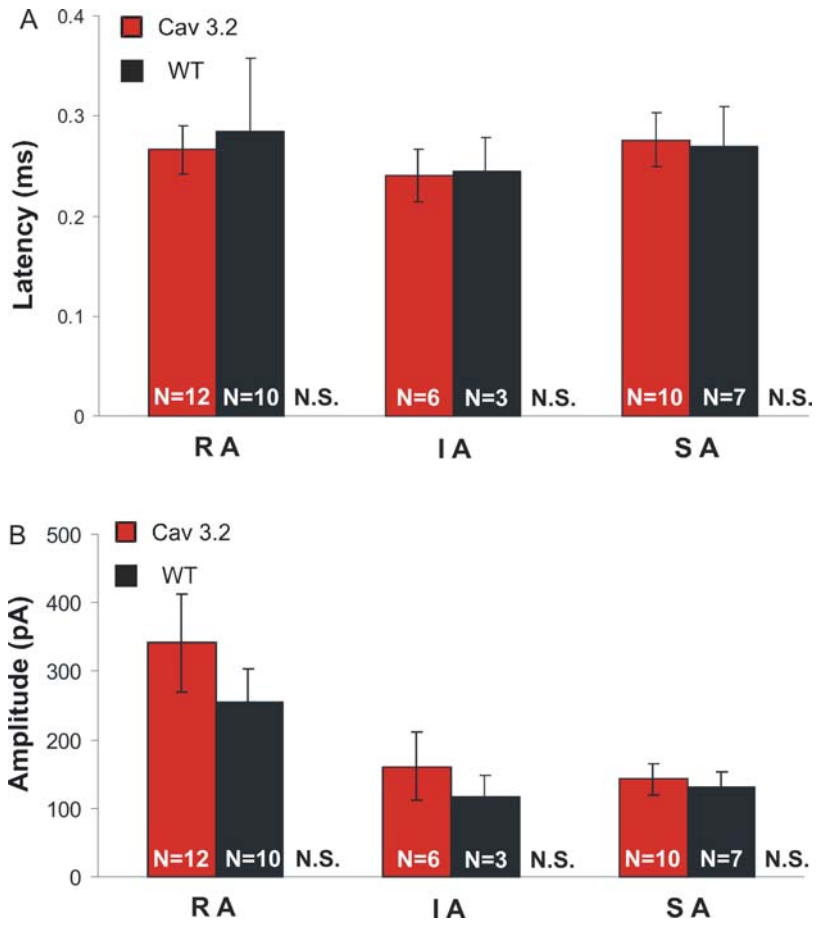

Fig. 26: The mean mechanical latency and mean of peak current amplitude for RA, IA and SA currents.

A: The RA, SA and IA currents were all activated within 300µs. The mean mechanical latencies of RA, SA and IA in $Ca_V3.2^{-/-}$ were also not significantly different from the wild type. **B:** the mean peak amplitudes of 3 types of mechanically gated currents evoked from neurite stimulation were also not significantly different between $Ca_V3.2^{-/-}$ and wild type. The amplitude of the displacement stimulus needed to evoke a current was not different between groups. Number of recorded neurons is indicated at bottom of each bar.

$Ca_V3.2$ is one of the T-type (low-voltage activated [LVA]) Ca^{2+} channels, which are activated at relatively negative membrane potentials. The opening of LVA Ca^{2+} channels around the resting potential may make a depolarizing current that brings the cell to firing threshold for a Na^+ spike. So another hypothesis would be the lack of depolarization helper $Ca_V3.2$ in $Ca_V3.2$ enriched sensory neurons would make it harder to generate AP. Therefore, I compared the somal threshold current for AP

generation, but the AP threshold in $Ca_V3.2^{-/-}$ (2800±256.79 pA, n=34) was quite comparable with that in the wild type (2838.24±189.66 pA, n=31; *P*>0.05, Unpaired t-test; Fig. 27)

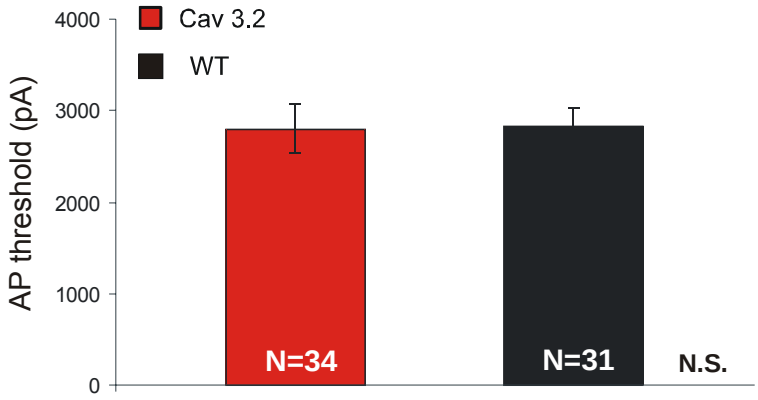

Fig. 27: Threshold current for somal AP initiation.
Under current clamp mode the current injection was applied to evoke AP on cell soma (step pulses was used: 200pA for middle sized neurons and 500 pA for big neurons). The threshold currents needed for generating APs in $Ca_V3.2^{-/-}$ and wild type were not dramatically different. Number of recorded neurons was indicated at bottom of each bar.

3.2.6 Summary

The characteristic response properties and mechanical latency was determined for each type of cutaneous mechanoreceptor in controls and $Ca_V3.2^{-/-}$ mice. The relative proportion of RAM and SAM in Aβ-fibers was unaltered between the genotypes. However, the ratio of AM to D-hair in Aδ-fibers was decreased. We reasoned this change due to the over sampling of D-hair receptors. Skin nerve experiments showed that the mice carrying a $Ca_V3.2$ null mutation had unchanged discharging frequency of RAMs, SAMs, AMs and C-fibres upon ramp and hold on mechanical stimuli compared to wild type mice. But interestingly, D-hair receptors in $Ca_V3.2^{-/-}$ mice had a dramatically lower firing frequency with increasing displacement. Furthermore, the lack of $Ca_V3.2$ also decreased the sensitivity of D-hairs in detecting changes in velocity. Further analysis revealed a delayed firing at the beginning of the ramp stimuli

in $Ca_V3.2^{-/-}$ accounted for the less mechanosensitivity. Moreover, both RAMs and D-hair receptors exhibited increased mechanical latency with increasing stimulus amplitude. Whole cell patch-clamp in characteristic mechanoreceptors indicated that the increased mechanical latency in RAMs and D-hairs and reduced mechanosensitivity in D-hair receptors were not due to delayed generation of a mechanosensitive current rather a delay in AP generation caused by the lack of $Ca_V3.2$ channels.

3.3 Tissue specific mechanosensitivity and distinct sensitization mechanism

Mechanically insensitive nociceptors (MIA) have long been noted in deep tissue, visceral organs and skin in rodents and primates (McMahon and Koltzenburg, 1990; Meyer et al., 1991). The proportion of MIA in different tissues is thought to contribute to different tissue sensation and inflammation induced hyperalgesia (Berberich et al., 1988; Grigg et al., 1986; Hoheisel et al., 2005; Schaible and Schmidt, 1988a). However, the reason for the mechanical insensitivity under physiological conditions and mechanisms of sensitization in the inflammatory state in these neurons is not yet understood. In this part of the study, retrograde labeling with a fluorescent labeled dextran amine give us the chance to back label target identified sensory neurons. With the whole cell patch-clamp technique, the reason for mechanical insensitivity can be tested at both mechanosensitive current generation level and membrane excitability level. Moreover, the effect of one of the inflammatory mediator and algesic drug NGF on mechanotransduction will be examined on both stages of the mechanotransduction processes.

3.3.1 Localization of Gastrocnimius Soleus (GS) muscle afferent neurons in DRG

Using fluorescence microscopy, Gastrocnimius Soleus (GS) muscle afferent neurons labeled with 3kMW Alexa Fluor 488 conjugated Dextran Amine (FDA) were visualized in sections from lumbosacral L1-L6 and S1-S3 DRG. Simultaneously, thoracic DRGs (T10-T13) were also removed and examined for evidence of spread. We found labeled GS muscle innervating neurons were mainly located in the lumbar ganglia (Fig. 28), as the thoracic and sacral DRG neurons were not labeled (Pictures were not shown). Among the Lumbar DRGs, L1 and L2 did not contain any labeled cells in any of the sections examined, whereas L3-L6 DRGs showed diverse labeling densities. L3 and L6 contained abundant FDA labeled nerurons. In the L6 DRG almost every

section contained labled neurons. In L4 and L 5 DRGs, sporadic labeled neurons (2-3 cells per section) were found but not in all sections.

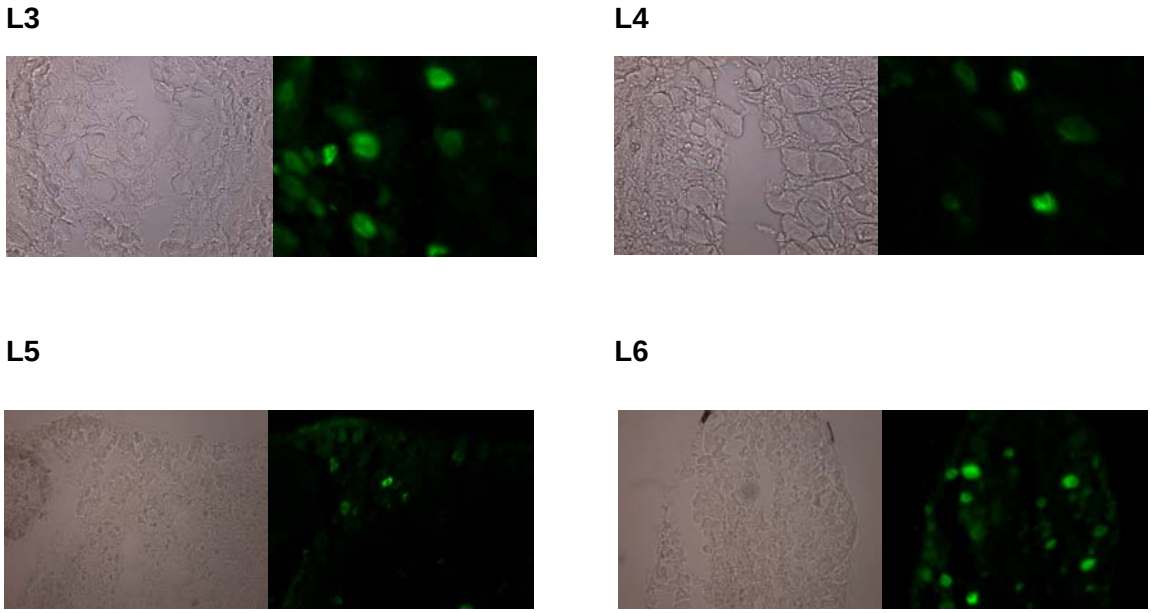

Fig. 28: Distribution of GS muscle retrogradely labeled afferents in lumber DRG. Left side showed the examples of bright field pictures from the indicated DRG segment. Right side showed the corresponding fluorescent image of GS muscle afferent neurons (green cells). The GS muscle afferent neurons were mainly distributed in L3 and L6 DRGs, whereas L4 and L5 contained fewer labeled neurons.

3.3.2 Different populations of DRG neurons labeled from muscle and cutaneous afferents.

FDA was injected into either the GS muscle or hind paw skin. Using the anatomical localization experiments as a guide, L3-L6 ganglia were harvested on average 3 days after injection and placed into culture for further electrophysiological analysis.

DRGs contain a heterogeneous population of sensory neurons and cell size in the DRG is closely related to sensory receptor type. Different tissues have distinct sensitivity to exogenous stimuli. I measured the cell size distribution of cultured neurons from retragradely labeled different target tissues. Seventeen (for GS muscle

from 6 experiments) and 28 (for hind paw skin from 2 experiments) random fields of cultured neurons were measured. The number and cell diameters of FDA + (green bar) and FDA- (black bar) neurons per field were counted and measured (Fig. 29A2, B2). From the cell size distribution histogram we observed that the total population of cultured DRG neurons (black plus green bar) from GS muscle and skin labeling both exhibited an approximately normal distribution. Most of the cells have diameters from 20-24μm (Fig. 29A1, B1). When the percentage of labeled neurons in 2μm bin size was plotted, we observed that muscle and cutaneous afferents contained both large and small DRG neurons. GS muscle labeled neurons had an equal distribution from small (18μm) to middle (30μm) sized neurons about 20% in each size. Nonetheless, there was also a large population of GS afferent neurons with very large cell diameters (38μm) (Fig. 29A3). The neurons in the small and middle size diameter range may represent the GS muscle afferents of C- and Aδ-fibers respectively, whereas the big neurons represent the Aα fibers. Cutaneous afferent neurons displayed a different neuron population composition, with a slightly wider range of cell size distribution from 14μm to 40μm. The percentage of skin labeled neurons was about 10% in each size from small (14μm) to middle (30μm) range, which may represent an overwhelming group of C- and Aδ-fibers from cutaneous afferent. There was also a high percentage of larger diameter neurons from skin, which may represent the Aβ mechanoreceptors (Fig. 29B3).

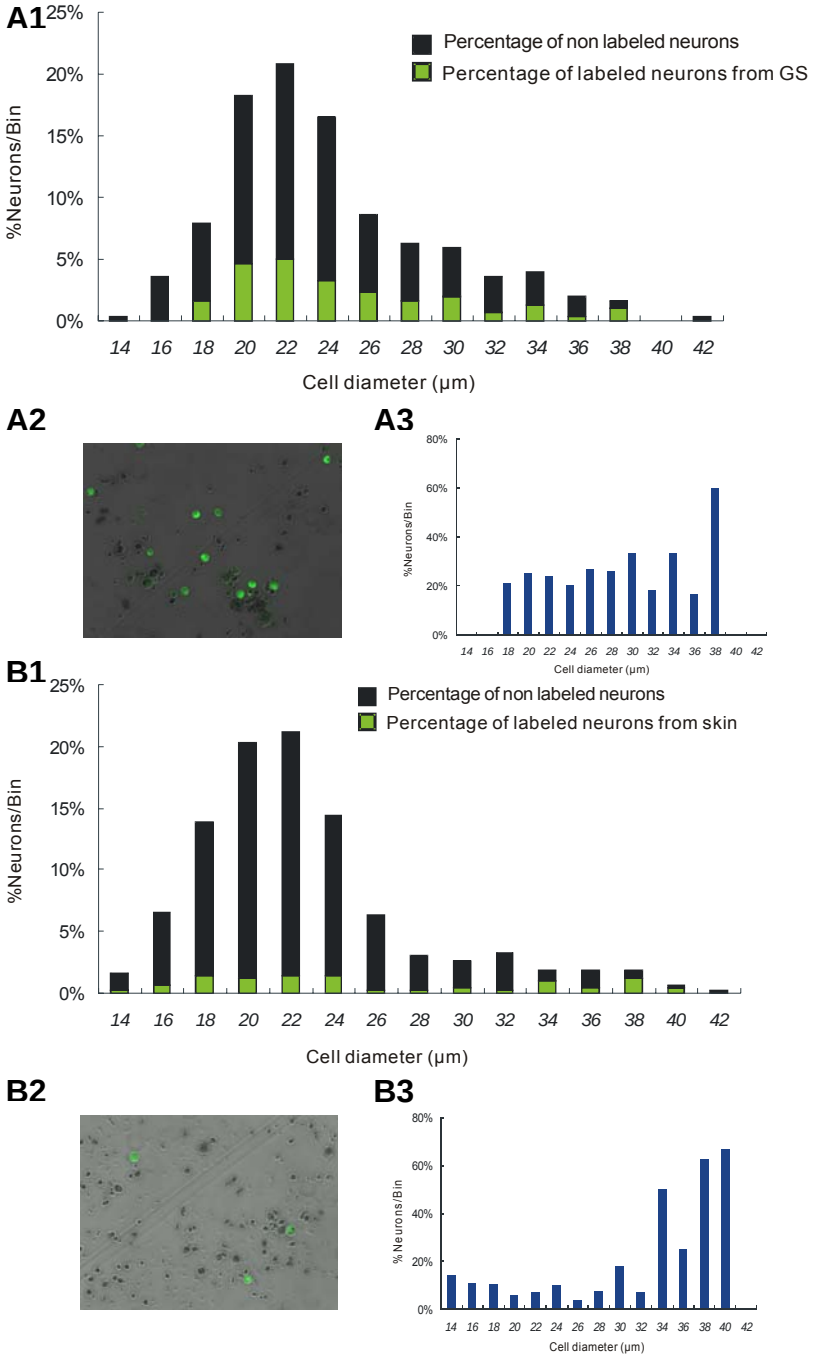

Fig. 29: Histograms of cell size distribution for GS muscle and skin labeled DRG neurons.

Bin size is 2µm. The percentages of GS muscle labeled neurons (green bars in **A1**) and skin labeled neurons (green bars in **B1**) in each size were plotted against non-labeled neurons (black bars in **A1** and **B1**, respectively). Example of bright field images superimposed with fluorescent images of GS muscle labeled (green cells in **A2**) and skin labeled (green cells in **B2**) DRGs in culture. The percentage of GS muscle (**A3**) and skin labeled neurons (**B3**) normalized with respect to the total

number of neurons in each size. The median cell body diameters for GS muscle and skin afferent neurons were 23.5μm and 24.5μm and were not significantly different.

3.3.3 Different mechanosensitivity in muscle and skin retrogradely labeled neurons

Muscle and knee joints are mostly innervated by Aδ- and C-fibers nociceptors, which have relatively small cell diameter somas in the DRG. Under normal conditions, extracellular recording studies showed 30% of Aδ and 40% of neurons innervating the knee joint are mechanically insensitive (Schaible and Grubb, 1993). In contrast, mechanoinsensitive fibers in the skin vary a lot between species. It has been reported that up to 30% of C-fibers and 50% of the Aδ-fibers are mechanically insensitive in humans and monkeys (Meyer et al., 1991), however about ~10% of C-fibers and 15% of AMs in rodent skin are found to be mechanical insensitive (Handwerker et al., 1991; Kress et al., 1992; Lewin and Mendell, 1994).

In the present study together with the whole cell patch-clamp recording, we used a computer-controlled nanomotor to stimulate neurites and soma of cultivated adult mouse sensory neurons. As described previously (Fig. 5), three types of mechanically activated currents are classified according to their different inactivation time constant, namely RA, SA and IA. With the combination of nanomotor and back labeling technique, we could determine whether there is tissue specific mechanosensitivity in the culture system as observed in single nerve recordings.

If mechanosensitive currents were evoked either on soma or neurite of a neuron, the neuron was counted as mechanosensitive. Compared to identified cutaneous afferent neurons, there were far fewer GS muscle afferent neurons responding to the mechanical stimuli (muscle: 58%; skin: 90%; $P<0.01$, χ^2; Fig. 30A). However, in GS labeled neurons the electrical excitabilities of GS and skin labeled neurons were comparable as measured by the threshold current needed to evoke an AP in current clamp [GS: 196.92±30.56 nA, n=26, skin: 183.33±35.66 nA, n=12 (Φ<25μm); GS: 2043.53±309.1 nA, n=17; skin: 2027.27±332.78 nA, n=11(Φ>25μm); Fig. 30B] and

amplitude of the AP [GS: 77.85±2.76 mV, n=26, skin: 71.23±3.75 mV, n=12 (Φ<25µm); GS: 79.4±3.1 mV, n=17; skin: 76.57±6.96 mV, n=11 (Φ>25µm): Fig. 30C, *P* >0.05, Unpaired T test]

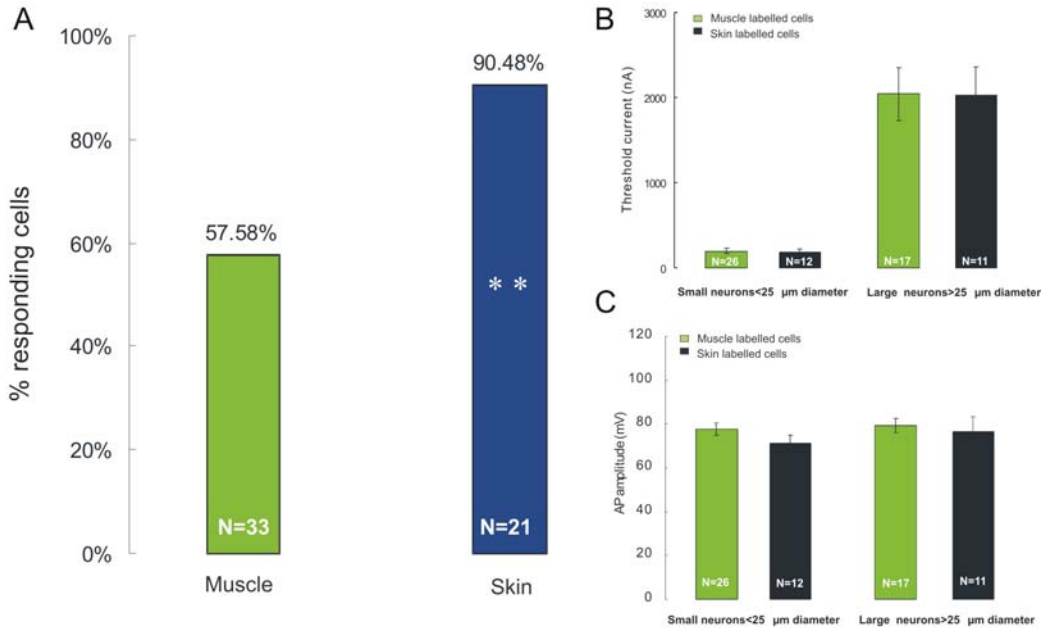

Fig. 30: Mechanical sensitivity and electrical excitability of GS muscle and cutaneous afferent neurons.
Histograms of the proportion of the mechanosensitive neurons in GS muscle (green) and skin (blue) labeled DRG neurons. The number of recorded neurons is indicated at the bottom of each histogram. The percentage of neurons with a mechanosensitive current in GS muscle labeled neurons is 30% less than those from cutaneous labeled neurons **(A)**. The threshold current for AP initiation **(B)** and AP amplitude **(C)** was measured in both GS and skin labeled neurons prior to the mechanical stimulation under current clamp mode for checking their electrical excitability and determine the mechanoreceptor and nociceptor properties.

3.3.4 Upregulation of mechanosensitive muscle afferent neurons after NGF treatment

Consistent with previous observations of mechanoinsensitive muscle fibers from single nerve recordings (Mense, 1993), we found a population of silent neurons in cultured GS muscle labeled DRG neurons. Previous studies have shown that afferents supplying deep tissues, such as muscle (Berberich et al., 1988) and joints

(Schaible and Schmidt, 1985; Schaible and Schmidt, 1988b), can respond to inflammatory agents with increased mechanosensitivity. One explanation would be sensitized silent or high threshold mechanoreceptors (HTM) exhibiting lowered mechanical thresholds in the innocuous range and responding to weak deformation of the muscle tissue. Another explanation might be a reduced threshold for firing and increased excitability of small diameter sensory neurons that communicate noxious information to the central nerves system. The single nerve recording technique bypasses receptor transduction and it is not possible to determine whether changes in transduction or excitability is produced. In inflammatory pain states, NGF is a peripheral pain mediator and has been found to be upregulated in a wide variety of inflammatory conditions (McMahon, 1996; Pezet and McMahon, 2006). NGF can potentiate the currents mediated by a number of ligand-gated ion channels, e.g.TRPV1 (Bron et al., 2003; Ji et al., 2002), P2X3 (Ramer et al., 2001) and ASIC3 (Mamet et al., 2002). Behavioral studies in rat have shown that NGF injection can cause acute thermal hyperalgesia (within minutes) and a delayed mechanical hyperalgesia (after7h) (Lewin et al., 1994). In human volunteers, a small subcutaneous or intramuscular injection of NGF also gave rise to pain and tenderness at the injection site, starting within minutes and persisting for several hours (Petty et al., 1994). Moreover, systemic injection of NGF in humans also causes a myalgia (Svensson et al., 2003). In the present study, we used cultured DRGs to examine whether increased mechanical sensitivity arises because of altered transduction properties of the endogenous mechanoreceptive proteins. We first put NGF (100ng/ml) directly in the culture for 4 hours and then replaced the NGF containing medium with normal medium. This mimics the in vivo inflammatory situation that boosts NGF to a high level in the tissue immediately after injury then decreases. Then we further injected NGF (1mg/g) systemically in mice in which the GS muscle afferents were labeled one day before preparation (Fig. 31A). Both 4hrs NGF culture (P <0.01, χ^2) and systemic NGF injected (P<0.01, χ^2) groups showed dramatically elevated proportion of mechanical responding cells in GS muscle afferent neurons (Fig. 31B).

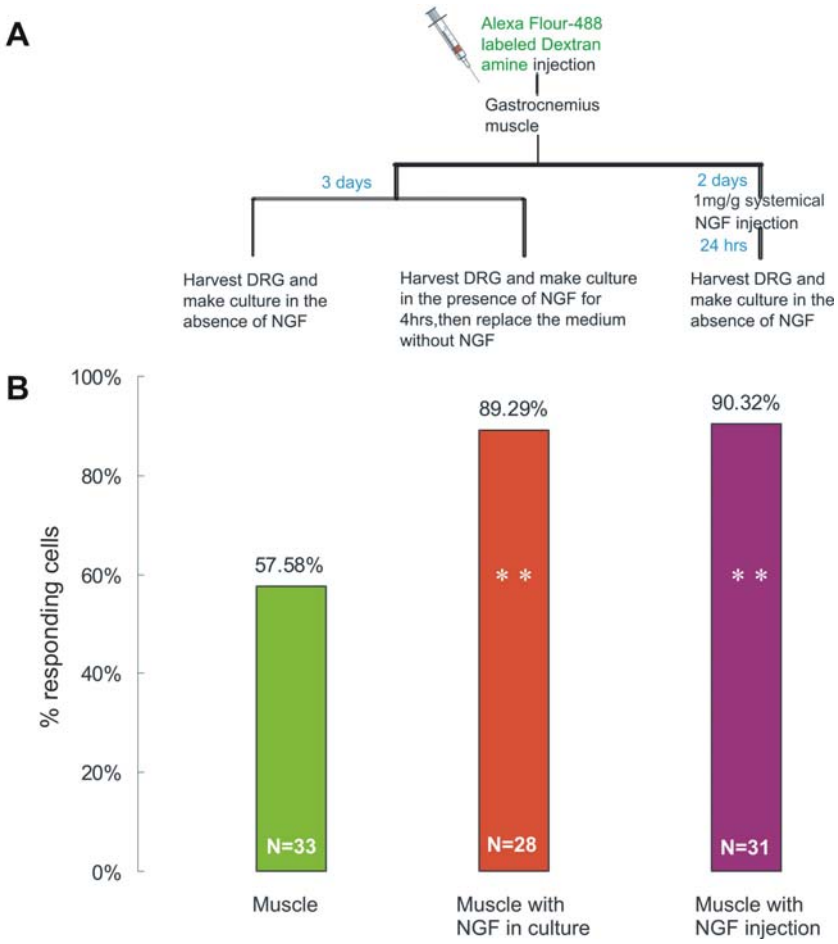

Fig. 31: The increased effect of NGF on mechanosensitivity in GS muscle afferent neurons.
A: Flow chart of NGF treatment on muscle afferent neurons and the effects of NGF in the culture and after systemic injection are shown in the corresponding bar graph in B. The 4hrs treatment of NGF in the culture and the systemic NGF injection both dramatically increased the proportion of mechanosensitive neurons in muscle labeled DRG neurons for more than 30% **(B)**. The number of recorded neurons is indicated at the bottom of each histogram.

3.3.5 Changes of excitability in mechanoreceptors and nociceptors after NGF treatment

NFG also regulates some voltage-gated ion channels, including potassium (Park et al., 2003) and particularly sodium channels, both TTX-sensitive and TTX-resistant sodium currents are increased in DRG neurons by treatment with NGF (Fjell et al., 1999; Leffler et al., 2002; Okuse et al., 1997; Ritter and Mendell, 1992). Furthermore, DRG neurons grown in the presence of NGF were reported to demonstrate spontaneous

activity (Kasai and Mizumura, 2001). The threshold current needed to evoke an AP changed in neither the 4hrs NGF culture treated group (117.89±22.73 nA, n=19, Φ<25μm; 2755.56±694.09 nA, n=9, Φ>25μm) nor in the systemic NGF injected group (291.43±140.73 nA, n=14,Φ<25μm; 1434.12±169.74 nA, n=17, Φ>25μm; *P*>0.05, Unpaired T test; Fig. 32A). However, the AP amplitude of neurons recorded in the systemic NGF injected group was dramatically increased in small nociceptive neurons (93.31±3.58 mV, n=14; *P*<0.05, Unpaired T test) but not in the large neurons (84.67±3.14 mV, n=17; *P*>0.05, Unpaired T test; Fig. 32B,). In contrast 4hrs treatment of NGF in the culture did not show any effect on AP amplitude in either small or large neurons (81.75±3.4 mV, n=19, Φ<25μm; 81.24±7.02 mV, n=9, Φ>25μm; *P*>0.05, Unpaired T test; Fig. 32B).

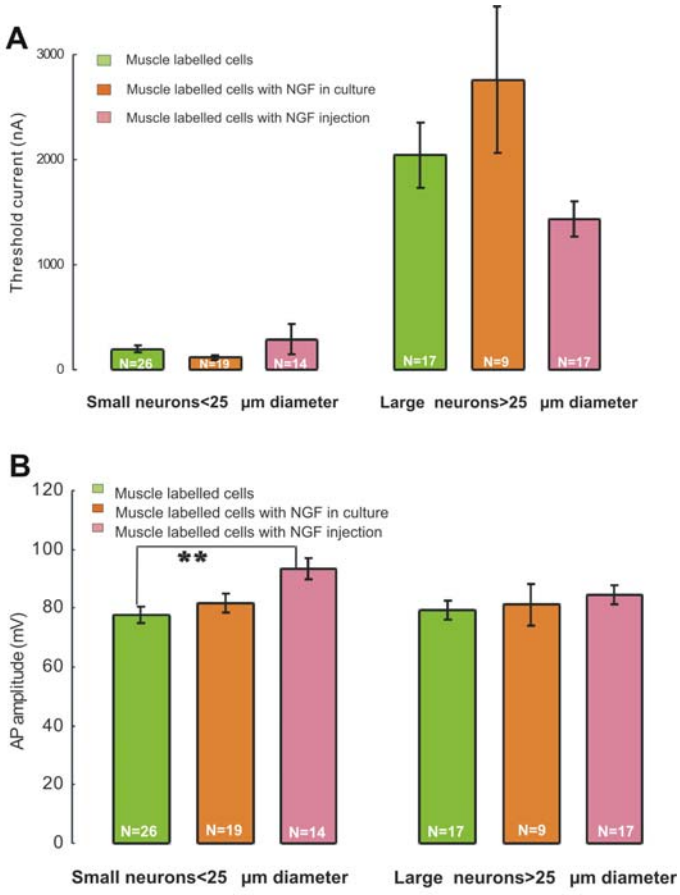

Fig. 32: The effect of NGF treatment on electrical excitability in GS muscle afferent neurons.
The electrical excitabilities of small nociceptors and large neurons were measured by the threshold current needed to evoke an AP and the amplitude of the AP prior to the mechanical stimulation. No differences were noted in the threshold current for AP initiation in either small or large neuron groups in either NGF treatment **(A)**. However, the AP amplitude was significantly increased in the small nociceptors in the systemic NGF injection group, but no difference was observed in the large neuron group or in either small or large neuron groups of 4hrs NGF treatment in the culture **(B)**.

3.3.6 Different types of mechanically-gated currents in tissue specific neurons and their alteration after NGF treatment.

Three types of mechanically activated current from neurite or soma stimuli have been identified in cultured DRG neurons (Fig. 33A). And there were 3 times more mechanoinsensitive neurons in muscle afferent neurons compared to cutaneous afferent neurons. As to those neurons with mechanosensitivtiy, we next asked which type of mechanosensitive current is present in tissue specific neurons. In muscle afferent neurons, around 48% of the neurons possessed SA type currents (16/33 cells) and 9% of the neurons possessed RA type currents (3/33 cells), whereas no neuron with an IA type current (0/33 cells) was observed (Fig.33B). In contrast in cutaneous afferent neurons, the three types of mechanosensitive currents were present in the following proportions, 38.1% for SA (8/21 cells), 38.1% for RA (8/21 cells) 14.29% and IA (3/21 cells). Therefore, the incidence of mechanosensitive currents in cutaneous afferent neurons represented the distribution of different mechanosensitive currents in the total population of DRG neurons (Hu and Lewin, 2006). The proportion of cutaneous afferent neurons possessing RA type was greater than in muscle afferents (about 3 times more, $P<0.01$, χ^2) and also for IA type currents (about 14% more, $P<0.05$, χ^2) than in identified muscle afferent neurons. After direct NGF treatment in the culture, muscle afferent neurons interestingly also displayed a dramatically elevated proportion of neurons with RA type currents from 9% (3/33 cells) to 29% (8/28 cells) ($P<0.05$, χ^2) and a new population of neurons with IA type currents (6/28 cells) with 21% ($P<0.01$, χ^2), but the proportion of neurons with SA type currents

(11/28 cells, 30%, *P*>0.05, χ^2) remained similar to the non-treated group. Similarly, systemic NGF injection also induced a significant increase in the proportion of neurons with RA type (11/31 cells, 35%, *P*<0.05, χ^2) and IA type currents (6/31 cells, 19%, *P*<0.01, χ^2) in muscle labeled cells, but not in the proportion of neurons with SA type currents (11/31 cells, 35%, *P*>0.05, χ^2). And the proportion of neurons with RA (*P*>0.05, χ^2) and IA type (*P*>0.05, χ^2) currents in muscle afferent neurons in both NGF treated groups (4hrs in culture and systemic injection) reached the same level as found in cutaneous afferents. The proportion of neurons with SA type currents was comparable in each group (*P*>0.05, χ^2; Fig. 33B).

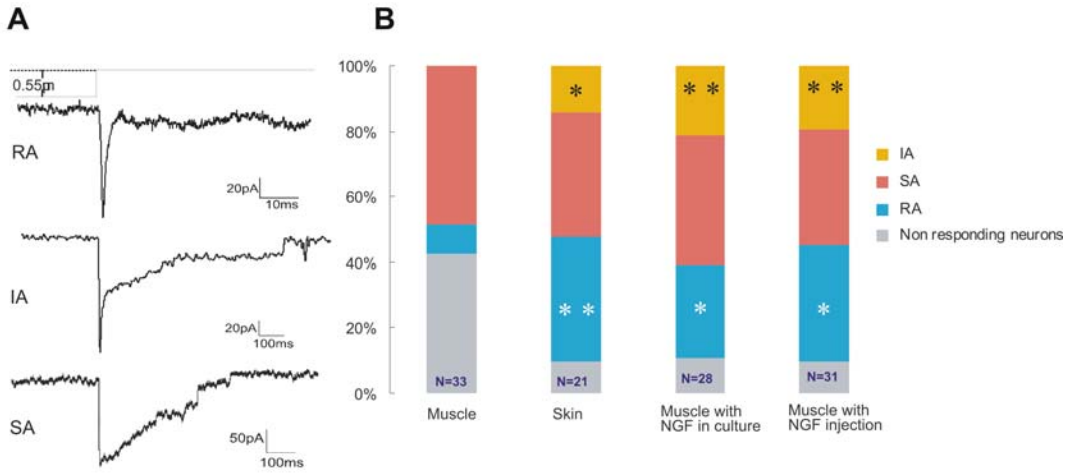

Fig. 33: Expression of different mechanically activated current in tissue specific neurons and NGF treated GS muscle labeled neurons.
Stacked histograms of the proportion of the three types of mechnosensitive currents observed in GS muscle labeled (first column) and skin labeled DRG neurons (second column). Muscle labeled neurons had a dramatically lower proportion of RA (blue) and IA type (yellow) currents compared to skin labeled ones. But the proportions of SA type neurons were almost the same in both tissue specific neurons (pink). And the proportion changes of different types of mechanosensitive currents by NGF treatment in GS muscle labeled neurons (third and forth column). RA and IA type currents could be induced by both 4hrs NGF treatment in the culture and systemic NGF injection in GS afferent neurons. So here we could see a significant increase in the proportion of muscle afferent neurons with RA and IA type currents in both NGF treated groups, but not in that of neurons with SA type currents.The number of recorded neurons is indicated at the bottom of each stacked histogram.

3.3.7 Unchanged kinetics of mechanosensitive current after NGF treatmeant

The kinetics of all three kinds of mechosensitive currents were measured by their mean peak amplitude, mean mechanical latency, mean activation time constant (τ_1) and mean inactivation time constant (τ_2). In spite of the difference in the proportion of mechanosensitive currents in tissue specific neurons and the elevation of the proportion of neurons with RA and IA type currents in NGF treated groups of GS afferent neurons, the four parameters mentioned above did not show any significant difference between either GS and skin labeled neurons or between NGF treated or non-treated GS muscle labeled neurons (P>0.05, Unpaired T test; Table. 3).

Tissue and its treatment	Amplitude (pA)			Latency (ms)			Activation time constant (τ_1) (ms)			Inactivation time constant (τ_2) (ms)		
	RA	**SA**	**IA**	**RA**	**SA**	**IA**	**RA**	**SA**	**IA**	**RA**	**SA**	**IA**
GS afferent neurons	588.71 ± 355.3 (n=2)	284.20 ± 58.78 (n=16)	n=0	0.27 (n=1)	0.49 ± 0.16 (n=14)	n=0	0.18 ± 0.04 (n=2)	0.93 ± 0.20 (n=16)	n=0	1.91 ± 0.29 (n=2)		n=0
Skin afferent neurons	511.88 ± 258.6 (n=2)	275.25 ± 61.65 (n=5)	390.89 ± 317.92 (n=3)	0.62 ± 0.4 (n=2)	0.30 ± 0.02 (n=5)	0.28 ± 0.02 (n=3)	0.47 ± 0.29 (n=2)	0.87 ± 0.16 (n=5)	0.71 ± 0.42 (n=3)	1.06 ± 0.31 (n=2)		11.53 ± 2.04 (n=3)
GS afferent neurons with NGF in the culture	642.75 ± 218.59 (n=5)	240.22 ± 49.91 (n=8)	607.92 ± 226.85 (n=5)	0.25 ± 0.01 (n=5)	0.34 ± 0.10 (n=8)	0.25 ± 0.03 (n=5)	0.17 ± 0.01 (n=5)	0.55 ± 0.11 (n=8)	0.52 ± 0.20 (n=5)	3.11 ± 0.62 (n=5)		22.11 ± 7.24 (n=5)
GS afferent neurons with systemic NGF injection	646.13 ± 137.28 (n=7)	239.28 ± 58.50 (n=9)	276.66 ± 84.60 (n=5)	0.26 ± 0.02 (n=7)	0.40 ± 0.12 (n=9)	0.24 ± 0.05 (n=5)	0.51 ± 0.02 (n=7)	0.47 ± 0.63 (n=9)	1.03 ± 0.38 (n=5)	1.93 ± 0.37 (n=7)		27.92 ± 5.91 (n=5)

Table. 3: Kinetics of mechanosensitive currents in tissue specific neurons and NGF treated GS muscle afferent neurons

Mean peak amplitude, mean mechanical latency, mean activation time constant (τ_1) and mean inactivation time constant (τ_2) measured from neurite stimulation was summarized above. There was no dramatic difference of these parameters in GS muscle afferent or skin afferent neurons. Neither the direct NGF treatment in the culture nor in vivo NGF injection significantly altered these parameters in GS muscle afferent neurons. Data shown as mean ± S.E.M.

3.3.8 Acute induction of mechanosensitivity in GS muscle labeled silent neurons by NGF.

Since both direct treatment with NGF in culture and systemic NGF injection increased the proportion of mechanosensitive neurons in muscle afferents from 58% to 90%, we now asked what the time course for this mechanosensitivity induction might be. A number of ion channels (e.g. TRPV1 and ASIC3) in TrKA-expressing neurons have been shown to be regulated by NGF at transcriptional, translational or postranslation levels. The expression and insertion of new channel caused by NGF-TrKA retrograde signal in the nucleus would require a long period (up to several hours), whereas the activation of a channel by NGF-TrKA signaling induced phosphorylation can happen within minutes (Zhang et al., 2005).

The timing of the effect could in someway elucidate the mechanism of mechanical sensitization. After the confirmation of a mechanoinsensitive GS muscle afferent neuron by stimulating 2-3 different locations on the neurite, we perfused 100ng/ml NGF for 10 to 15 minutes and found some small diameter (20.63±1.30μm, n=4) nociceptors now exhibited mechanosensitive currents by stimulating the locations which had been stimulated before (Fig. 34A). A previous study has shown that IB4 expression is negatively correlated with TrKA expression (Molliver et al., 1997). Therefore, the mechanosensitivities of IB4 negative neurons (mostly likely to be TrKA+) are more likely to be regulated by NGF treatment. In IB4- GS muscle labeled mechanoinsensitive nociceptors, 43% (3/7 cells) of them acquired mechanosensitivity after acute NGF treatment (Fig. 34B). The newly acquired mechanosensitive current was either RA or SA type current (Fig. 34A, B).

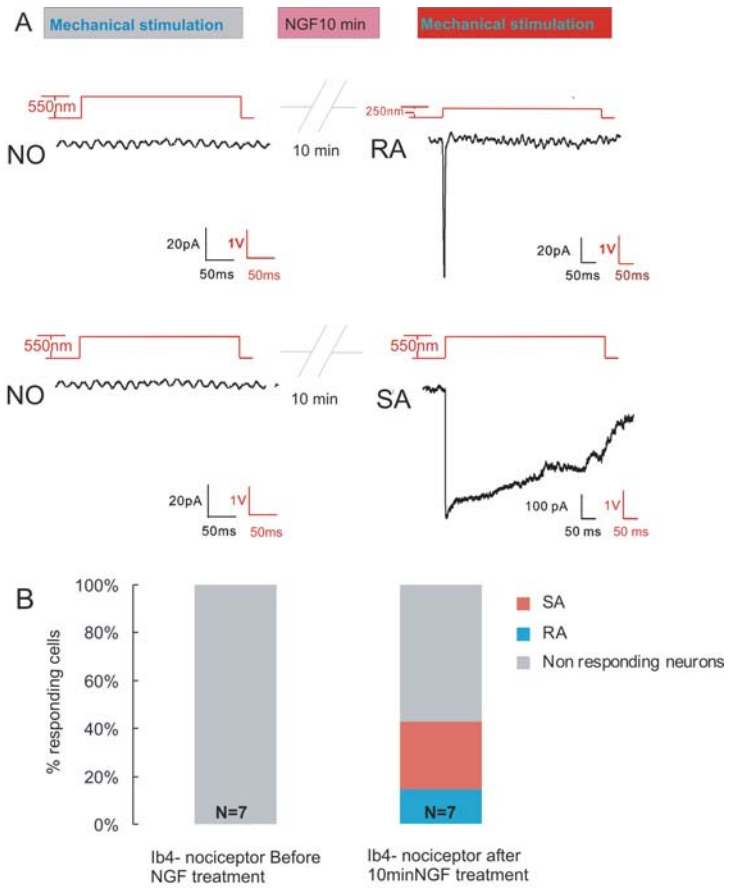

Fig. 34: Acute effect of NGF on mechanoinsensitive GS muscle labeled neurons.
A: Example traces of mechanosensitive currents induced by 10 to 15 minutes NGF treatment in originally mechanoinsensitive nociceptors. Upper red trace is the mechanical stimulus threshold. The newly acquired mechanosensitive currents are diverse, which could be either RA or SA currents. **B:** Summarized the proportion of IB4- nociceptors whose mechanosensitivity could be induced by short NGF treatment. 43% of the mechanoinsensitive IB4- nociceptors acquired mechanosensitive currents after NGF application.

3.3.9 Summary

Combining the retrograde labeling with whole cell patch-clamp techniques, the mechanosensitivity of target identified sensory neurons can be examined in cultured DRG neurons. My results showed that mechanoinsensitive neurons do exist in both muscle and cutaneous innervating neurons in culture. The proportion of mechanoinsensitive neurons in muscle is 4 times as high as that found in the skin.

But the electrical excitability of sensory neurons innervating muscle and skin was not dramatically different. We conclude that tissue specific mechanosensitivity is in part due to the RP generation level rather than the AP generation level. In addition, an important inflammatory mediator NGF can significantly elevate the proportion of mechanosensitive neurons in muscle afferents. This mechanosenstive current induction occurs rapidly, as fast as 15 min in 40% of the TrKA+ silent neurons. Moreover, the long-term treatment of NGF also changed neuron excitability in AP amplitude.

4. Discussion

Mechanoreceptor neurons usually transform a continuously varying mechanical stimulus into trains of discrete APs. This transformation has traditionally been viewed as a three-stage process. Firstly, the input stimulus modulates the opening of mechanically sensitive ion channels, generating a transmembrane ion flux called the receptor current. Secondly, the receptor current passing through other membrane conductances creates a voltage across the membrane, the RP. Thirdly, the RP is encoded into APs by voltage-sensitive ion channels (Eyzaguirre and Kuffler, 1955; Loewenstein, 1959). Extensive intracellular and extracellular recording studies have shown that the RP and AP are different events mediated by different mechanisms. Both exhibit rapid and slow adaptation. Adaptation describes a phemonenon whereby the response is initially large at stimulus onset and falls off in amplitude (RP) or in firing frequency (AP) despite a constant stimulus. Adaptation at the RP level is thought to be introduced by the external specializations produced by the viscosity of accessory muscle fibers (crayfish stretch receptors) (Rydqvist and Purali, 1993) or membrane lamellae (Pacinian corpuscle) (Loewenstein and Skalak, 1966; Mendelson and Lowenstein, 1964) or by an intrinsic mechanism in which mechanical force is coupled to the mechanosensitive ion channel (hair cell) (Assad and Corey, 1992). AP adaptation is in part the result of a difference in the voltage-gated channels in the receptor membrane (crayfish stretch receptor and spider slit sensilla) (Eyzaguirre and Kuffler, 1955; Juusola and French, 1998). The unanswered questions are: are the RPs and APs acquired distinctively during development? Secondly, whether one or both of the processes contribute to different receptor mechanosensitivity? Thirdly, whether adaptation of the receptor current contributes significantly to the overall adaptation of the AP firing?

4.1 Developmental acquisition of electrical excitability and mechanosensitivity in mouse DRG neurons

4.1.1 Sequential emergence and maturation of electrical excitability in specified sensory neurons

How and when DRG neurons acquire the remarkable ability to detect and transmit information about mechanical stimuli has not been investigated. Previous studies using extracellular recording indicated that mechanical responses cannot be elicited before embryonic day 17 in the rat, whereas electrical responses can already be evoked at E16 (Fitzgerald, 1987b). Here we examined the acquisition sequence and functional maturation of the two distinct events, namely the electrical excitability of sensory neurons and their mechanosensitivity, in the mouse during developmental stages between E11.5 and postnatal day 0 using the whole cell patch-clamp techniques. We showed that sensory neurons with characteristic mechanoreceptor APs (narrow and no hump) appeared at E11.5, shortly after neuronal crest cells (NCC) migrate from the neuronal tube (between embryonic day E8.5 and E10) (Serbedzija et al., 1990), whereas nociceptors characterized by wider APs with humps were born later and observed in significant numbers only from E13.5 onwards (Fig. 12,13). Cell lineage studies from retroviral tracing of single NCCs labeled in the chick neuronal tube showed that there are two consecutive waves of neurogenesis that form the early DRG from migrating NCCs. Putative mechanoreceptors and proprioceptors that are $TrkC^+$ and/or $TrkB^+$ are the first sensory neurons born, between E10 and E11, and arise from one third of the migrating NCCs that express the transcription factors neurogenin 2 (*ngn2*) and runt-related transcription factor-3 (runx3). The second neurogenic wave (E11-E13) of NCCs expresses *ngn1* and *runx1* and gives rise to all subtypes of DRG neurons, the majority of which are $TrkA^+$ nociceptive neurons (Chen et al., 2006; Kramer et al., 2006; Ma et al., 1999). The stage of appearance and the numbers of neurons generated with characterstics of mechanoreceptors and

nociceptors in the present study corroborate the NCCs lineage studies in that the functional electrical excitability of mechanoreceptors and nociceptors is gained just after the sequential migrations of two waves of NCCs. The sensory neural specification is rather genetically determined before NCCs migration (at E9) rather than a phenotype switch from one type of early born neurons to the later born neuron types.

The acquisition of mechanoreceptive and nociceptive AP was accompanied by the clear appearance of voltage-gated sodium currents (Fig. 12). Electrogenesis in neurons has been considered to be the product of activity of the sodium channel and potassium channel. Now we know that multiple isoforms of voltage-gated sodium channels (Na_v) and potassium channels (K_v) are present within mammalian DRG neurons. Sodium channels are broadly divided in to TTX-sensitive (TTX-S) channels with fast inactivation kinetics, which are predominantly expressed in large DRG neurons, and TTX-resistent (TTX-R) channels with slow inactivation kinetics, which are mainly in small DRG neurons. The expression pattern of genes encoding various Na_v channels during development in DRG has not been adequately studied. Only $Na_v1.8$ and $Na_v1.9$ channels have been shown to be expressed at E15 and E17 in rat DRG, respectively (Benn et al., 2001). As to potassium channels, three genes *m-erg1, m- erg2* and *m-erg3* (mice ether a-go-go related gene1-3) have been found to encode K_v channels in mammalian DRG neurons (Polvani et al., 2003). All three *m-erg* genes can be detected as early as E13.5 in mice DRG using whole-mount in situ hybridization. In our study, we showed that TTX-S Na_v channels and K_v channel are already present in small numbers of DRG neurons as early as E11.5. Sensory neurons at this stage possess functional fast inactivating Na^+ and delayed rectifier K^+ currents under depolarization state (Fig. 12). K_v channels might be expressed earlier than Na_v channels, since the delayed rectifier K^+ currents are already observed in immature DRG neurons in which the Na^+ current has not been evoked by depolarization (Fig. 12).

The electrical properties characterized by AP amplitude and half-peak duration were also fine tuned during development in both mechanoreceptors and nociceptors (Fig. 14). The dramatic increase in AP amplitude of nociceptors between E13.5 and E15.5 is perhaps attributable to the progressive developmental acquisition of additional types of Na_v and voltage-dependent sodium conductance. However, the relative stable AP amplitudes of mechanoreceptors might indicate that the types and the amount of Na_v have been already expressed in their mature form as in adult since they first present in these neurons at the earliest stage E11.5. The AP width is determined mainly by the inactivation speed of Na_v channels and activation speed of K_v channels. The general tendency of widening in nociceptive APs and narrowing of mechanoreceptive APs is supposed to be accomplished by the expression of TTX-R sodium channel in nociceptors and maturation or transition of various potassium channels (Polvani et al., 2003). Moreover, the hump of AP in nociceptors, which appeared after E13.5 and contribute at least in part to the broad AP, is also thought to be the major product of the TTX-R sodium channel expression and high voltage-activated calcium current (Blair and Bean, 2002; Yoshida et al., 1978). In addition, repetitive firing of APs was observed only in nociceptors and first emerged at E18.5. The proportion of repetitively firing nociceptors showed an increasing tendency during the first two postnatal weeks (Fig. 15). The TTX-R sodium channels, $Na_v1.8$ and $Na_v1.9$ are supposed to be responsible for repetitive firing by different mechanisms, $Na_v1.8$ channel has depolarized voltage dependence of inactivation and rapid recovery from inactivation (Blair and Bean, 2003; Renganathan et al., 2001), whereas $Na_v1.9$ enhances and prolongs the response to depolarization that are subthreshold for AP electrogenesis (Herzog et al., 2001) and lowers threshold for repetitive firing (Baker et al., 2003). Moreover the contribution of hyperpolarization-activated, cyclic nucleotide-gated channels (HCN) in repetitive firing has also been noticed in DRG neurons (Tu et al., 2004). The appearance of spike adaptation in the late embryonic stage may indicate the functional expression of these channels.

4.1.2 Correlation of mechanosensitivity acquisition with target innervation and genetic switch in DRG neurons

Under voltage clamp mode, the membrane voltage was kept at a constant value using the voltage-clamp circuit, therefore Na_v and K_v channels could have made no contribution to the receptor current evoked by mechanical stimulation. Several previous studies have shown that mechanosensitivity is present after the target innervation is completed. The supramaximal stimulation of lumbosacral spinal nerves of chick embryo could be elicited at E10, whereas the lateral femoral cutaneous nerve reaches the skin at E5 (Honig, 1982). And the innervation of the embryonic rat hindlimb reached the limb distal part by E16.5 (Mirnics and Koerber, 1995), while single nerve recordings showed that cutaneous mechanosensitivity was clearly observed from E17 on (Fitzgerald, 1987b). Both studies indicate that the induction of mechanosensitivity correlates with the onset of target innervation. However, the real responding stage might be still earlier since the extracellular recording in these two studies might miss small numbers of excitable neurons. Our results showed that the mechanosensitive current first appeared at E13.5 with the major form being the RA type and less commonly the IA type mechanosensitive current, which occurred 2 days later than AP appearance (Fig. 16B). This coincides with the study in rat that the electrical property is acquired prior to the mechanosensitivity (Fitzgerald, 1987b) although there is 1.5 day developmental delay between rat and mice (Theiler, 1972; Wischi, 1962). Interestingly, E13.5 is also the time point by which sensory axons reached the distal margin of the forelimb and proliferation of sensory neurons precursors in mouse is completed (Berg and Farel, 2000). Neurotrophins are target-derived trophic factors essential for the survival and maintenance of neurons. Among these, NGF and neurotrophin-3 (NT-3) are particularly important for sensory neurons. Both neurotrophin factors' mRNAs are detectable as early as E10.5, but are expressed in different regions of the developing peripheral nervous system. NT-3 mRNA is particularly intense in the ventral horn adjacent to the DRG, whereas NGF mRNA is more intense over the developing

superficial epithelium at E13.5 (White et al., 1996). By E15.5, NT-3 expression is downregulated, but NGF mRNA is increasingly and intensely expressed in the epithelium of the hindlimb epidermis (White et al., 1996). The temporal and spatial expression of two neurotrophic factors indicate that NGF rather than NT-3 is more likely to be the inductive factor of mechanosensitivity because the timing of its upregulated expression level and restricted expression position in the superficial epithelium are correlated well with the onset of the mechanosensitivity at E13.5. The receptors, TrkA for NGF (Kaplan et al., 1991) and TrkC for NT-3 (Lamballe et al., 1991), are the genetic markers for nociceptors and mechanoreceptors, respectively (Marmigere and Ernfors, 2007). It has been shown that TrKA+ axons first approach cutaneous target fields in proximal hindlimb at E13.5. By E15.5, the TrKA+ fibers have reached the most distal portion of the developing hindlimb and arborize extensively in the cutaneous epithelium of the distal hindlimb, where NGF is intensely expressed (White et al., 1996). The sequential target innervation of nociceptors could explain the findings that the proportions of mechanosensitive neurons in large neurons (>14μm) were constant from the stage when they acquired the mechanosensitivity, whereas the small neurons (<14μm) showed a gradually increased proportion of mechanosensitivity. We suppose that at E13.5, part of the early born nociceptors and most mechanoreceptors have reached their target and acquired mechanosensitivity upon the stimulation of target-derived factors, however the small neurons (<14μm) might be born later and reached their target and acquired mechanosensitivity at E15.5 when the difference of the incidence of mechanosensitive neurons in the large and small groups were eliminated (Fig. 16C).

The SA type mechanosensitive current only emerged with a very low incidence at E16.5 with its mature kinetics and exhibited an increasing proportion at birth. In the adult, the SA type current is almost exclusively observed in the nociceptors and is pharmacologically distinct from the RA type current (Drew et al., 2007; Hu and Lewin, 2006). The appearance and increased proportion of SA type current around birth do not coincide with target contact as the innervation of the limb is largely complete

before birth (Berg and Farel, 2000). Several genetic changes observed around birth in nociceptors might be correlated with the emergence of neurons with SA type current. Firstly, around birth, and during the first 2-3 postnatal weeks, a fraction of nociceptive neurons switch their neurotrophic factor dependence by downregulating expression of TrkA and upregulating that of Ret, a signaling subunit of the receptor complex for members of the GDNF (glial cell line derived neurotrophic factor) ligand family (Molliver and Snider, 1997; Molliver et al., 1997). This neurotrophic factor dependence switch from NGF to GDNF in a subpopulation of nociceptors around birth may stimulate a different signaling pathway mediated by GFLs/GFR (GDNF family ligands/ GFL receptor) binding (Ernsberger, 2008), which might affect or induce mechanosensitivity of the new population of neurons with SA type current. Secondly, nociceptor specific transcription factor Runx1 is downregulated in some nociceptors (Chen et al., 2006; Marmigere et al., 2006). The change of Runx 1 during the late embryonic and postnatal stages is the reason for the above mentioned neurotrophic factor switch (Chen et al., 2006). Therefore, Runx1 could directly or indirectly affect the expression of certain unknown mechanosensitive ion channels or the formation of the molecular machinery, which mediates the SA type current. Runx1 can repress ASIC3 channel and μ-class opioid receptors and upregulate the expression of some ion channels, e.g. P_2X_3 and $Na_v1.9$ (Chen et al., 2006). Although $Runx1^{-/-}$ mice did not show any deficit in responses to mechanical stimuli (Chen et al., 2006), we cannot exclude the possibility that changes in only one population of mechanosensitive neurons induced by the lack of Runx1 would not be noticed in the absence of physiological recordings.

This study showed the two distinct checkpoints for mechanotransduction are developmentally acquired in sequence. In addition, the maturation of electrical properties and appearance of different forms of the mechanosensitive current are also developmentally regulated. The highly regulated appearance of mechanosensitive currents *in vivo* during development allowed us to screen for candidate ion channels whose expression profile matches mechanosensitive current appearance. Upon the

results of mRNA expression profile screen done in our lab, the expression pattern of Degenerin/ENaC sodium channel super family (ASIC2b and ASIC3) and TRP channel family member (TRPC4) coincided well with the mechanosensitivity acquisition (Lechner et al., 2009). However, the requirement of ASIC2b and ASIC3 in forming mechanosensitive currents in sensory neurons has been precluded in cultured adult and embryonic DRG neurons (Drew et al., 2004; Lechner et al., 2009). Further experiments with TRPC4$^{-/-}$ mice will be required to validate the involvement of TRPC4 in mechanotransduction. So far, analysis of TRPC4 mutant mice has not indicated a strong sensory phenotype (Freichel et al., 2005). We conclude that it is most likely that an unknown or uncharacterized membrane protein constitutes the ion channel that underlies mechanosensitive currents in sensory neurons.

4.2 $Ca_v3.2$ is required for cutaneous mechanoreceptor function in mice

4.2.1 $Ca_v3.2$ is necessary for the mechanosensitivity of rapidly adapting mechanoreceptors in detecting displacement and velocity

Extracellular recording from teased cutaneous fibers in mouse (Koltzenburg et al., 1997) has characterized basically five kinds of cutaneous mechanoreceptors according to their conduction velocities and adaptation properties in response to a standardized ramp and hold indentation stimuli (Fig. 1). These five kinds of mechanoreceptors have quite distinct mechanical thresholds (measured by Von Frey test) and spike frequency adaptations. They are either slowly adapting (SAM, AM and C-fibres) or rapidly adapting (RAM and D-hairs). The reason why they have different mechanical threshold and respond with persistent firing or ceased firing to a hold-on stimuli is probably attributable to different RPs and interplay of several voltage-gated ion channels on the nerve endings (Fig. 4). Until now, besides distinguishing the mechanoreceptors according to their physiological characteristics, no molecular

markers uniquely identify specific mechanoreceptor subtypes. An exception is the T-type calcium channel $Ca_v3.2$ which was found to be exclusively expressed in D-hair receptors (Shin et al., 2003). Moreover, $Ca_v3.2$ expression was also detected by in situ hybridization in a subset of small and medium primary afferent neurons (Talley et al., 1999). Despite the observed expression pattern in subtypes of DRG neurons and small or large T-type Ca2+ currents recorded in small and medium diameter neurons (Scroggs and Fox, 1992), respectively, the function of $Ca_v3.2$ in sensory neurons is still controversial (Andre et al., 2003; Baccei and Kocsis, 2000; Barton et al., 2005; Heppenstall and Lewin, 2006; Todorovic et al., 2001).

In this part of the study, we compared the stimulus response properties of all five kinds of cutaneous mechanoreceptors in both wild type and $Ca_v3.2^{-/-}$ mice with a standard series of stimuli applied using a computer controlled mechanical stimulator. The physiological properties (with regard to CV, von Frey threshold and proportion in total DRG population) of individual primary afferent mechanoreceptors in $Ca_v3.2^{-/-}$ were comparable with those in wild type (Table. 2). The firing frequency of each mechanoreceptor was calculated by dividing the spike numbers by the duration of the stimulus (slowly adapting receptors) or its responding time (rapidly adapting receptors). Slowly adapting mechanoreceptors (SAM, AM and C-fibres) exhibited increasing firing rates to increasing displacement amplitude and thus coded the amplitude of the stimulus. Of the rapidly adapting receptors (RAM and D-hairs), D-hairs exhibited a constant firing rate, whereas RAMs had decreased firing rate with increasing displacement, which reflects most likely adaptation during the movement phase. Statistical analysis with repeated-measures ANOVA showed that lack of $Ca_v3.2$ did not alter the mechanical sensitivity of RAMs, SAMs, AMs and C-fibers. However, strikingly, the mechanical sensitivity of D-hairs was dramatically decreased in the mutant mice. Because rapidly adapting mechanoreceptors do not increase their firing rate with increasing displacement amplitude, it suggests that firing rate of D-hair receptor codes the speed of the ramp (which is constant at 1432μm/s) rather than stimulus amplitude. Therefore, we also plotted firing rate against stimulus velocity with

constant amplitude (velocity ranging from 6μm/s-3000μm/s at 96μm). Both of the RA mechanoreceptors code increasing ramp velocity with increased firing rates (Fig. 23). The lack of $Ca_v3.2$ did not affect the ability of RAMs to detect changes in velocity, but dramatically decreased the sensitivity of D-hairs in detecting velocity, especially at slow velocities (Fig. 23). Detailed analysis at velocity of 356μm/s and 1432μm/s on D-hairs during the ramp phase by dividing the responding phase into five equal duration (54ms at 356μm/s and 13.4ms at 1432μm/s) revealed that firing frequency of wild type D-hair reached its plateau within 162ms (356μm/s) and 40ms (1432μm/s) of the stimulation time, which remained constant until the end of the movement phase of the stimulus, whereas the firing frequency in $Ca_v3.2^{-/-}$ was much lower at the beginning and only reached the same level as in wild type much later in the ramp. Therefore, a delayed increase in firing in the $Ca_v3.2^{-/-}$ fiber is the cause of the decreased D-hair mechanosensitivity.

For each receptor type, mechanical threshold was measured as mechanical latency calculated between onset of the mechanical stimulus and the first spike corrected for conduction delay (Fig. 24). In both wild type and $Ca_v3.2^{-/-}$ mice, the slowly adapting mechanoreceptors (SAM, AM and C fibers) displayed decreasing mechanical latency with increasing displacement amplitude, whereas the rapidly adapting mechanoreceptors (D-hair and RAM) showed tendency of increased mechanical latency with increasing stimulus amplitude, which may reflect desensitization of these receptors. Recording from nociceptors in monkeys showed that 30s interstimulation interval is enough for AMs to recover from fatigue and 150s for C fibers (Slugg et al., 2000). We supposed the interstimulation interval used in our experiment (30s) should be enough for most mechanoreceptors to recover from fatigue. However, the attribution of observed possible desensitization can be solved by shuffling the higher displacement amplitude to the front of the small displacement stimuli. Mechanical latency is thought to be dependent on several factors, including stimulus strength, transduction time and the excitability of the membrance adjacent to the site of transduction. As all the stimuli applied are suprathreshold stimuli, the different

behavior of mechanical latency in slowly and rapidly adapting mechanoreceptors could be attributable either to their different RP latency or variety of voltage-gated ion channels which influence the transformation of the RP into APs. As to the contribution of $Ca_v3.2$, the mechanical latencies of the three types of slowly adapting mechanoreceptors were not changed between wild type and $Ca_v3.2^{-/-}$ mice, but the latencies of both RAMs and D-hairs in $Ca_v3.2^{-/-}$ mice were dramatically prolonged (Fig. 21,22). The prolonged mechanical latency was also observed in $Ca_v3.2^{-/-}$ D-hairs with increasing ramp speed, but not in RAMs (Fig. 24). The delayed mechanical latency together with slowered acceleration of firing frequency in the ramp phase suggest slower onset of depolarization.

4.2.2 The lack of $Ca_v3.2$ does not affect the function of mechanosensitive ion channels

To further dissect the function of $Ca_v3.2$ channel in mechanotransduction, mechanosensitive currents was measured with the whole cell patch-clamp method after mechanical stimulation of mechanoreceptors (narrow AP no hump) in culture. Three types of mechanosensitive currents were observed in the mechanoreceptors: 43%(RA), 21% (IA) and 36% (SA) in $Ca_v3.2^{-/-}$ mice and 50% (RA), 15%(IA), 35%(SA) in wild type (Fig. 26). These mechanosensitive currents have comparable latencies of around 300μs in both wild type and $Ca_v3.2^{-/-}$ mice (Fig. 26). We hypothesized that the reduced mechanical sensitivity and higher mechanical threshold of rapidly adapting mechanoreceptors might be due to an impairment in the initiation of AP, since $Ca_v3.2$ is low a voltage-gated ion channel. But this hypothesis was not confirmed. When the threshold currents required to evoke AP were measured in both genotypes under current-clamp mode, they were found to be no different (Fig. 27). The explanation could be due to the lower density of $Ca_v3.2$ on soma than on nerve ending, which masks the function of this low threshold voltage-gated ion channel on the soma in the wild type. The difference in excitability between soma and neurite are also noticed. Current injection on cell body of mechanoreceptive neurons grown in culture would

never evoke more than one spike, whereas the mechanical stimulation on the nerve ending connected with the peripheral structure always induce a cluster of AP trains.

Since the first description of T type Ca^{2+} channels in peripheral sensory neurons (Carbone and Lux, 1984b), expression of functional T-type channel in small capsaicin sensitive DRG neurons suggested its role in painful sensation (Todorovic et al., 2001). Several pieces of experimental evidence support this hypothesis. Redox agents increase T-type currents and exacerbate painful stimuli in rodent models (Todorovic et al., 2001). Conversely, mibefradil, ethosuximide and redox agents that attenuate T-type currents reduce perception of painful stimuli (Barton et al., 2005; Bilici et al., 2001; Matthews and Dickenson, 2001; Todorovic et al., 2001). Similarly, antisense targeting of $Ca_v3.2$ channel, reduced T-type currents in rat sensory neurons and resulted in antinociceptive and antihyperalgesia effects (Bourinet et al., 2005). Moreover $Ca_v3.2^{-/-}$ mice showed decreased pain responses to tonic noxious stimuli (Choi et al., 2007). In spite of this evidence showing the involvement of the $Ca_v3.2$ in behavioural measures of nociception, our results showed that the lack of $Ca_v3.2$ does not affect the mechanical sensitivity and threshold of peripheral nociceptors under normal conditions. However, the mechanical sensitivity in response to stimuli strength of D-hairs and RAMs was dramatically decreased in the $Ca_v3.2^{-/-}$ mice and the mechanical threshold and sensitivity of D-hairs in response to changing velocity were also impaired in $Ca_v3.2^{-/-}$ mice. LVA Ca^{2+} channels activate at potentials near the resting membrane potential, which allow calcium influx below threshold (Magee et al., 1996). This depolarizing current brings the cell to firing threshold for a Na^+ spike. It has been proposed to be a crucial component in shaping subthreshold membrane fluctuations, rebound burst firing (Llinas and Yarom, 1981), rhythmic oscillation (Bal and McCormick, 1993; Gutnick and Yarom, 1989) and pacemaker activity (Bal and McCormick, 1993; Puil et al., 1994). In the present study, the lack of T-type Ca^{2+} current in the neuron, in which the $Ca_v3.2$ was enriched previously, will make the transformation from mechanical RPI into AP become much harder without the help of this fast Ca^{2+} current. This might be the reason that there is a long delay to reach the threshold for opening the Na_v channel directly (Fig. 35).

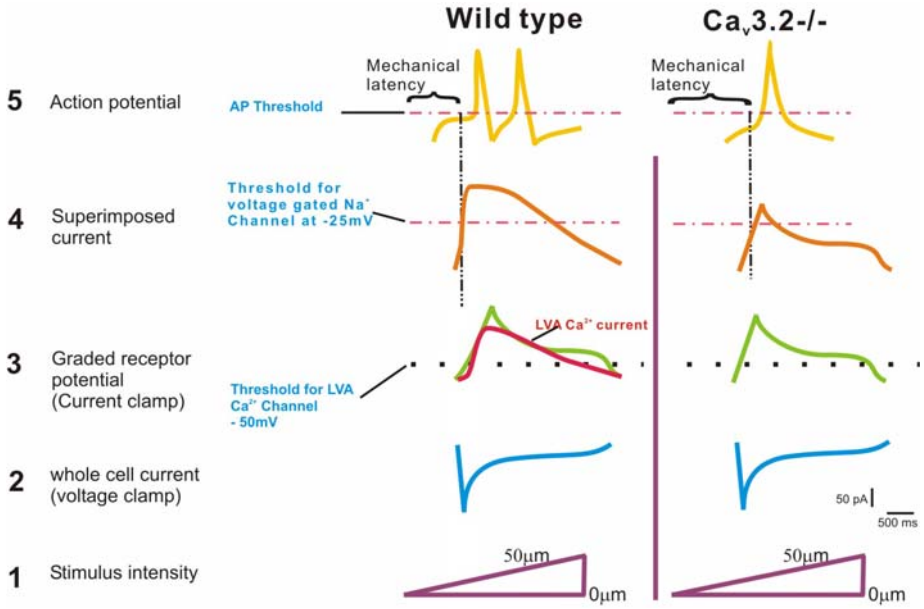

Fig. 35: A schematic diagram showing the assumed AP generation processes in response to increasing stimuli at the nerve terminal of D-hair receptors in wild type and $Ca_V3.2^{-/-}$ mice.

Moving stimuli evoke inward currents **(row 1)**, which can be measured at the receptor ending under voltage clamp and reflect opening of mechanically gated cation channels **(row 2)**. The RP (green) caused by the inward current under current clamp reaches the threshold for activation of the LVA Ca^{2+} channel (dotted black line) in wild type but not in $Ca_v3.2^{-/-}$ **(row 3)**. The summation of RP and transient Ca^{2+} currents bring the small deflection in membrane potential up to the activation threshold of Na_v quickly in wild type (pink dotted line). In contrast, only when the RP alone reaches the threshold of Na_v, can be AP generated in $Ca_v3.2^{-/-}$ (**row 4**). Therefore, the AP is generated with a shorter latency in wild type than in $Ca_v3.2^{-/-}$ (**row 5**).

4.3 Tissue specific mechanosensitivity and distinct sensitization mechanism

4.3.1 The proportion of mechanoinsensitive neurons innervating different tissue gives rise to tissue specific mechanosensation

Deep tissue and visceral pain differ in many ways from cutaneous pain. Pain associated with muscle and visceral lesion is described as aching and cramping, while cutaneous pain is characterized by its sharp, pricking, stabbing or burning nature. Muscle and visceral pain is difficult to localize, whereas, cutaneous pain is localized with great accuracy. It is known that innervation density decreases in the following order skin > muscle > viscera (Mense, 1993). Considering the different tissue specific mechanosensitivity, the question arises: firstly, whether there are different types of transducer in deep sensor afferents? Secondly, whether electrical excitability of such neurons gives rise to distinct sensations. It has been shown that the electrical activation of thin myelinated and non-myelinated afferent fibers in a muscle nerve elicited the same dull and aching quality as nociceptive mechanical stimulation did (Torebjork et al., 1984). Moreover, a class of nociceptors that were termed mechanically insensitive nociceptors (MIA) have been identified and thought to contribute to different tissue sensation and inflammation induced hyperalgesia (Meyer et al., 1991). Because they do not respond to acute noxious mechanical or thermal stimuli, they are sometimes called “silent” or “sleeping” nociceptors. This situation has been well demonstrated for different painful joint and visceral conditions. A large number of primary afferents (particularly in the C-fibre range) in joint (Schaible and Grubb, 1993; Schaible and Schmidt, 1988a; Schaible and Schmidt, 1988b) and urinary bladder (Habler et al., 1990; Sengupta and Gebhart, 1994) cannot be excited by noxious stimuli, but some of them begin to respond to innocuous mechanical stimuli after inflammatory insult. This type of nociceptors has also been described in primate (Meyer et al., 1991; Schmidt et al., 1995; Weidner et al., 1999) and rodent skin (Handwerker et al., 1991; Kress et al., 1992; Lewin and Mendell, 1994), but is

much less common in skin than in joint and viscera. In skeletal muscle such receptors have not been examined in detail (Mense, 1993).

In the current study, GS muscle and hindpaw cutaneous innvervating neurons were separately labeled by fluorescent labeled dextran amine. With the whole cell patch-clamp technique we are able to dissect the mechanotransduction current from membrane excitability in target identified sensory neurons. If the mechanosensitive current is neither evoked on soma nor on neurite, this neuron will be counted as a mechanoinsensitive one. My results showed that MIA do exist in both muscle and cutaneous innervating neurons in culture, but the proportion of MIA in muscle is 4 times as high as that found in the skin (Fig. 30A). However, the electrical excitability measured by AP activation threshold and AP amplitude (Fig. 30B and C) in sensory neurons innervating different tissues was comparable. Here we conclude that tissue specific mechanosensitivity is produced in part at the level of RP generation rather than at the level of different voltage-gated ion channels on the nerve endings.

4.3.2 Muscle sensitization induced by NGF happens at both the generation of mechanosensitive current and electrical excitability level

In vivo recordings have shown that the silent neurons innervating the cat knee joint (Schaible and Schmidt, 1988a), urinary bladder (Habler et al., 1990) and skin (Meyer and Campbell, 1988; Meyer et al., 1991) could be excited by inflammatory agents or irritant chemicals. These silent afferents first developed ongoing activity induced by irritant chemicals directly and then began to respond to innocuous mechanical stimuli, such as joint movement or storage of fluid in the urinary bladder. Among various inflammatory mediators, neurotrophic factor NGF has been shown to have an algesic effect. NGF plays an important role in the development of nociceptive neurons (Lewin and Mendell, 1993) but is also involved in sensory modulation of the adult nervous system (Lewin et al., 1993; Merighi et al., 2004). A single systemic injection of NGF in adult rats initiated thermal hyperalgesia within minutes that lasted for days and also

induced a delayed mechanical hyperalgesia with 7 hours latency (Lewin et al., 1994). Also, transgenic mice overexpressing NGF in the skin show a marked mechanical hyperalgesia (Davis et al., 1993a). In human studies, systemic or intradermal administration of recombinant human NGF cause diffuse myalgias and pressure allodynia on NGF-injected side (Dyck et al., 1997; Petty et al., 1994), while intramuscularly injected NGF evoked long-lasting mechanical allodynia and hyperalgesia (Svensson et al., 2003). Based on the previous findings, we examined the effect of NGF on the mechanosensitivity in previously found muscle innervating "silent" neurons. Our results indicated that both 4 hours treatment of NGF in culture and a single systemic NGF injection 24 hours before harvesting DRGs dramatically elevated the proportion of mechanosensitive neurons from 60% to 90% in muscle labeled neurons. The "unsilenced" muscle afferent neurons mainly fell into groups with RA and IA type mechanosensitive currents. In addition the electrical excitabilities of neurons were not affected in the 4 hour culture NGF treated group, but an elevated AP amplitude was recorded in the 24 hour NGF systemic injection group. A short-term perfusion experiment with a high dose of NGF (100ng/ml) induced a mechanosensitive current in 40% of IB4- silent neurons within 15 minutes indicating the mechanical sensitization might be mediated in part by posttranslational processing. But this mechanical sensitization has to be ruled out by the repeated stimulation in the absence of NGF since repetitive mechanical stimulation may also cause mechanical sensitization (Handwerker et al., 1991).

4.3.3 Possible signaling pathway involved in NGF induced muscle mechanical sensitization

A number of ion channels involved in hyperalgesia are regulated by NGF. Both TTX-S and TTX-R sodium currents are increased in DRG neurons by NGF as a result of increased expression level of these sodium ion channels (Leffler et al., 2002; Okuse et al., 1997). These NGF-induced changes are likely to have a major impact on the excitability of nociceptive neurons. Moreover, extensively studied TRPV1 and ASIC3

channels are regulated by NGF through post-translational and transcription controls (Mamet et al., 2002; Stucky and Lewin, 1999). The binding of NGF to TrKA stimulates homodimer formation and activation of tyrosine kinase activity, resulting in the activation of a series of signaling pathways, notably the ras-raf-MAPK, PI3K-Akt-GSKIII, PLCγ-DAG-PKC and S6kinase. More recent data have shown that short-term sensitization of TRPV1 by NGF is mediated by two pathways (Zhang et al., 2005): one is the PI3K-Src induced TRPV1 phosphorylation, leading to trafficking and insertion of the channel into the surface membrane. The other is PLCγ/PKCε signalling pathway caused phosphorylation of TRPV1, sensitizing the channel basal activity. However, the increase in TRPV1 expression induced by NGF has also been found to be mediated by the TrkA-dependent MAPK pathways (Bron et al., 2003). Similarly, NGF controls ASIC3 basal expression through constitutive activation of a TrKA/ PLCγ/PKC pathway (Mamet et al., 2003). As for the mechanosensitive ion channel, due to the lack of its molecular identity, understanding of the molecular mechanisms and intracellular signaling pathway of mechanical sensitization lags behind that of thermal or chemical sensation. However, it has been shown in our lab that NGF can induce the mechanosensitive current of embryonic DRG neurons and modulate the kinetics of the current from RA type into IA type current in postnatal stage (Lechner et al., 2009). Di Castro and colleagues also showed that mainly in peptidergic nociceptors, activation the PKC signaling cascade increased the mechanosensitivity of DRG neurons in current amplitude by inducing insertion of new transduction channels into the cell membrane, whereas NGF acted at the transcriptional level to increase the availability of these channels or a factor that allow PKC-dependent membrance insertion of the channel (Di Castro et al., 2006).

Here we showed that NGF alone recruited mechanosensitive ion channels to the membrane surface or activated these ion channels from their silent state by an unknown mechanism. In addition the long term but not short-term treatment with NGF could also increase the neuronal excitability.

The present findings are in agreement with the hypothesis that inflammatory processes sensitized at least part of the unresponsive units. These units then become responsive to mechanical stimuli. In this case inflammatory pain and hyperalgesia may be more a function of the recruitment of a larger population of thin afferent units than of the sensitization of C-MHs, and spatial summation at central synapses will be more important than temporal summation.

5. Summary

The mechanotransduction process utilized by auditory/vestibular system and somatosensory system is broadly viewed as a two-stage process: mechanical stimuli open the mechanosensitive ion channels, generating a RP, which is encoded into APs by voltage sensitive ion channels. The mechanosensitivity of cutaneous and deep tissue mechanoreceptors is profoundly affected by unidentified mechanosenstive ion channel at the first stage and interplay of various voltage-gated ion channels at the second stage. The contribution of these two types of ion channels underlying target dependent sensitivity and mechanical sensitization has not been adequately studied.

In the present study, we took a well-established mouse DRG culture as a model to study the mechanotransduction processes. By using the whole cell patch-clamp technique, three types of mechanosensitive currents are evoked by stimulating the cell soma or neurite with a nanomotor.

In the first part of this study, we showed that the two processes involved in somatosensory mechanotransduction are sequentially acquired during development. The electrical excitability of DRG neurons is acquired prior to the mechanosensitivity and characteristic electrical excitabilities of mechanoreceptors and nociceptors are fine tuned during the whole developmental stages. As to mechanosensitivity, the RA type mechanosensitive current is gained by most DRG neurons at E13.5, which is correlated with the peripheral target innervation, whereas neurons with SA type current only appear later at E16.5 and reach in significant number at birth. Therefore, the highly regulated appearance of mechanosensitive currents *in vitro* allowed us to screen candidate genes involved in mechanotransduction, whose expression profile matches mechanosensitive current appearance.

$Ca_v3.2$ is a low voltage activated calcium ion channel, which has been found highly

expressed in subtypes of DRG neurons. Our lab showed that it is enriched in the most sensitive cutaneous mechanoreceptors, D-hairs, and may be required for the normal D-hair mechanosensitivity. However, $Ca_v3.2$ is also implicated in nociception by pharmacological and behavior studies from other groups. In the second part of the work, I used an *in vitro* skin nerve preparation to investigate the function of $Ca_v3.2$ in mechanosensitivity of all cutaneous mechanoreceptors by using $Ca_v3.2^{-/-}$ mice. Our results showed that only the mechanosensitivity of D-hair was dramatically reduced in mutant mice. In addition the mechanical latency of both rapidly adapting mechanoreceptors (D-hair and RAM) was delayed. Further experiments with patch-clamp technique showed that the properties of the receptor current were unaltered in mutant mechanoreceptors. Although we did not provide the direct evidence that the lack of $Ca_v3.2$ elevated the threshold of AP generation, from the above experiments we could conclude that the reduced mechanosensitivity in $Ca_v3.2^{-/-}$ mice was caused by delayed AP initiation due to the lack of $Ca_v3.2$.

In the third part of my study, we combined retrograde labeling with patch-clamp techniques to investigate the contribution of ion channels involved in two stages of mechanotransduction to target dependent mechanosensitivity. Here we found that differences in mechanosensitivity from skin and deep tissue (gastrocnemius-soleus muscle in this particular case) under normal conditions is attributable mainly to the silence or the lack of unidentified mechanosensitive ion channels in muscle afferent neurons rather than the AP generation level controlled by voltage-gated ion channels. Furthermore, the algesic drug, NGF modulated the mechanosensitivity at both mechanotransduction sites under inflammatory conditions. But the signaling pathway underlying the mechanical sensitization induced by NGF has to be further unraveled.

In conclusion, our work provides for the first time direct evidence that the mechanotransduction is a two-stage developmental process, that the mechanosensitivity of different mechanoreceptors could be endowed by ion channels involved at any level of the transduction process. Finally, inflammatory mediators can

modulate the mechansensitivity from both processes.

6. Zusammenfassung

Der Mechanotransduktionsprozess des auditären/vestibulären Systems and des somato-sensorischen Systems wird allgemein als zwei-Stufen Prozess angesehen. Mechanische Stimuli öffnen mechanosensitive Inonenkanäle und generieren ein RP, welches durch spannungsabhängige Inonenkanäle in APs kodiert wird. Die Sensibilität der kutanen Mechanorezeptoren und Mechanorezeptoren des tieferliegenden Gewebes wird auf der ersten Stufe von unbekannten mechanosensitiven Ionenkanälen, und auf der zweiten Stufe durch ein Wechselspiel unterschiedlicher spannungsabhängiger Ionenkanäle hochgradig beeinflusst. Die Beteiligung dieser beiden Kanaltypen bezüglich der gewebspezifischen mechanischen Sensibilisierung wurde bisher kaum untersucht.

In der vorliegenden Arbeit verwendeten wir ein etabliertes Maus DRG Zellkultur-Modell um den Mechanotransduktionsprozess zu untersuchen. Durch vorhergehende Arbeiten mittels der whole-cell patch clamp Methode ist bekannt, dass ducrh mechanische Stimulation des Zellsomas oder der Neuriten durch einen Nanomotor drei unterschiedliche Typen an Strömen erzeugt werden.

Im ersten Teil dieser Arbeit konnten wir zeigen, dass die beiden an somatosensorischer Mechanotransduktion beteiligten Prozesse während der embryonalen Entwicklung sequentiell erworben werden. Die elektrische Erregbarkeit von DRG Neuronen wird vor der Mechanosensisitivität erworben, und die charakteristische elektrische Erregbarkeit wird während aller Entwicklungsstadien abgestimmt. Die meisten DRG Neurone erhalten den mechanosensitive Strom des RA-Typs zum Embryonalstadium E13.5, was mit der Innervation peripheren Gewebes einhergeht, während der Strom des SA-Typs bei E16.5 erscheint und erst bei der Geburt eine signifikante Anzahl erreicht. Die streng regulierte Erscheinung mechanosensitiver Ströme *in vitro* ermöglichte es uns, mögliche an der Mechanotransduktion beteiligten Gene, deren Expressionsprofil mit dem Vorkommen

mechanosensitiver Ströme übereinstimmt, zu screenen.

$Ca_v3.2$ ist ein spannungsaktivierter Kalzium-Ionenkanal, der in Subtypen von DRG Neuronen stark exprimiert wird. In unserem Labor konnte gezeigt werden, dass er in den sensitivsten cutanen Mechanorezeptoren, den D-hairs, angereichert ist, und er könnte für die normale D-hair Mechanosensitivität notwendig sein. Andere Arbeitsgruppen zeigten durch pharmakologische Versuche und Verhaltensexperimente, dass $Ca_v3.2$ auch bei der Schmerzempfindung eine Rolle zu spielen scheint. Im zweiten Teil dieser Arbeit führten wir *in vitro* Experimente mittels Haut-Nerv-Preparationen an $Ca_v3.2^{-/-}$-Mäusen durch, um die Funktion von $Ca_v3.2$ bei der Mechanosensitivität aller cutanen Mechanorezeptoren zu untersuchen. Wir beobachteten, dass die Mechanosensitivität bei $Ca_v3.2^{-/-}$-Mäusen nur in D-Hairs signifikant reduziert war. Ausserdem war die mechanische Latenzzeit beider “rapidly-adapting” Mechanorezeptoren (D-Hair und RAM) verlängert. Anhand der Patch Clamp Methode konnten wir zeigen, dass die Eigenschaften des Rezeptorstromes in $Ca_v3.2^{-/-}$-Mäusen unverändert blieb. Auch wenn wir nicht den direkten Beweis dafür erbrachten, dass das Fehlen von $Ca_v3.2$ zu einer Erhöhung des Grenzwertes zur AP Generierung führt, so können wir dennoch aus obigen Ergebnissen schliessen, dass die reduzierte Mechanosensitivität in $Ca_v3.2^{-/-}$-Mäusen durch eine verspätete AP Initiierung mangels $Ca_v3.2$ verursacht wird.

Im dritten Teil dieser Arbeit kombinierten wir retrograde Markierungs-Experimente mit der Patch Clamp Methode, um die Beteiligung von an beiden Stufen der Mechanotransduktion involvierten Ionenkanälen bezüglich gewebspezifischer Mechanosensitivität zu untersuchen. Wir konnten zeigen, dass unter Normalbedingungen Unterschiede bezüglich der Mechanosensitivität der Haut and des teferliegenden Gewebes (hier: gastrocnemius-soleus-Muskel) hauptsächlich der nicht-Aktivierung oder den Mangel an unidentifizierten machanosensitiven Ionenkanälen in den Muskel innervierenden Neuronen, und weniger der durch spannungsabhängige Ionenkanäle kontrollierten AP Generation zuzuordnen ist.

Ausserdem beobachteten wir, dass NGF unter inflammatorischen Bedingungen die Mechanosensitivität von sowohl Mechanorezeptoren der Haut als auch des tieferliegenden Gewebes moduliert. Der dieser Sensitivierung zugrundeliegende und durch NGF induzierte Signalweg sollte weiter untersucht werden.

Diese Arbeit liefert den ersten direkten Beweis dafür, dass Mechanotransduktion ein zwei-stufiger Entwicklungsprozess ist und dass die Mechanosensitivität unterschiedlicher Mechanorezeptoren an jeder Stelle des Transduktionsprozesses durch beteiligte Ionenkanäle erbracht wird. Schliesslich wurde gezeigt, dass inflammatorische Mediatoren die Mechanosensitivität beider Prozesses modulieren.

7. References

Adriaensen, H., Gybels, J., Handwerker, H. O., and Van Hees, J. (1983). Response properties of thin myelinated (A-delta) fibers in human skin nerves. J Neurophysiol *49*, 111-122.

Adrian, E. D., and Umrath, K. (1929). The impulse discharge from the pacinian corpuscle. J Physiol *68*, 139-154.

Ahmed, Z. M., Goodyear, R., Riazuddin, S., Lagziel, A., Legan, P. K., Behra, M., Burgess, S. M., Lilley, K. S., Wilcox, E. R., Griffith, A. J.*, et al.* (2006). The tip-link antigen, a protein associated with the transduction complex of sensory hair cells, is protocadherin-15. J Neurosci *26*, 7022-7034.

Andre, S., Puech-Mallie, S., Desmadryl, G., Valmier, J., and Scamps, F. (2003). Axotomy differentially regulates voltage-gated calcium currents in mice sensory neurones. Neuroreport *14*, 147-150.

Assad, J. A., and Corey, D. P. (1992). An active motor model for adaptation by vertebrate hair cells. J Neurosci *12*, 3291-3309.

Baccei, M. L., and Kocsis, J. D. (2000). Voltage-gated calcium currents in axotomized adult rat cutaneous afferent neurons. J Neurophysiol *83*, 2227-2238.

Baker, M. D., Chandra, S. Y., Ding, Y., Waxman, S. G., and Wood, J. N. (2003). GTP-induced tetrodotoxin-resistant Na+ current regulates excitability in mouse and rat small diameter sensory neurones. J Physiol *548*, 373-382.

Bal, T., and McCormick, D. A. (1993). Mechanisms of oscillatory activity in guinea-pig nucleus reticularis thalami in vitro: a mammalian pacemaker. J Physiol *468*, 669-691.

Barton, M. E., Eberle, E. L., and Shannon, H. E. (2005). The antihyperalgesic effects of the T-type calcium channel blockers ethosuximide, trimethadione, and mibefradil. Eur J Pharmacol *521*, 79-85.

Baumann, T. K., Simone, D. A., Shain, C. N., and LaMotte, R. H. (1991). Neurogenic hyperalgesia: the search for the primary cutaneous afferent fibers that contribute to capsaicin-induced pain and hyperalgesia. J Neurophysiol *66*, 212-227.

Benn, S. C., Costigan, M., Tate, S., Fitzgerald, M., and Woolf, C. J. (2001). Developmental expression of the TTX-resistant voltage-gated sodium channels Nav1.8 (SNS) and Nav1.9 (SNS2) in primary sensory neurons. J Neurosci *21*, 6077-6085.

Berberich, P., Hoheisel, U., and Mense, S. (1988). Effects of a carrageenan-induced myositis on the discharge properties of group III and IV muscle receptors in the cat. J Neurophysiol *59*, 1395-1409.

Berg, J. S., and Farel, P. B. (2000). Developmental regulation of sensory neuron number and limb innervation in the mouse. Brain Res Dev Brain Res *125*, 21-30.

Bilici, D., Akpinar, E., Gursan, N., Dengiz, G. O., Bilici, S., and Altas, S. (2001). Protective effect of T-type calcium channel blocker in histamine-induced paw inflammation in rat. Pharmacol Res *44*, 527-531.

Blair, N. T., and Bean, B. P. (2002). Roles of tetrodotoxin (TTX)-sensitive Na+ current, TTX-resistant Na+ current, and Ca2+ current in the action potentials of nociceptive sensory neurons. J Neurosci *22*, 10277-10290.

Blair, N. T., and Bean, B. P. (2003). Role of tetrodotoxin-resistant Na+ current slow inactivation in adaptation of action potential firing in small-diameter dorsal root ganglion neurons. J Neurosci *23*, 10338-10350.

Bourinet, E., Alloui, A., Monteil, A., Barrere, C., Couette, B., Poirot, O., Pages, A., McRory, J., Snutch, T. P., Eschalier, A., and Nargeot, J. (2005). Silencing of the Cav3.2 T-type calcium channel gene in sensory neurons demonstrates its major role in nociception. Embo J *24*, 315-324.

Bron, R., Klesse, L. J., Shah, K., Parada, L. F., and Winter, J. (2003). Activation of Ras is necessary and sufficient for upregulation of vanilloid receptor type 1 in sensory neurons by neurotrophic factors. Mol Cell Neurosci *22*, 118-132.

Brown, A. G., and Iggo, A. (1967). A quantitative study of cutaneous receptors and afferent fibres in the cat and rabbit. J Physiol *193*, 707-733.

Burgess, P. R., and Perl, E. R. (1967). Myelinated afferent fibres responding specifically to noxious stimulation of the skin. J Physiol *190*, 541-562.

Carbone, E., and Lux, H. D. (1984a). A low voltage-activated calcium conductance in embryonic chick sensory neurons. Biophys J *46*, 413-418.

Carbone, E., and Lux, H. D. (1984b). A low voltage-activated, fully inactivating Ca channel in vertebrate sensory neurones. Nature *310*, 501-502.

Caterina, M. J., Leffler, A., Malmberg, A. B., Martin, W. J., Trafton, J., Petersen-Zeitz, K. R., Koltzenburg, M., Basbaum, A. I., and Julius, D. (2000). Impaired nociception and pain sensation in mice lacking the capsaicin receptor. Science *288*, 306-313.

Chalfie, M. (1997). A molecular model for mechanosensation in Caenorhabditis elegans. Biol Bull *192*, 125.

Chen, C. C., Lamping, K. G., Nuno, D. W., Barresi, R., Prouty, S. J., Lavoie, J. L., Cribbs, L. L., England, S. K., Sigmund, C. D., Weiss, R. M*., et al.* (2003). Abnormal coronary function in mice deficient in alpha1H T-type Ca2+ channels. Science *302*, 1416-1418.

Chen, C. L., Broom, D. C., Liu, Y., de Nooij, J. C., Li, Z., Cen, C., Samad, O. A., Jessell, T. M., Woolf, C. J., and Ma, Q. (2006). Runx1 determines nociceptive sensory neuron phenotype and is required for thermal and neuropathic pain. Neuron *49*, 365-377.

Choi, S., Na, H. S., Kim, J., Lee, J., Lee, S., Kim, D., Park, J., Chen, C. C., Campbell,

K. P., and Shin, H. S. (2007). Attenuated pain responses in mice lacking Ca(V)3.2 T-type channels. Genes Brain Behav *6*, 425-431.

Chung, Y. D., Zhu, J., Han, Y., and Kernan, M. J. (2001). nompA encodes a PNS-specific, ZP domain protein required to connect mechanosensory dendrites to sensory structures. Neuron *29*, 415-428.

Corey, D. P., Garcia-Anoveros, J., Holt, J. R., Kwan, K. Y., Lin, S. Y., Vollrath, M. A., Amalfitano, A., Cheung, E. L., Derfler, B. H., Duggan, A.*, et al.* (2004). TRPA1 is a candidate for the mechanosensitive transduction channel of vertebrate hair cells. Nature *432*, 723-730.

Davis, B. M., Lewin, G. R., Mendell, L. M., Jones, M. E., and Albers, K. M. (1993a). Altered expression of nerve growth factor in the skin of transgenic mice leads to changes in response to mechanical stimuli. Neuroscience *56*, 789-792.

Davis, J. B., Gray, J., Gunthorpe, M. J., Hatcher, J. P., Davey, P. T., Overend, P., Harries, M. H., Latcham, J., Clapham, C., Atkinson, K.*, et al.* (2000). Vanilloid receptor-1 is essential for inflammatory thermal hyperalgesia. Nature *405*, 183-187.

Davis, K. D., Meyer, R. A., and Campbell, J. N. (1993b). Chemosensitivity and sensitization of nociceptive afferents that innervate the hairy skin of monkey. J Neurophysiol *69*, 1071-1081.

Di Castro, A., Drew, L. J., Wood, J. N., and Cesare, P. (2006). Modulation of sensory neuron mechanotransduction by PKC- and nerve growth factor-dependent pathways. Proc Natl Acad Sci U S A *103*, 4699-4704.

Drew, L. J., Rohrer, D. K., Price, M. P., Blaver, K. E., Cockayne, D. A., Cesare, P., and Wood, J. N. (2004). Acid-sensing ion channels ASIC2 and ASIC3 do not contribute to mechanically activated currents in mammalian sensory neurones. J Physiol *556*, 691-710.

Drew, L. J., Rugiero, F., Cesare, P., Gale, J. E., Abrahamsen, B., Bowden, S., Heinzmann, S., Robinson, M., Brust, A., Colless, B.*, et al.* (2007). High-threshold mechanosensitive ion channels blocked by a novel conopeptide mediate pressure-evoked pain. PLoS ONE *2*, e515.

Drew, L. J., Wood, J. N., and Cesare, P. (2002). Distinct mechanosensitive properties of capsaicin-sensitive and -insensitive sensory neurons. J Neurosci *22*, RC228.

Du, H., Gu, G., William, C. M., and Chalfie, M. (1996). Extracellular proteins needed for C. elegans mechanosensation. Neuron *16*, 183-194.

Dyck, P. J., Peroutka, S., Rask, C., Burton, E., Baker, M. K., Lehman, K. A., Gillen, D. A., Hokanson, J. L., and O'Brien, P. C. (1997). Intradermal recombinant human nerve growth factor induces pressure allodynia and lowered heat-pain threshold in humans. Neurology *48*, 501-505.

Ernsberger, U. (2008). The role of GDNF family ligand signalling in the differentiation

of sympathetic and dorsal root ganglion neurons. Cell Tissue Res *333*, 353-371.

Ernstrom, G. G., and Chalfie, M. (2002). Genetics of sensory mechanotransduction. Annu Rev Genet *36*, 411-453.

Eyzaguirre, C., and Kuffler, S. W. (1955). Processes of excitation in the dendrites and in the soma of single isolated sensory nerve cells of the lobster and crayfish. J Gen Physiol *39*, 87-119.

Ferrington, D. G., Hora, M. O., and Rowe, M. J. (1984). Functional maturation of tactile sensory fibers in the kitten. J Neurophysiol *52*, 74-85.

Fitzgerald, M. (1987a). Cutaneous primary afferent properties in the hind limb of the neonatal rat. J Physiol *383*, 79-92.

Fitzgerald, M. (1987b). Spontaneous and evoked activity of fetal primary afferents in vivo. Nature *326*, 603-605.

Fjell, J., Cummins, T. R., Fried, K., Black, J. A., and Waxman, S. G. (1999). In vivo NGF deprivation reduces SNS expression and TTX-R sodium currents in IB4-negative DRG neurons. J Neurophysiol *81*, 803-810.

Freichel, M., Vennekens, R., Olausson, J., Stolz, S., Philipp, S. E., Weissgerber, P., and Flockerzi, V. (2005). Functional role of TRPC proteins in native systems: implications from knockout and knock-down studies. J Physiol *567*, 59-66.

Fricke, B., Lints, R., Stewart, G., Drummond, H., Dodt, G., Driscoll, M., and von During, M. (2000). Epithelial Na+ channels and stomatin are expressed in rat trigeminal mechanosensory neurons. Cell Tissue Res *299*, 327-334.

Fukushige, T., Siddiqui, Z. K., Chou, M., Culotti, J. G., Gogonea, C. B., Siddiqui, S. S., and Hamelin, M. (1999). MEC-12, an alpha-tubulin required for touch sensitivity in C. elegans. J Cell Sci *112 (Pt 3)*, 395-403.

Garcia-Anoveros, J., Samad, T. A., Zuvela-Jelaska, L., Woolf, C. J., and Corey, D. P. (2001). Transport and localization of the DEG/ENaC ion channel BNaC1alpha to peripheral mechanosensory terminals of dorsal root ganglia neurons. J Neurosci *21*, 2678-2686.

Geleoc, G. S., and Holt, J. R. (2003). Developmental acquisition of sensory transduction in hair cells of the mouse inner ear. Nat Neurosci *6*, 1019-1020.

Gillespie, P. G., and Walker, R. G. (2001). Molecular basis of mechanosensory transduction. Nature *413*, 194-202.

Gong, Z., Son, W., Chung, Y. D., Kim, J., Shin, D. W., McClung, C. A., Lee, Y., Lee, H. W., Chang, D. J., Kaang, B. K.*, et al.* (2004). Two interdependent TRPV channel subunits, inactive and Nanchung, mediate hearing in Drosophila. J Neurosci *24*, 9059-9066.

Goodman, M. B., Ernstrom, G. G., Chelur, D. S., O'Hagan, R., Yao, C. A., and Chalfie,

M. (2002). MEC-2 regulates C. elegans DEG/ENaC channels needed for mechanosensation. Nature *415*, 1039-1042.

Gopfert, M. C., Albert, J. T., Nadrowski, B., and Kamikouchi, A. (2006). Specification of auditory sensitivity by Drosophila TRP channels. Nat Neurosci *9*, 999-1000.

Grigg, P., Schaible, H. G., and Schmidt, R. F. (1986). Mechanical sensitivity of group III and IV afferents from posterior articular nerve in normal and inflamed cat knee. J Neurophysiol *55*, 635-643.

Gu, G., Caldwell, G. A., and Chalfie, M. (1996). Genetic interactions affecting touch sensitivity in Caenorhabditis elegans. Proc Natl Acad Sci U S A *93*, 6577-6582.

Gutnick, M. J., and Yarom, Y. (1989). Low threshold calcium spikes, intrinsic neuronal oscillation and rhythm generation in the CNS. J Neurosci Methods *28*, 93-99.

Habler, H. J., Janig, W., and Koltzenburg, M. (1990). Activation of unmyelinated afferent fibres by mechanical stimuli and inflammation of the urinary bladder in the cat. J Physiol *425*, 545-562.

Handwerker, H. O., Kilo, S., and Reeh, P. W. (1991). Unresponsive afferent nerve fibres in the sural nerve of the rat. J Physiol *435*, 229-242.

Hardy, J. D., Wolff, H. G., and Goodell, H. (1950). Experimental evidence on the nature of cutaneous hyperalgesia. J Clin Invest *29*, 115-140.

Heppenstall, P. A., and Lewin, G. R. (2006). A role for T-type Ca2+ channels in mechanosensation. Cell Calcium *40*, 165-174.

Herzog, R. I., Cummins, T. R., and Waxman, S. G. (2001). Persistent TTX-resistant Na+ current affects resting potential and response to depolarization in simulated spinal sensory neurons. J Neurophysiol *86*, 1351-1364.

Hoheisel, U., Unger, T., and Mense, S. (2005). Excitatory and modulatory effects of inflammatory cytokines and neurotrophins on mechanosensitive group IV muscle afferents in the rat. Pain *114*, 168-176.

Holt, J. R., Gillespie, S. K., Provance, D. W., Shah, K., Shokat, K. M., Corey, D. P., Mercer, J. A., and Gillespie, P. G. (2002). A chemical-genetic strategy implicates myosin-1c in adaptation by hair cells. Cell *108*, 371-381.

Honig, M. G. (1982). The development of sensory projection patterns in embryonic chick hind limb. J Physiol *330*, 175-202.

Hu, J., and Lewin, G. R. (2006). Mechanosensitive currents in the neurites of cultured mouse sensory neurones. J Physiol *577*, 815-828.

Hu, J., Milenkovic, N., and Lewin, G. R. (2006). The high threshold mechanotransducer: a status report. Pain *120*, 3-7.

Huang, M., Gu, G., Ferguson, E. L., and Chalfie, M. (1995). A stomatin-like protein necessary for mechanosensation in C. elegans. Nature *378*, 292-295.

Hudspeth, A. J. (1992). Hair-bundle mechanics and a model for mechanoelectrical transduction by hair cells. Soc Gen Physiol Ser *47*, 357-370.

Hunt, C. C., Wilkinson, R. S., and Fukami, Y. (1978). Ionic basis of the receptor potential in primary endings of mammalian muscle spindles. J Gen Physiol *71*, 683-698.

Iggo, A., and Andres, K. H. (1982). Morphology of cutaneous receptors. Annu Rev Neurosci *5*, 1-31.

Ji, R. R., Samad, T. A., Jin, S. X., Schmoll, R., and Woolf, C. J. (2002). p38 MAPK activation by NGF in primary sensory neurons after inflammation increases TRPV1 levels and maintains heat hyperalgesia. Neuron *36*, 57-68.

Julius, D., and Basbaum, A. I. (2001). Molecular mechanisms of nociception. Nature *413*, 203-210.

Juusola, M., and French, A. S. (1998). Adaptation properties of two types of sensory neurons in a spider mechanoreceptor organ. J Neurophysiol *80*, 2781-2784.

Kamikouchi, A., Inagaki, H. K., Effertz, T., Hendrich, O., Fiala, A., Gopfert, M. C., and Ito, K. (2009). The neural basis of Drosophila gravity-sensing and hearing. Nature *458*, 165-171.

Kaplan, D. R., Hempstead, B. L., Martin-Zanca, D., Chao, M. V., and Parada, L. F. (1991). The trk proto-oncogene product: a signal transducing receptor for nerve growth factor. Science *252*, 554-558.

Kaufman,MH The atlas of mouse development. 515-525 (Acadenuc Oress, London, 1994)

Kasai, M., and Mizumura, K. (2001). Increase in spontaneous action potentials and sensitivity in response to norepinephrine in dorsal root ganglion neurons of adjuvant inflamed rats. Neurosci Res *39*, 109-113.

Kim, J., Chung, Y. D., Park, D. Y., Choi, S., Shin, D. W., Soh, H., Lee, H. W., Son, W., Yim, J., Park, C. S.*, et al.* (2003). A TRPV family ion channel required for hearing in Drosophila. Nature *424*, 81-84.

Kocher, L., Anton, F., Reeh, P. W., and Handwerker, H. O. (1987). The effect of carrageenan-induced inflammation on the sensitivity of unmyelinated skin nociceptors in the rat. Pain *29*, 363-373.

Koerber, H. R., Druzinsky, R. E., and Mendell, L. M. (1988). Properties of somata of spinal dorsal root ganglion cells differ according to peripheral receptor innervated. J Neurophysiol *60*, 1584-1596.

Koltzenburg, M. (2000). Neural mechanisms of cutaneous nociceptive pain. Clin J Pain *16*, S131-138.

Koltzenburg, M., and Lewin, G. R. (1997). Receptive properties of embryonic chick

sensory neurons innervating skin. J Neurophysiol *78*, 2560-2568.

Koltzenburg, M., Lundberg, L. E., and Torebjork, H. E. (1992). Dynamic and static components of mechanical hyperalgesia in human hairy skin. Pain *51*, 207-219.

Koltzenburg, M., Stucky, C. L., and Lewin, G. R. (1997). Receptive properties of mouse sensory neurons innervating hairy skin. J Neurophysiol *78*, 1841-1850.

Kramer, I., Sigrist, M., de Nooij, J. C., Taniuchi, I., Jessell, T. M., and Arber, S. (2006). A role for Runx transcription factor signaling in dorsal root ganglion sensory neuron diversification. Neuron *49*, 379-393.

Kress, M., Koltzenburg, M., Reeh, P. W., and Handwerker, H. O. (1992). Responsiveness and functional attributes of electrically localized terminals of cutaneous C-fibers in vivo and in vitro. J Neurophysiol *68*, 581-595.

Kwan, K. Y., Allchorne, A. J., Vollrath, M. A., Christensen, A. P., Zhang, D. S., Woolf, C. J., and Corey, D. P. (2006). TRPA1 contributes to cold, mechanical, and chemical nociception but is not essential for hair-cell transduction. Neuron *50*, 277-289.

Lamballe, F., Klein, R., and Barbacid, M. (1991). trkC, a new member of the trk family of tyrosine protein kinases, is a receptor for neurotrophin-3. Cell *66*, 967-979.

Lechner, S. G., Frenzel, H., Wang, R., and Lewin, G. R. (2009). Developmental waves of mechanosensitivity acquisition in sensory neuron subtypes during embryonic development. Embo J.

Leem, J. W., Willis, W. D., and Chung, J. M. (1993). Cutaneous sensory receptors in the rat foot. J Neurophysiol *69*, 1684-1699.

Leffler, A., Cummins, T. R., Dib-Hajj, S. D., Hormuzdiar, W. N., Black, J. A., and Waxman, S. G. (2002). GDNF and NGF reverse changes in repriming of TTX-sensitive Na(+) currents following axotomy of dorsal root ganglion neurons. J Neurophysiol *88*, 650-658.

LeMasurier, M., and Gillespie, P. G. (2005). Hair-cell mechanotransduction and cochlear amplification. Neuron *48*, 403-415.

Lewin, G. R., and McMahon, S. B. (1991). Physiological properties of primary sensory neurons appropriately and inappropriately innervating skeletal muscle in adult rats. J Neurophysiol *66*, 1218-1231.

Lewin, G. R., and Mendell, L. M. (1993). Nerve growth factor and nociception. Trends Neurosci *16*, 353-359.

Lewin, G. R., and Mendell, L. M. (1994). Regulation of cutaneous C-fiber heat nociceptors by nerve growth factor in the developing rat. J Neurophysiol *71*, 941-949.

Lewin, G. R., and Moshourab, R. (2004). Mechanosensation and pain. J Neurobiol *61*, 30-44.

Lewin, G. R., Ritter, A. M., and Mendell, L. M. (1992). On the role of nerve growth

factor in the development of myelinated nociceptors. J Neurosci *12*, 1896-1905.

Lewin, G. R., Ritter, A. M., and Mendell, L. M. (1993). Nerve growth factor-induced hyperalgesia in the neonatal and adult rat. J Neurosci *13*, 2136-2148.

Lewin, G. R., Rueff, A., and Mendell, L. M. (1994). Peripheral and central mechanisms of NGF-induced hyperalgesia. Eur J Neurosci *6*, 1903-1912.

Llinas, R., and Yarom, Y. (1981). Electrophysiology of mammalian inferior olivary neurones in vitro. Different types of voltage-dependent ionic conductances. J Physiol *315*, 549-567.

Loewenstein, W. R. (1959). The generation of electric activity in a nerve ending. Ann N Y Acad Sci *81*, 367-387.

Loewenstein, W. R., and Altamiranoorrego, R. (1958). The refractory state of the generator and propagated potentials in a pacinian corpuscle. J Gen Physiol *41*, 805-824.

Loewenstein, W. R., and Cohen, S. (1959a). After-effects of repetitive activity in a nerve ending. J Gen Physiol *43*, 335-345.

Loewenstein, W. R., and Cohen, S. (1959b). Post-tetanic potentiation and depression of generator potential in a single non-myelinated nerve ending. J Gen Physiol *43*, 347-376.

Loewenstein, W. R., and Skalak, R. (1966). Mechanical transmission in a Pacinian corpuscle. An analysis and a theory. J Physiol *182*, 346-378.

Ma, Q., Fode, C., Guillemot, F., and Anderson, D. J. (1999). Neurogenin1 and neurogenin2 control two distinct waves of neurogenesis in developing dorsal root ganglia. Genes Dev *13*, 1717-1728.

Magee, J. C., Avery, R. B., Christie, B. R., and Johnston, D. (1996). Dihydropyridine-sensitive, voltage-gated Ca2+ channels contribute to the resting intracellular Ca2+ concentration of hippocampal CA1 pyramidal neurons. J Neurophysiol *76*, 3460-3470.

Mamet, J., Baron, A., Lazdunski, M., and Voilley, N. (2002). Proinflammatory mediators, stimulators of sensory neuron excitability via the expression of acid-sensing ion channels. J Neurosci *22*, 10662-10670.

Mamet, J., Lazdunski, M., and Voilley, N. (2003). How nerve growth factor drives physiological and inflammatory expressions of acid-sensing ion channel 3 in sensory neurons. J Biol Chem *278*, 48907-48913.

Mannsfeldt, A. G., Carroll, P., Stucky, C. L., and Lewin, G. R. (1999). Stomatin, a MEC-2 like protein, is expressed by mammalian sensory neurons. Mol Cell Neurosci *13*, 391-404.

Marmigere, F., and Ernfors, P. (2007). Specification and connectivity of neuronal

subtypes in the sensory lineage. Nat Rev Neurosci *8*, 114-127.

Marmigere, F., Montelius, A., Wegner, M., Groner, Y., Reichardt, L. F., and Ernfors, P. (2006). The Runx1/AML1 transcription factor selectively regulates development and survival of TrkA nociceptive sensory neurons. Nat Neurosci *9*, 180-187.

Martinez-Salgado, C., Benckendorff, A. G., Chiang, L. Y., Wang, R., Milenkovic, N., Wetzel, C., Hu, J., Stucky, C. L., Parra, M. G., Mohandas, N., and Lewin, G. R. (2007). Stomatin and sensory neuron mechanotransduction. J Neurophysiol *98*, 3802-3808.

Matthews, E. A., and Dickenson, A. H. (2001). Effects of ethosuximide, a T-type Ca(2+) channel blocker, on dorsal horn neuronal responses in rats. Eur J Pharmacol *415*, 141-149.

McCarter, G. C., Reichling, D. B., and Levine, J. D. (1999). Mechanical transduction by rat dorsal root ganglion neurons in vitro. Neurosci Lett *273*, 179-182.

McMahon, S. B. (1996). NGF as a mediator of inflammatory pain. Philos Trans R Soc Lond B Biol Sci *351*, 431-440.

McMahon, S. B., and Koltzenburg, M. (1990). Novel classes of nociceptors: beyond Sherrington. Trends Neurosci *13*, 199-201.

Mendelson, M., and Lowenstein, W. R. (1964). Mechanisms of Receptor Adaptation. Science *144*, 554-555.

Mense, S. (1993). Nociception from skeletal muscle in relation to clinical muscle pain. Pain *54*, 241-289.

Merighi, A., Carmignoto, G., Gobbo, S., Lossi, L., Salio, C., Vergnano, A. M., and Zonta, M. (2004). Neurotrophins in spinal cord nociceptive pathways. Prog Brain Res *146*, 291-321.

Meyer, R. A., and Campbell, J. N. (1988). A novel electrophysiological technique for locating cutaneous nociceptive and chemospecific receptors. Brain Res *441*, 81-86.

Meyer, R. A., Davis, K. D., Cohen, R. H., Treede, R. D., and Campbell, J. N. (1991). Mechanically insensitive afferents (MIAs) in cutaneous nerves of monkey. Brain Res *561*, 252-261.

Milenkovic, N., Wetzel, C., Moshourab, R., and Lewin, G. R. (2008). Speed and temperature dependences of mechanotransduction in afferent fibers recorded from the mouse saphenous nerve. J Neurophysiol *100*, 2771-2783.

Mirnics, K., and Koerber, H. R. (1995). Prenatal development of rat primary afferent fibers: I. Peripheral projections. J Comp Neurol *355*, 589-600.

Molliver, D. C., and Snider, W. D. (1997). Nerve growth factor receptor TrkA is down-regulated during postnatal development by a subset of dorsal root ganglion neurons. J Comp Neurol *381*, 428-438.

Molliver, D. C., Wright, D. E., Leitner, M. L., Parsadanian, A. S., Doster, K., Wen, D.,

Yan, Q., and Snider, W. D. (1997). IB4-binding DRG neurons switch from NGF to GDNF dependence in early postnatal life. Neuron *19*, 849-861.

Nelson, M. T., Joksovic, P. M., Perez-Reyes, E., and Todorovic, S. M. (2005). The endogenous redox agent L-cysteine induces T-type Ca2+ channel-dependent sensitization of a novel subpopulation of rat peripheral nociceptors. J Neurosci *25*, 8766-8775.

Okuse, K., Chaplan, S. R., McMahon, S. B., Luo, Z. D., Calcutt, N. A., Scott, B. P., Akopian, A. N., and Wood, J. N. (1997). Regulation of expression of the sensory neuron-specific sodium channel SNS in inflammatory and neuropathic pain. Mol Cell Neurosci *10*, 196-207.

Park, S. Y., Choi, J. Y., Kim, R. U., Lee, Y. S., Cho, H. J., and Kim, D. S. (2003). Downregulation of voltage-gated potassium channel alpha gene expression by axotomy and neurotrophins in rat dorsal root ganglia. Mol Cells *16*, 256-259.

Perl, E. R. (1968). Myelinated afferent fibres innervating the primate skin and their response to noxious stimuli. J Physiol *197*, 593-615.

Petty, B. G., Cornblath, D. R., Adornato, B. T., Chaudhry, V., Flexner, C., Wachsman, M., Sinicropi, D., Burton, L. E., and Peroutka, S. J. (1994). The effect of systemically administered recombinant human nerve growth factor in healthy human subjects. Ann Neurol *36*, 244-246.

Pezet, S., and McMahon, S. B. (2006). Neurotrophins: mediators and modulators of pain. Annu Rev Neurosci *29*, 507-538.

Polvani, S., Masi, A., Pillozzi, S., Gragnani, L., Crociani, O., Olivotto, M., Becchetti, A., Wanke, E., and Arcangeli, A. (2003). Developmentally regulated expression of the mouse homologues of the potassium channel encoding genes m-erg1, m-erg2 and m-erg3. Gene Expr Patterns *3*, 767-776.

Price, M. P., Lewin, G. R., McIlwrath, S. L., Cheng, C., Xie, J., Heppenstall, P. A., Stucky, C. L., Mannsfeldt, A. G., Brennan, T. J., Drummond, H. A.*, et al.* (2000). The mammalian sodium channel BNC1 is required for normal touch sensation. Nature *407*, 1007-1011.

Price, M. P., McIlwrath, S. L., Xie, J., Cheng, C., Qiao, J., Tarr, D. E., Sluka, K. A., Brennan, T. J., Lewin, G. R., and Welsh, M. J. (2001). The DRASIC cation channel contributes to the detection of cutaneous touch and acid stimuli in mice. Neuron *32*, 1071-1083.

Puil, E., Meiri, H., and Yarom, Y. (1994). Resonant behavior and frequency preferences of thalamic neurons. J Neurophysiol *71*, 575-582.

Ramer, M. S., Bradbury, E. J., and McMahon, S. B. (2001). Nerve growth factor induces P2X(3) expression in sensory neurons. J Neurochem *77*, 864-875.

Reeh, P. W., Kocher, L., and Jung, S. (1986). Does neurogenic inflammation alter the

sensitivity of unmyelinated nociceptors in the rat? Brain Res *384*, 42-50.

Renganathan, M., Cummins, T. R., and Waxman, S. G. (2001). Contribution of Na(v)1.8 sodium channels to action potential electrogenesis in DRG neurons. J Neurophysiol *86*, 629-640.

Ritter, A. M., and Mendell, L. M. (1992). Somal membrane properties of physiologically identified sensory neurons in the rat: effects of nerve growth factor. J Neurophysiol *68*, 2033-2041.

Rose, R. D., Koerber, H. R., Sedivec, M. J., and Mendell, L. M. (1986). Somal action potential duration differs in identified primary afferents. Neurosci Lett *63*, 259-264.

Rydqvist, B., and Purali, N. (1993). Transducer properties of the rapidly adapting stretch receptor neurone in the crayfish (Pacifastacus leniusculus). J Physiol *469*, 193-211.

Savage, C., Hamelin, M., Culotti, J. G., Coulson, A., Albertson, D. G., and Chalfie, M. (1989). mec-7 is a beta-tubulin gene required for the production of 15-protofilament microtubules in Caenorhabditis elegans. Genes Dev *3*, 870-881.

Schaible, H. G., and Grubb, B. D. (1993). Afferent and spinal mechanisms of joint pain. Pain *55*, 5-54.

Schaible, H. G., and Schmidt, R. F. (1985). Effects of an experimental arthritis on the sensory properties of fine articular afferent units. J Neurophysiol *54*, 1109-1122.

Schaible, H. G., and Schmidt, R. F. (1988a). Excitation and sensitization of fine articular afferents from cat's knee joint by prostaglandin E2. J Physiol *403*, 91-104.

Schaible, H. G., and Schmidt, R. F. (1988b). Time course of mechanosensitivity changes in articular afferents during a developing experimental arthritis. J Neurophysiol *60*, 2180-2195.

Schmidt, R., Schmelz, M., Forster, C., Ringkamp, M., Torebjork, E., and Handwerker, H. (1995). Novel classes of responsive and unresponsive C nociceptors in human skin. J Neurosci *15*, 333-341.

Schmidt, R., Schmelz, M., Ringkamp, M., Handwerker, H. O., and Torebjork, H. E. (1997). Innervation territories of mechanically activated C nociceptor units in human skin. J Neurophysiol *78*, 2641-2648.

Scott, S. A. (1982). The development of the segmental pattern of skin sensory innervation in embryonic chick hind limb. J Physiol *330*, 203-220.

Scroggs, R. S., and Fox, A. P. (1992). Calcium current variation between acutely isolated adult rat dorsal root ganglion neurons of different size. J Physiol *445*, 639-658.

Sengupta, J. N., and Gebhart, G. F. (1994). Mechanosensitive properties of pelvic nerve afferent fibers innervating the urinary bladder of the rat. J Neurophysiol *72*,

2420-2430.

Serbedzija, G. N., Fraser, S. E., and Bronner-Fraser, M. (1990). Pathways of trunk neural crest cell migration in the mouse embryo as revealed by vital dye labelling. Development *108*, 605-612.

Shin, J. B., Martinez-Salgado, C., Heppenstall, P. A., and Lewin, G. R. (2003). A T-type calcium channel required for normal function of a mammalian mechanoreceptor. Nat Neurosci *6*, 724-730.

Si, F., Brodie, H., Gillespie, P. G., Vazquez, A. E., and Yamoah, E. N. (2003). Developmental assembly of transduction apparatus in chick basilar papilla. J Neurosci *23*, 10815-10826.

Siemens, J., Lillo, C., Dumont, R. A., Reynolds, A., Williams, D. S., Gillespie, P. G., and Muller, U. (2004). Cadherin 23 is a component of the tip link in hair-cell stereocilia. Nature *428*, 950-955.

Simone, D. A., Baumann, T. K., and LaMotte, R. H. (1989). Dose-dependent pain and mechanical hyperalgesia in humans after intradermal injection of capsaicin. Pain *38*, 99-107.

Simone, D. A., Sorkin, L. S., Oh, U., Chung, J. M., Owens, C., LaMotte, R. H., and Willis, W. D. (1991). Neurogenic hyperalgesia: central neural correlates in responses of spinothalamic tract neurons. J Neurophysiol *66*, 228-246.

Slugg, R. M., Meyer, R. A., and Campbell, J. N. (2000). Response of cutaneous A- and C-fiber nociceptors in the monkey to controlled-force stimuli. J Neurophysiol *83*, 2179-2191.

Stacey, M. J. (1969). Free nerve endings in skeletal muscle of the cat. J Anat *105*, 231-254.

Stauffer, E. A., Scarborough, J. D., Hirono, M., Miller, E. D., Shah, K., Mercer, J. A., Holt, J. R., and Gillespie, P. G. (2005). Fast adaptation in vestibular hair cells requires myosin-1c activity. Neuron *47*, 541-553.

Stucky, C. L., DeChiara, T., Lindsay, R. M., Yancopoulos, G. D., and Koltzenburg, M. (1998). Neurotrophin 4 is required for the survival of a subclass of hair follicle receptors. J Neurosci *18*, 7040-7046.

Stucky, C. L., and Lewin, G. R. (1999). Isolectin B(4)-positive and -negative nociceptors are functionally distinct. J Neurosci *19*, 6497-6505.

Svensson, P., Cairns, B. E., Wang, K., and Arendt-Nielsen, L. (2003). Injection of nerve growth factor into human masseter muscle evokes long-lasting mechanical allodynia and hyperalgesia. Pain *104*, 241-247.

Talley, E. M., Cribbs, L. L., Lee, J. H., Daud, A., Perez-Reyes, E., and Bayliss, D. A. (1999). Differential distribution of three members of a gene family encoding low voltage-activated (T-type) calcium channels. J Neurosci *19*, 1895-1911.

Tavernarakis, N., and Driscoll, M. (1997). Molecular modeling of mechanotransduction in the nematode Caenorhabditis elegans. Annu Rev Physiol *59*, 659-689.

Theiler, K. (1972). The House Mouse, Berlin: Spring-Verlag

Todorovic, S. M., Jevtovic-Todorovic, V., Meyenburg, A., Mennerick, S., Perez-Reyes, E., Romano, C., Olney, J. W., and Zorumski, C. F. (2001). Redox modulation of T-type calcium channels in rat peripheral nociceptors. Neuron *31*, 75-85.

Toma, S., and Nakajima, Y. (1995). Response characteristics of cutaneous mechanoreceptors to vibratory stimuli in human glabrous skin. Neurosci Lett *195*, 61-63.

Torebjork, H. E., Schady, W., and Ochoa, J. L. (1984). A new method for demonstration of central effects of analgesic agents in man. J Neurol Neurosurg Psychiatry *47*, 862-869.

Treede, R. D., Meyer, R. A., Raja, S. N., and Campbell, J. N. (1992). Peripheral and central mechanisms of cutaneous hyperalgesia. Prog Neurobiol *38*, 397-421.

Tu, H., Deng, L., Sun, Q., Yao, L., Han, J. S., and Wan, Y. (2004). Hyperpolarization-activated, cyclic nucleotide-gated cation channels: roles in the differential electrophysiological properties of rat primary afferent neurons. J Neurosci Res *76*, 713-722.

Walker, R. G., Willingham, A. T., and Zuker, C. S. (2000). A Drosophila mechanosensory transduction channel. Science *287*, 2229-2234.

Weidner, C., Schmelz, M., Schmidt, R., Hansson, B., Handwerker, H. O., and Torebjork, H. E. (1999). Functional attributes discriminating mechano-insensitive and mechano-responsive C nociceptors in human skin. J Neurosci *19*, 10184-10190.

Wetzel, C., Hu, J., Riethmacher, D., Benckendorff, A., Harder, L., Eilers, A., Moshourab, R., Kozlenkov, A., Labuz, D., Caspani, O*., et al.* (2007). A stomatin-domain protein essential for touch sensation in the mouse. Nature *445*, 206-209.

White, F. A., Silos-Santiago, I., Molliver, D. C., Nishimura, M., Phillips, H., Barbacid, M., and Snider, W. D. (1996). Synchronous onset of NGF and TrkA survival dependence in developing dorsal root ganglia. J Neurosci *16*, 4662-4672.

Winston, J., Toma, H., Shenoy, M., and Pasricha, P. J. (2001). Nerve growth factor regulates VR-1 mRNA levels in cultures of adult dorsal root ganglion neurons. Pain *89*, 181-186.

Witschi, E. (1962). Development: Rat. (VII. Prenatal vertebrate development.) In Biological Handbook of Federation of American Societies for Experimental Biology, Washington,D.C. (ed. P. L. Altmann & D. S. Dittmer), pp. 304-314

Yoshida, S., Matsuda, Y., and Samejima, A. (1978). Tetrodotoxin-resistant sodium and calcium components of action potentials in dorsal root ganglion cells of the adult

mouse. J Neurophysiol *41*, 1096-1106.

Zhang, X., Huang, J., and McNaughton, P. A. (2005). NGF rapidly increases membrane expression of TRPV1 heat-gated ion channels. Embo J *24*, 4211-4223.

Zhuang, Z. Y., Xu, H., Clapham, D. E., and Ji, R. R. (2004). Phosphatidylinositol 3-kinase activates ERK in primary sensory neurons and mediates inflammatory heat hyperalgesia through TRPV1 sensitization. J Neurosci *24*, 8300-8309.

Erklärung

„Ich, Rui Wang, erkläre, dass ich die vorgelegte Dissertation mit dem Thema: ‚*Electrical excitability and mechanosensitive currents in sensory neurons: developmental onset, calcium channels and NGF-mediated modulation of mechanotransduction'* selbst verfasst und keine anderen als die angegebenen Quellen und Hilfsmittel benutzt, ohne die (unzulässige) Hilfe Dritter verfasst und auch in Teilen keine Kopien anderer Arbeiten dargestellt habe."

Berlin, den

Rui Wang